THE BOUNDARY CONDITIONS IN DIRECT SIMPLE SHEAR TESTS

Developments for peat testing at low normal stress

Matthieu Grognet

September 2011

The boundary conditions in direct simple shear tests, development for peat testing at low vertical stress

M.Sc. thesis of Matthieu Grognet

Supervised by:
Prof. M. Hicks
Dr. E. Den Haan
Dr. D. N-Gan Tillard
Ir J. Van der Schrier

September 2011

Delft University of Technology
Faculty of applied Earth Science
Engineering Geology

Preface

The present study has been performed at Deltares between 12/02/2011 and 13/09/2011. This report report is a graduation project both for the degree of Master of Science (Engineering Geology) at the Delft University of Technology (The Netherlands) and for the *diplome d'ingénieur* at the *Ecole Nationale Superieure de Géologie* in *option Géotechnique* (France).

Many people contributed to the elaboration of this report, I would like to express them my gratitude.

First thank you to the members of the graduation committee and especially to Dr. Evert den Haan (Deltares) who gave me the chance to study this fascinating topic. He has been available, even during his holidays to answer to all my questions and always managed to keep me focus in the good direction.

Dr. Dominique N-Gan Tillard (TU Delft) who has been an invaluable support not only for this thesis but also for my entire stay at TU Delft. She made this experience very enriching for me.

Prof. Dr. Hicks (TU Delft) who remained available at any moment to answer to my questions and contributes daily to the good development of the Geo-engineering department.

Ir. Joost van der Schrier (Royal Haskoning) who spent some of his precious time on supervising this work and revised it always in a very constructive way.

In Deltares, I would like to thank Aad Schapers who spent a lot of his time on teaching me all the secrets of the Geonor device. He always contributes to make the working environment as pleasant as possible.

Goof Leendertse who has entirely built the prototype in addition to his routine work. He has shown a remarkable patience with my infinite demands to improve the device. Nothing would have been possible without him.

Jack van der Vegt who has supported this work in many ways, "Super" Lambert Smidt for his kindness and his ability to fix any problem on any kind of device and Thijs van Dijk who contributed to the elaboration of the prototype.

Cor Zwanenburg who helped me with identifying the peat sampled at the IJKDijk project.

Leo Voogt and Bas Hemmen for having found rooms to make this work possible.

Vera van Beck who provided valuable help with the Particle Image velocimetry analysis.

From Plaxis, I would like to thank sincerely Ronald Brinkgreve for all his advices and answers about Plaxis. His natural ability to provide clear explanations makes enriching any discussion or course given by him.

Finally, Jelke Dykstra who showed interest for this subject and especially for the physical modelling.

And all the others I forgot to mention here.

The organisations involved in this research study are listed below:

Deltares
Stieltjesweg 2
P.O. Box 177
2600 MH Delft, The Netherlands

Delft University of Technology
Geo Engineering section
P.O. Box 5048
2600 GA Delft, The Netherlands

Ecole National Supérieure de Géologie
Rue du Doyen Roubault
B.P. 40
54500 Vandoeuvre lès Nancy, France

Abstract

More than the half of the Netherlands is under the high level of sea and rivers. Therefore, evaluating the safety of dykes is primordial. A specific interest is given to peat dykes safety which suffer of a lack of knowledge which manifested recently by some peat dykes failures (Van Baars 2005). The behaviour of peat is also of interest in others countries, for assessing peat slope stability for instance (Long and Jennings 2006). Due to its high anisotropy and fibrosity, peat cannot be tested with any device in the laboratory. The direct simple shear test is routinely used since it can mimic several in situ conditions and provides conservative results for peat dyke stability evaluation. Furthermore, it does not show the inconvenience of triaxial testing with peat (Landva 1980). Larger samples than for usual testing are desirable to investigate the effect of fibres on tests results.

The Direct simple shear testing devices remain imperfect since it is unable to provide additional shear stresses on the sides of the specimen. As consequence, non uniformities develop on all the faces of the specimen, in particular compression in the obtuse corners and tension in the acute corners. In practice, thin samples are used (height over diameter around 0,2 to 0,3) to limit the nonhomogeneities to the sides and leave the major part of the sample in an homogenous state of stress. Testing peat at low vertical stress, remains a challenge and necessities the development of adapted devices (Boylan and Long 2009).

A series of tests has been performed on a wood and sedge peat with the Geonor device in order to compare the effect of two boundary conditions on tests results. The first one is a classical reinforced membrane (Bjerrum and Landva 1966) and the second is an unreinforced membrane enclosed in a stack of rings. The vertical stresses applied during the tests varied between 10kPa and 120kPa. The results show small differences when the Mohr Coulomb parameters are determined. The comparison is limited considering the variability of the material tested. A more accurate calibration of the stack of rings would be desirable. Some improvements are needed on the actual apparatus to test peat at low vertical stress. Removing the membrane between the soil and the rings would give more accuracy in the results.

A direct simple shear prototype has been developed in order to test larger samples (with height over diameter ratio of 0.5) at low vertical stress. The effect of two innovative rough boundaries on the stress-strain homogeneity of the sample has been investigated. The sidewalls of the device are transparent and make possible a visual assessment of the deformation of the sample. The Particle Image Velocimetry analysis is also considered to assess the shear strain homogeneity in the sample. The results show an improving shear strain homogeneity and reduced tension forces in the acute corners. Slippage is also observed between the top cap and the sample and the normal load could not be measured. Further research is needed to validate the utility of this prototype. Stress-strain curves obtained from the three boundaries should be compared to quantify the improvement of rough boundaries. A finite element analysis of the prototype boundaries has been performed with two models (Mohr Coulomb and Soft Soil Creep model). The boundaries considered were perfectly rough at the top and bottom and perfectly smooth at the sides. The presence of strips and even more the presence of vanes increase the stress – strain homogeneity inside the sample with both models. Reliable stress – strain curves as measured in classical devices could not be obtained with such boundaries. Interfaces should be preferred to model more realistic conditions.

TABLE OF CONTENT

INTRODUCTION

More than the half of the Netherlands is below the high water level of the rivers and sea. In order to prevent the lowlands from flooding, primary and secondary dykes have been built along rivers and sea. A large amount of these dykes (3500 of the 14000km of secondary dykes) are built on very soft material such as peat. Recent disorders (Van Baars 2005) have pointed out an important lack of knowledge concerning peat behaviour and assessment of peat dyke stability. Understanding peat behaviour is also of major interest in some countries such as Ireland or Canada in consequence of peat dyke failures (Pigott et al. 1992) and peat slope failure (Long and Jennings 2006, Boylan et al. 2008). One example of peat dyke failure is illustrated in figure1 and an Irish peat slope failure is illustrated in figure 2.

Laboratory testing methods to evaluate the shear strength of peat are generally the same as for traditional soils. Nevertheless, some limitations are encountered due to the strong anisotropy and fibrosity of peat with a notable influenced of the fibres and wood remains. Since peat has a disposition towards horizontal sliding, the direct simple shear test is routinely used with such a material (Farrell and Hebib 1998, Den Haan and Kruse 2007). Classical sample dimensions are tested with classical devices but larger samples (with larger height over diameter ratio) would be desirable to investigate the influence of peat structure. One direct simple shear test apparatus has been recently developed especially for peat testing under low stresses (Boylan and Long 2009).

Figure 1: Horizontal failure of the Wilnis peat dyke (Van Baars 2005)

Figure 2: Peat slope failure in Ireland (Long and Jennings 2006)

Initially, the direct simple shear device was developed as an improvement of the direct shear box. In both device, shear is applied directly to a soil sample, unlike the triaxial device in which shear develops from a difference of applied principal stresses. Although the direct application of shear stress closely mimics many modes of shear in situ, the direct shear device in particular suffers from inhomogeneity of the applied stresses and resultant strains. In the direct simple shear device, these are alleviated but not completely removed. Furthermore, the significance of these inhomogeneities is increased by increasing the height over diameter ratio. In the project described here, it is attempted to further improve the direct simple shear device to obtain a more homogenous distribution of both shear and normal stresses and resulting strains.

First, a review of the literature about direct simple shear device is given. A special emphasis is put on the stress-strain conditions in direct simple shear tests. Secondly, a series of tests has been performed on peat with a classical Geonor device, in order to investigate the effect of two different boundary conditions on the test results. The reinforced membrane is compared to an unreinforced membrane enclosed in a stack of rings. The comparison is done on the basis of typical results such as friction angle, cohesion and initial shear modulus. A detailed study of the peat tested is given as well as a description of the device and the routine testing procedure. An assessment of the Geonor device for peat testing at low vertical stress is done. Thirdly, a prototype has been developed in order to investigate the effect of innovative boundary conditions on the stress strain distribution in the sample at low vertical stress. The experimental work consisted in a visual assessment of the deformation of the soil as well as a Particle Image Velocimetry analysis allowing for shear strain measurements. Finally, a finite element analysis of the prototype boundary conditions is performed with the software Plaxis 2D. Two models, one linear elastic (Mohr Coulomb) and one visco-elasto-plastic (Soft Soil Creep) are used. The choice of rigid or smoother boundaries using interfaces is discussed.

1. THE DIRECT SIMPLE SHEAR DEVICE: RESEARCH AND PRACTICE

Shear tests have been developed in order to investigate the failure of soil which occurs by sliding along a surface when a critical value of shear stress is reached. The direct shear box and then its improvement, the direct simple shear device are two examples of such tests. For fifty years, a substantial amount of research has been lead about simple shear and created controversy due to the stress and strain inhomogeneities developing in the soil specimen during the test. A summary of the important points concerning simple shear are presented. First, the development of the direct simple shear device is detailed as well as the different conditions to perform a direct simple shear and the different methods of interpretation. Then, an emphasis is put on the stress-strain conditions developing in direct simple shear tests. Finally, the utility of such a test to reproduce in situ conditions is detailed before presenting the interest of the direct simple shear test for peat testing at low vertical stress.

1.1 DEVELOPMENT OF THE DIRECT SIMPLE SHEAR DEVICE

It is not known when the direct shear apparatus was invented and if Coulomb, whose formula it uses had anything to do with it. In its present form, the direct shear test (credited to Krey, Terzaghi and Casagrande) is performed on circular or rectangular specimen encased in a splitspacebox. In a first phase, a normal force is applied at the top of the box and in a second phase, a shearing force is applied at the top (or bottom) of the split box, causing the soil to shear along the plane between the two parts of the box. The shear and vertical stresses are measured in function of the horizontal displacement. A peak in the stress-strain curves is often observed. The evolution of the vertical displacement in function of the horizontal deformation provides information concerning the contractant or dilatant behaviour of the soil. In this device, the shear stress-strain distribution is highly non uniform for different reasons. First, a high concentration of stresses develops at the front and rear edges of the specimen. This condition creates a progressive failure so that the total shear strength of the specimen is not mobilized. Furthermore, the strain restraints which force the failure in one direction create an unknown state of stress in the specimen (Terzaghi, Peck and Mesri 1996).

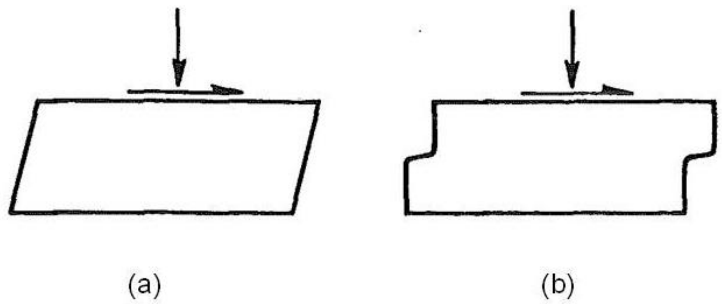

Figure 3: Distinction between direct simple shear (a) and direct shear (b)

Because of the shortcomings of the direct shear tests, various attempts were made in the hope of imposing a more uniform stress and strain conditions to the soil specimen and the direct simple shear apparatus was introduced. A distinction between direct simple shear and direct shear is illustrated in figure 3. Kjellman (1951) developed an apparatus to test circular soil specimens (h=60mm and D=20mm) enclosed in a rubber membrane and surrounded by aluminium rings as illustrated in figure 4. Two porous stones at the top and bottom of the soil specimen allow drainage during consolidation which can be compared to an oedometer one dimensional compression. The specimen is then sheared from the top plate with the possibility to maintain either the load or the height constant. Often, the top and bottom cap are furnished with little teeth to avoid slippage between the boundaries and the soil specimen. Vertical and horizontal load cells and displacement gauges are used to obtain vertical stress, shear stress vertical strain and shear strain. The major advantages of this device are to impose a constant area of potential sliding (compared to the direct shear box) and also to obtain a better homogeneity of the stress distribution. In a comparable way to the direct shear box, the direction of the major principal stress sig1 is vertical during consolidation (the minor being horizontal) and then it rotates during shearing. The amplitude and direction of principal stresses remain difficult to trace during shearing in such a device.

The Kjellman's apparatus has been improved then by Landva at the Nowegian Geotechnical Institute (NGI) (Bjerrum and Landva, 1966). The major new feature of this device was the use of a reinforced membrane to surround the sample laterally and to enforce constant area. The reinforcement consists of a spiral winding of wire having a diameter of 0.15mm and being wound at 25 turns per cm. This reinforced membrane is applied on the sample with vacuum and fit perfectly to the lateral boundaries. The reinforced membrane is supposed to be stiff enough to ensure one dimensional consolidation of the soil specimen and to have the capacity to conserve a constant volume during shearing. The NGI device accommodates samples of h=10mm and D=80mm.

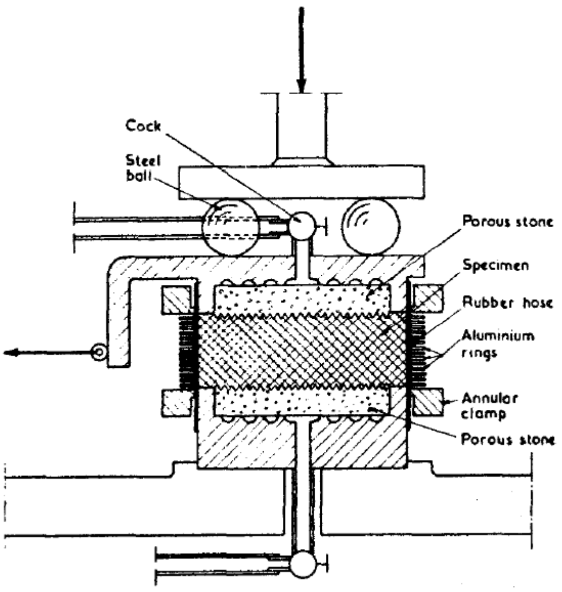

Figure 4: Direct simple shear apparatus testing cylindrical samples (Kjellman 1951)

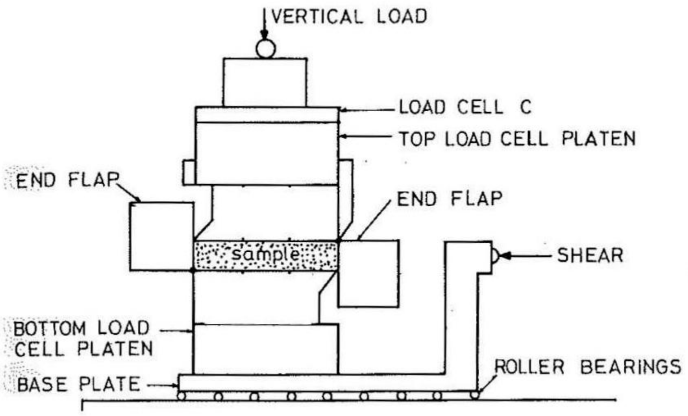

Figure 5: Cambridge direct simple shear device testing cubical sample (Roscoe 1953)

Other developments of direct simple shear device lead to the development of the Cambridge apparatus presented in figure 5. A device using a square sample (dimensions 60x60x20 mm) was designed with straight lateral boundaries (Roscoe 1953) in order to improve on the previous devices. The lateral boundaries are frictionless whereas the top and bottom boundaries are rough. This experimental device is the first of a long series developed in Cambridge University and thoroughly studied in details by several researchers during the following decades. These devices could not perform truly undrained tests since no back pressure could be applied for full saturation. Later, Direct Simple Shear device testing samples enclosed in a pressurized cell were developed (Franke 1979, Dyvik 1987) with the objective to ensure a full saturation of the sample and provide accurate pore pressure measurements in the soil specimen.

1.2 DIRECT SIMPLE SHEAR TEST RESULTS

The shear strain (γ) in simple shear is defined as the horizontal displacement divided by the height of the specimen. The typical results obtained from direct simple shear tests are the shear stress, the change in vertical stress (or the change in vertical displacement) in function of the shear strain. The shear modulus can be deduced from the slope of the shear stress-shear strain curve. Several tests at different vertical loads permit to obtain the Mohr Coulomb parameters: cohesion (c) and friction angle (φ). The different methods of interpretations of Direct Simple Shear tests are discussed later.

The same kind of results can be obtained from other shear devices but are not likely to provide similar results. Saada et al. (1983) compared results from various shear tests such as triaxial or hollow cylinder. For both clay and sand, shear strength and shear moduli are among the lowest compared to the results from others apparatuses. Bjerrum and Landva (1966) also observed the same trend. It can be explained by the difference in the stress conditions in the simple shear and in other devices. For instance, in simple shear tests the intermediate principal stress (σ_2) is neither independent of nor it is equal to either the major or minor principal stress (contrary to triaxial test which impose σ_1 and σ_2=σ_3). Furthermore, the simple shear conditions allow the rotation of principal stress during the test. In this way it is closer to the in situ conditions compared to the triaxial device which is only able to exchange major and minor principal stress.

1.3 CONSTANT VOLUME / CONSTANT LOAD TESTS

Two main procedures are in use for the shear phase of direct simple shear tests: maintaining a constant vertical load during shearing or maintaining the volume of the soil specimen constant by keeping the height of the sample constant. The former is considered to yield drained shear strength parameters; the latter undrained shear strength parameters

For granular soils (sand), Direct Simple Shear tests are usually performed time drained with a constant load since the drained parameters are most likely to be investigated.

For soft soils (clay, peat), the parameters of interest are more likely to be investigated in undrained conditions. In most of the simple shear apparatus, it is not possible to perform truly undrained tests since no back pressure can be applied with mean of cell pressure around the sample. So, the undrained simple shear response is normally investigated by performing drained tests at constant volume. Bjerrum and Landva (1966) proposed this equivalence between the two tests and furthermore stated that the change in vertical stress observed in a constant volume test is similar to the change in pore pressure that would have occurred in a constant load undrained test. The equivalence of constant volume and constant load tests is illustrated in figure 6. Low rate of strain prevents generation of excess pore pressure internally by allowing time for equalisation.

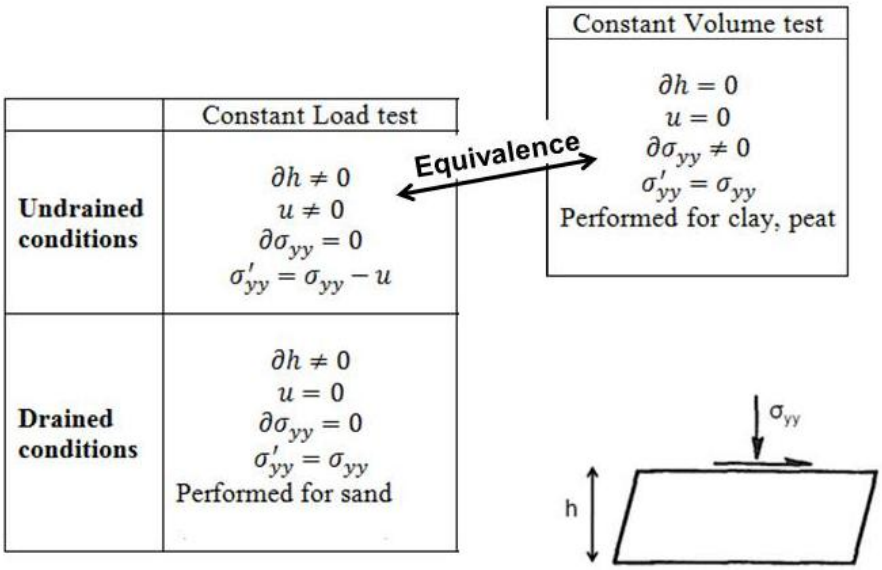

Figure 6: Equivalence between constant load test and constant volume test

Dyvik et al. (1987) performed tests to validate the ”constant volume” hypothesis. They designed a chamber for the NGI Direct Simple Shear device that provides the capability of performing truly undrained tests with pore pressure measurements inside the soil specimen. The authors compared truly undrained tests and constant volume drained test results on normally consolidated clay and obtained very similar results in both case. These conclusions only apply to normally consolidated saturated clay for shear strain lower than 10%. Unfortunately, it was not investigated for other materials. It needs not be correct for unsaturated soils. Budhu and Britto. (1987) performed a finite element modelling of the evolution of pore pressure in the core of the NGI specimen. Using Speswhite Kaolin properties and the modified Cam Clay model, they obtained results in accordance with Bjerrum’s predictions for the same range of shear strain.

1.4 INTERPRETATION OF DIRECT SIMPLE SHEAR TEST RESULTS

In most Direct Simple Shear devices, only the average vertical stress and average shear stress is measured. Horizontal stress cannot be measured. Since uncertainties remain on the actual stress state inside the specimen during testing, several methods of interpretation have emerged.

Three possibilities are usually considered as illustrated in figure 7. The determination of undrained parameters is presented here but the method of determination is also valid for drained parameters. The numbering refers to the equations below.

- The horizontal plane is a plane of maximum stress obliquity so that the angle of friction mobilized in the soil is determined by equation (1).

$$tan(\varphi) = \frac{\tau_{yx}}{\sigma_{yy}} \tag{1}$$

- The horizontal plane is a plane of maximum shear stress so that the angle of friction mobilized in the soil is determined by equation (2).

$$sin(\varphi) = \frac{\tau_{yx}}{\sigma_{yy}} \tag{2}$$

- The vertical plane is a plane of maximum stress obliquity. De Josselin de Jong (1971) proposed this option using a book stack analogy. This proposal assumes a vertical failure associated with a body rotation of magnitude gamma in the anticlockwise direction (where gamma is the amount of engineering strain applied to the specimen externally). The angle of friction mobilized in the soil is then determined by equation (3).

$$\frac{sin(\varphi).cos\,(\varphi)}{(1+sin^2(\varphi))} = \frac{\tau_{yx}}{\sigma_{yy}} \tag{3}$$

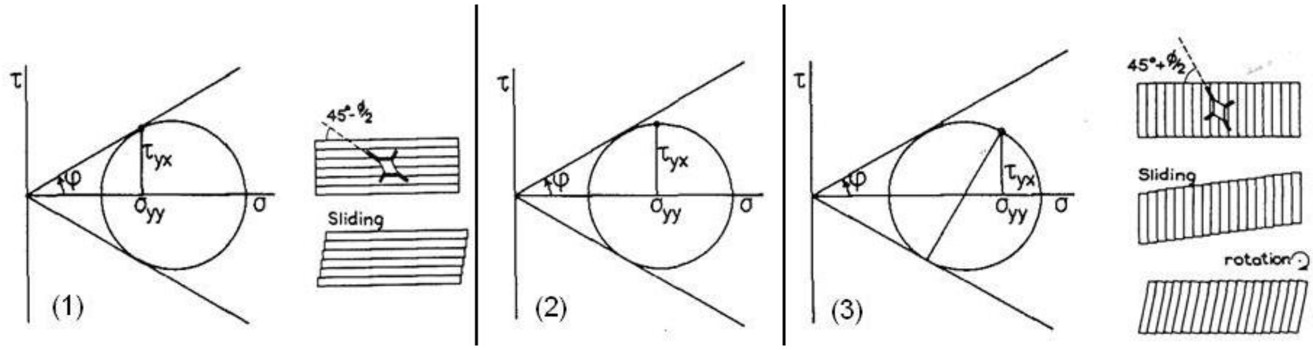

Figure 7: Different methods of interpretation of the direct simple shear test (de Josselin de Jong 1971)

De Josselin de Jong argues that the three mechanisms are possible, and that if the boundary condition of the test – or the engineering situation – allows the soil element a choice between the three modes, the selected mode is the one which requires the least resistance.

One single test performed by Borin (1973) on kaolin with a special simple shear device (in which the sample is completely surrounded by load cells so that the stress state can be completely defined, see 1.5.4) confirms the de Josselin de Jong hypothesis. In general, the first hypothesis is used since it provides conservative design parameters.

Several authors performed finite element analysis of the simple shear test in order to investigate this question of interpretation (Farrell et al. 1999, Doherty and Fahey 2011). Some uncertainties remain on the appropriate method of interpretation of the Direct Simple Shear test. The mode of failure certainly depends on the material considered. Other methods of interpretation have been proposed for granular material (Oda and Konishi 1974) but are not detailed here.

All the methods of interpretation detailed previously assume an homogeneity of the stresses inside the sample. The next section will show that this assumption cannot be true.

1.5 STRESS – STRAIN INHOMOGENEITY IN DIRECT SIMPLE SHEAR

It is intended with all laboratory tests that the behaviour of a test sample should be representative of a point in the ground. This can only be true if the stresses and strains are uniform, a requirement that no laboratory test can completely satisfy. Laboratory tests are always “a compromise between the theoretically possible and the practically feasible” (Lacasse 1981). The inhomogeneities developing in the simple shear test due to its imperfect boundary conditions are detailed here.

1.5.1 SIMPLE SHEAR / PURE SHEAR

To understand the differences between the ideal case and the real case, a distinction must be made between pure shear and simple shear in strain state and stress state. The term “pure shear” is a state of plane strain which consists of a uniform extension in the x direction and a uniform compression in the y direction of such an amount that the volume remains unchanged as illustrated in figure 8. The term “simple shear” refers to a state of plane strain in which the points are displaced only in one direction (parallel to the x-axis). In this case all planes parallel to the x-z plane slide in the direction of the x axis without changing their distance from each other. It is also a constant volume deformation. Simple shear is equal to pure shear plus a rotation. From an engineering point of view, both the simple shear state of strain and the pure shear state of strain need shear stresses applied along the four sides to maintain an uniform deformation.

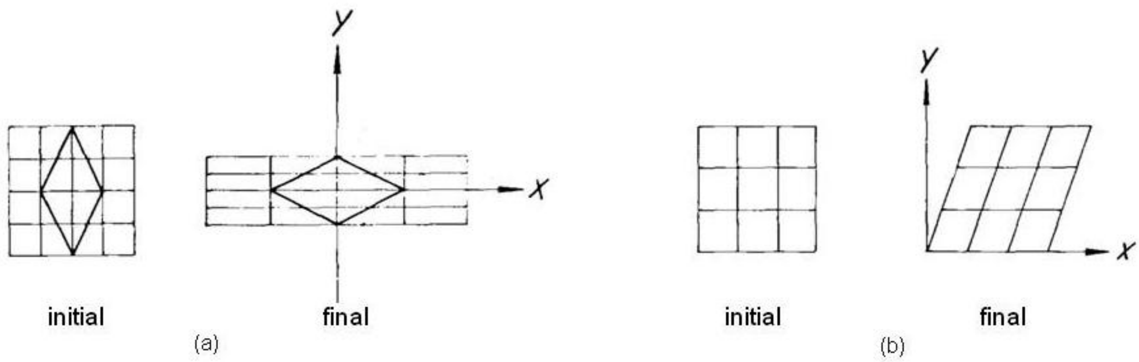

Figure 8: Pure shear state of strain (a) and simple shear state of strain (b) (Saada and Townsend 1981)

The purpose of direct simple shear tests is to apply to the sample a simple shear strain deformation. However, no shear stress can be applied on the sides of the sample compared to ideally pure shear stress condition. This absence of shear stress along the sides makes a difference between the pure shear state of stress (desired) and the simple shear state of stress as illustrated in figure 9. From advanced direct simple shear device (detailed in 1.5.4), it was deduced that the pure shear state of stress is experienced in the core of the specimen as illustrated by the dashed arrows in figure 9. Ideally, the stress and strain should be measured from this core during a test. But most of the simple shear devices only measure stresses and displacement from the boundaries of the specimen. For practical purposes, the simple shear state of stress is considered close enough to the pure shear state of stress to justify the interpretation of test results.

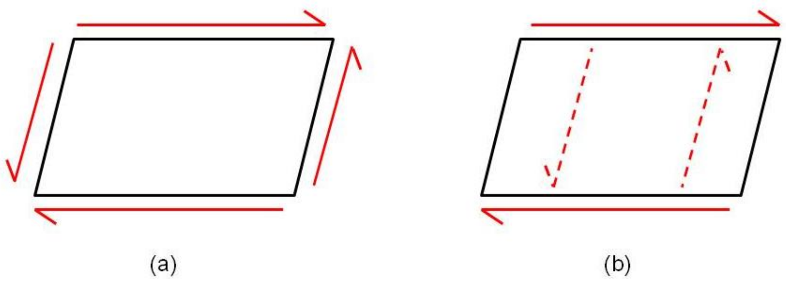

Figure 9: Pure shear state of stress (a) and simple shear state of stress (b)

1.5.2 STRESS DISTRIBUTION

From the early developments of the direct simple shear device, it was already realized that the stress – strain distribution inside the specimen was non-uniform. Indeed, because of the eccentricity developing between the top and bottom normal forces and the incapability of the devices to provide shear stress at the edges, normal forces appear on all the faces (top, bottom and sides) of the sample. Therefore, the normal stress and shear stress are non uniformly distributed in the specimen.

In order to obtain some indication of the magnitude of stresses and displacement in the sample, several analytical studies have been performed. Roscoe (1953) carried out a mathematical analysis assuming a linear elastic material. The solutions should apply to soils in the first stages of deformation and can be considered as a guide to the behaviour for large deformations. His results show both compression and tensile forces on upper and lower faces of the sample as well as on the sides as presented in figures 10 and 11. On the figure 10 the shear stress and vertical stress at the top and bottom of the sample are presented. On the figure 11 the horizontal stresses on the front and back sides are presented. s is the external horizontal force applied to the sample divided by the horizontal cross sectional area of the sample. The stress distribution can be considered as uniform only on the central third of the sample. His results were experimentally checked on a plasticine specimen sheared in the Cambridge direct simple shear test. The result at small vertical stress (12kPa) is illustrated in figure 12. The tensile forces as predicted in his theoretical analysis are seen to actually appear: a void develops between the sample and the platen in the acute angles. This separation is more easily observed at low normal stress (12kPa) than at high vertical stress (495kPa).

Prevost and Hoeg (1976) took Roscoe's analysis a step further by taking into account the slippage which can occur at the platen-soil interface in the Cambridge device. Such slippage occurs as a differential displacement between the top cap and the soil just under it. The slippage induces significant variation of normal and shear stresses on the upper and lower faces of the specimen. Complementary experimental work on plasticine samples has been performed by Finn et al. (1971). They suggested that with smooth upper and lower plates, the sample could deform so that only a region near the centre was resisting the shear load while a significant proportion of the sample near the surfaces was unstrained The apparent strength of the soil would then be substantially less than the real strength in this case. Most of the devices are now equipped with teeth or pins on top and bottom faces to avoid this phenomenon. Slippage is a real issue at low vertical stress since a minimum vertical stress has to be applied to create grip on the sample. It remains difficult to check if it occurs or not since the sample is enclosed in a box or between rings in most of the apparatuses.

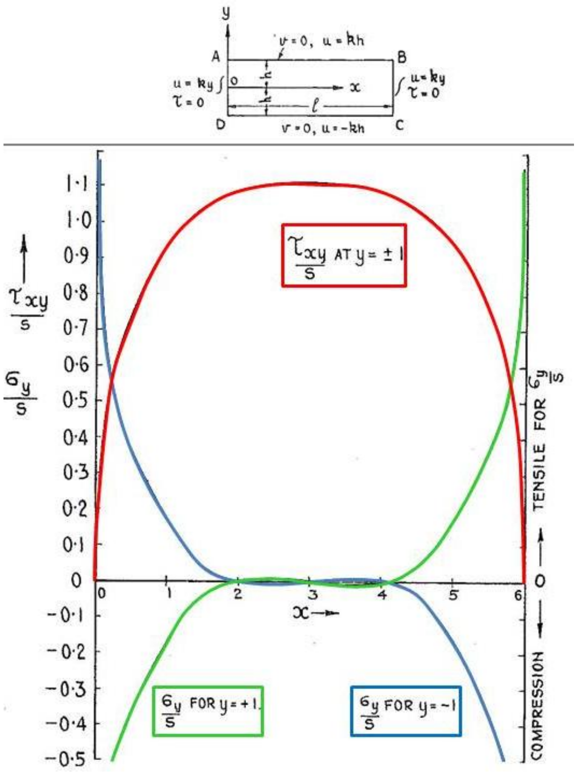

Figure 10: Distribution of the vertical stress and shear stress on top and bottom of the specimen (Roscoe 1953)

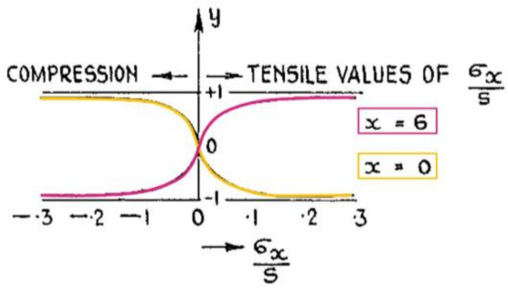

Figure 11: Distribution of the horizontal stress on the sides (Roscoe 1953)

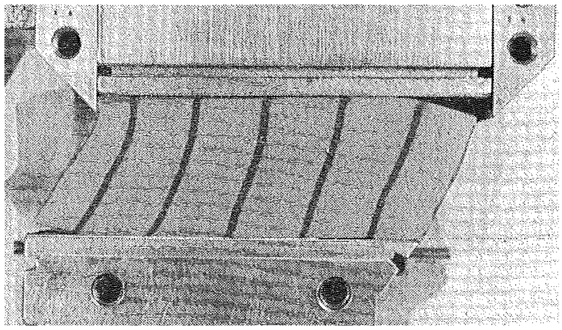

Figure 12 : Side view of a plasticine sample after shearing with a vertical stress of 12kPa (Roscoe 1953)

A three dimensional finite element analysis of the NGI Direct Simple Shear test has been performed by Lucks et al. (1972) assuming linearly elastic isotropic material and in consequence only valid for infinitesimal strain (practically up to γ=2%). The dimensions of the sample considered are 80mm diameter and 20mm height and the consolidation phase is modelled for σ_v=98kPa. The boundary conditions and the results of the analysis are presented in figure 13 and figure 14 respectively. The results show that a stress concentration can be experienced at the edges but approximately 70% of the sample is found to have a remarkably uniform stress condition. No confining effect of the reinforced membrane was considered here.

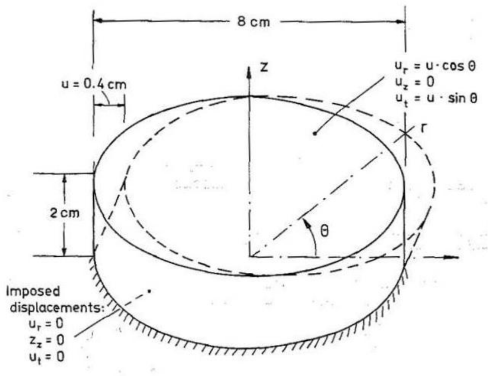

Figure 13: Boundary condition of the finite element study (Lucks at al. 1972)

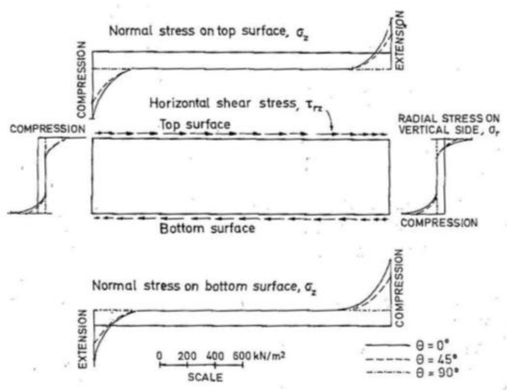

Figure 14: Stress distribution in the NGI direct simple shear sample (Lucks et al. 1972)

1.5.3 EFFECTS OF THE GEOMETRY OF THE SPECIMEN

It has been explained earlier that due to the differences between the pure shear state of stress and the simple shear state of stress, stress inhomogeneities develop at the edges of the specimen. The geometry must have an influence in the significance of theses inhomogeneities. A theoretical distribution of the stresses is presented in figure 15 for a slice with infinitesimal unit thickness, taken from the middle of the specimen along the direction of shearing. The moment equilibrium leads to equation (4).

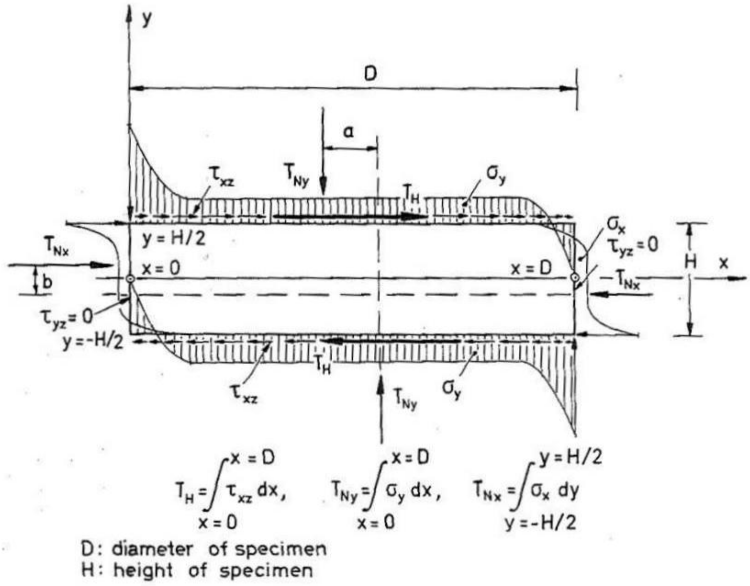

Figure 15: Stress distribution in middle of specimen and corresponding external forces (Vucetic and Lacasse 1982)

$$\sum M = T_H * H - T_{NY} * a + T_{NX} * b = 0 \tag{4}$$

If the diameter D increases while H, τ_{xy} and σ_y are kept constant, the forces T_H and T_{Ny} will increase and T_{Nx} remains constant. Using equation (4), it can be deduced that the increase in the length arm a will always be smaller than the increase of the diameter D. Thus increasing D reduces the influence of the moment on the stress distribution and then a decreasing H/D ratio is increasing the stress uniformity in the specimen. These edge effects have to be minimized to ensure that the stress and strain measured at the boundaries are close to the stress and strain experienced by the major part of the specimen. To investigate experimentally this geometry effect, Vucetic and Lacasse (1982) tested a medium stiff laminated clay with three different H/D ratio specimens (0.32; 0.20 and 0.14). The tests were carried out at two over-consolidation ratios. The results show very close results for the three different H/D ratios and the authors concluded that the H/D ratio has no significant influence on the strength and deformation characteristics of this soil. These results should be considered with caution regarding the specific laminated structure of the material tested.

The effects of the H/D ratio has been investigated by Shen et al. (1978) through a three dimensional finite element analysis (linear elastic isotropic model) taking into account the wire reinforced membrane confinement. The boundary condition and some of the results are illustrated in figure 16. The deviation is given in function of the external shear strain applied. The authors obtained the logical conclusion that the inhomogenous shear strain distribution at the edges of the specimen is diminished by reducing the height/diameter ratio. Kovacs (1973) observed experimentally differences in Direct Simple Shear test results due to the sample geometry.

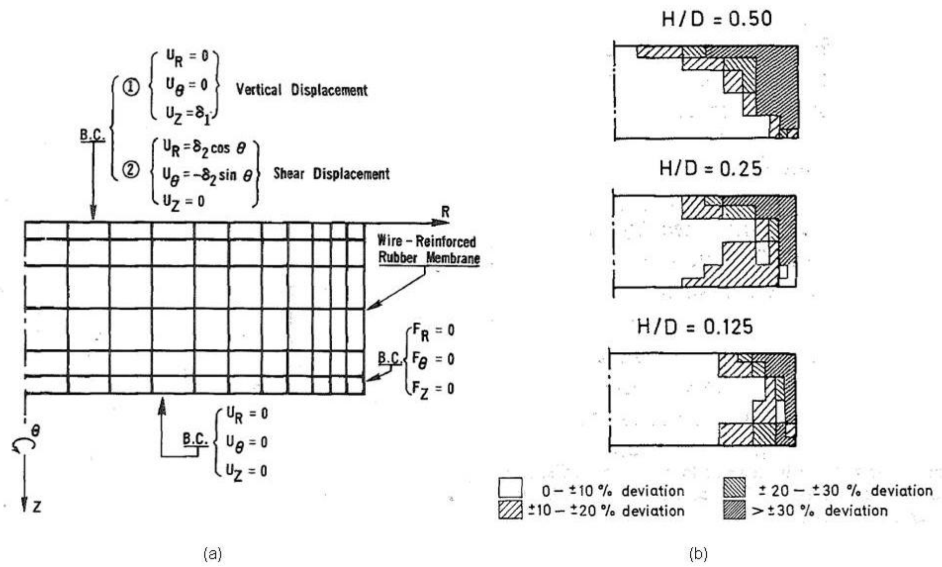

Figure 16: Boundary conditions (a) and effect of heigth to diameter ratio on shear strain distribution in the R-Z plane (θ=0)) (Shen et al. 1978)

1.5.4 RESULTS FROM ADVANCED DIRECT SIMPLE SHEAR DEVICES DEVELOPED AT CAMBRIDGE UNIVERSITY

Even if the stress distribution is criticized, the pure shear state of stress is assumed to be encountered in the core of the specimen as detailed in figure 9. Since only the average displacement and average stress can be measured in most of the Direct Simple Shear devices, it is desirable to know how significant is the difference between the measured values and the ideal “pure shear” values experienced by the core of the specimen. For this purpose, a series of advanced direct simple shear device has been developed at Cambridge. It encloses a square cross sectional specimen by an array of load cells at the top and at the sides (Roscoe 1967) as detailed in figure 17. A device has been built in order to test cylindrical samples and to produce results that could be compared to the Geonor device.

Budhu (1984) compared experimental results from identically prepared samples of sand tested in both circular and square sections apparatus. The specimens are in both cases surrounded by a special arrangement of load cells. Some of his results are presented in figure 18. The stress deduced from measurements over the whole horizontal boundary (as measured in the regular NGI device) was found to underestimate the stress ratio that is developing in the core of the sample by 6% in the NGI device and by 12% in the Cambridge device. Similar experimental studies have been performed on clay by Airey et al. (1987) in the Cambridge device. The authors observed an underestimation of the stiffness and shear strength by using the average stresses of about 10% “which from a practical point of view is not very significant”.

Furthermore, the author noticed also that the rigid boundaries of the Cambridge apparatus force the sample to deform in a simple shear configuration but the flexible vertical boundary of the NGI device cannot do so except perhaps at small shear strains.

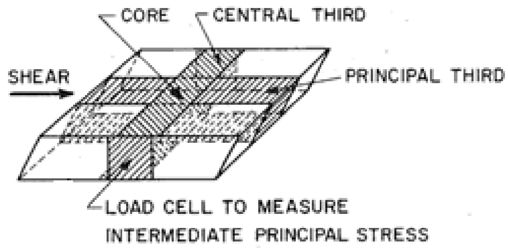

Figure 17: Arrangement of load cells in the Cambridge direct simple shear apparatus (Roscoe 1967)

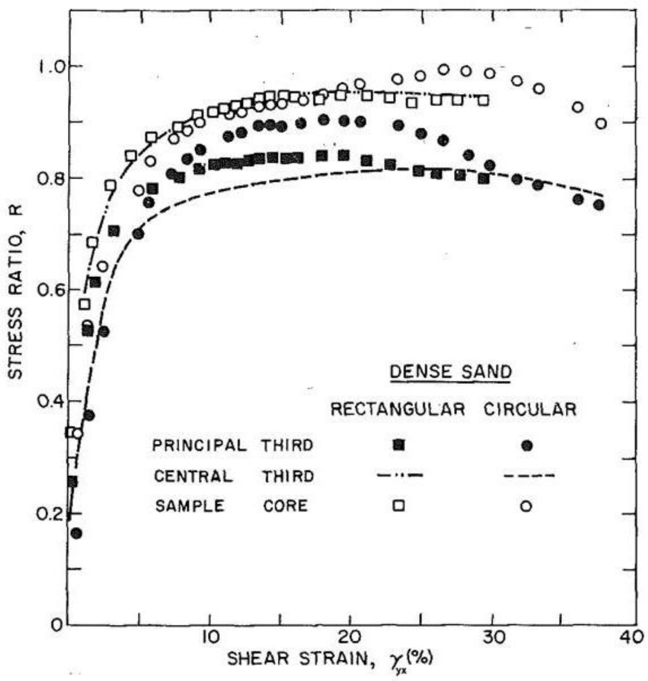

Figure 18: Stress strain curves obtained from three locations in the sample (Budhu 1984)

As a comparison to these results, one can refer to finite element modelling providing the stress state of the specimen core subjected to simple shear. Lucks et al. (1972) obtained from a finite element analysis at infinitesimal shear strain (linear elastic material) that the average shear stress increment applied is within 2% of the horizontal shear stress in the core of the specimen. This difference between the average shear stress increment applied and the horizontal shear stress in the core is around 10% in Doherty et al. (2011) finite element modelling study (for a device equipped with a cell pressure). The first result assumes a linear elastic material whereas the second considers a modified Cam Clay model.

1.5.5 PLANE STRAIN HYPOTHESIS

In Direct Simple Shear tests, the soil specimen is assumed to deform in plane strain deformation and the interpretation of test results in done on this assumption. Wright et al. (1978) investigated analytically the validity of this assumption for both circular and rectangular specimens. They applied the Saint Venant solution (linear elastic assumption) which involves a fixed end beam of square and circular cross section subjected to an end load P. The boundary conditions are different from simple shear but, the results are supposed to provide a constructive contribution. The axes considered are presented at the top of the figure. 19. According to these axes, a plane strain deformation would mean that the displacement in the z-direction is zero as well as τ_{xz} and τ_{zy}.

The results are presented in figure 19 (a), (b) and (c) refer to the square cross section whereas (a'), (b') and (c') refer to the round cross section. τ_{yx} (a, b and a', and b') is the shearing stress in the direction of the applied shearing force, τ_{yz} (c and c') is the perpendicular to it. Comparing the magnitude of shearing stresses for a square cross section, τ_{yz} is very small compared to τ_{yx} except at the edges. If the condition of smooth lateral restraint is applied the assumption of plane strain can be acceptable. For a circular cross section, neglecting τ_{yz} compared to τ_{yx} seems unacceptable since they have the same order of magnitude.

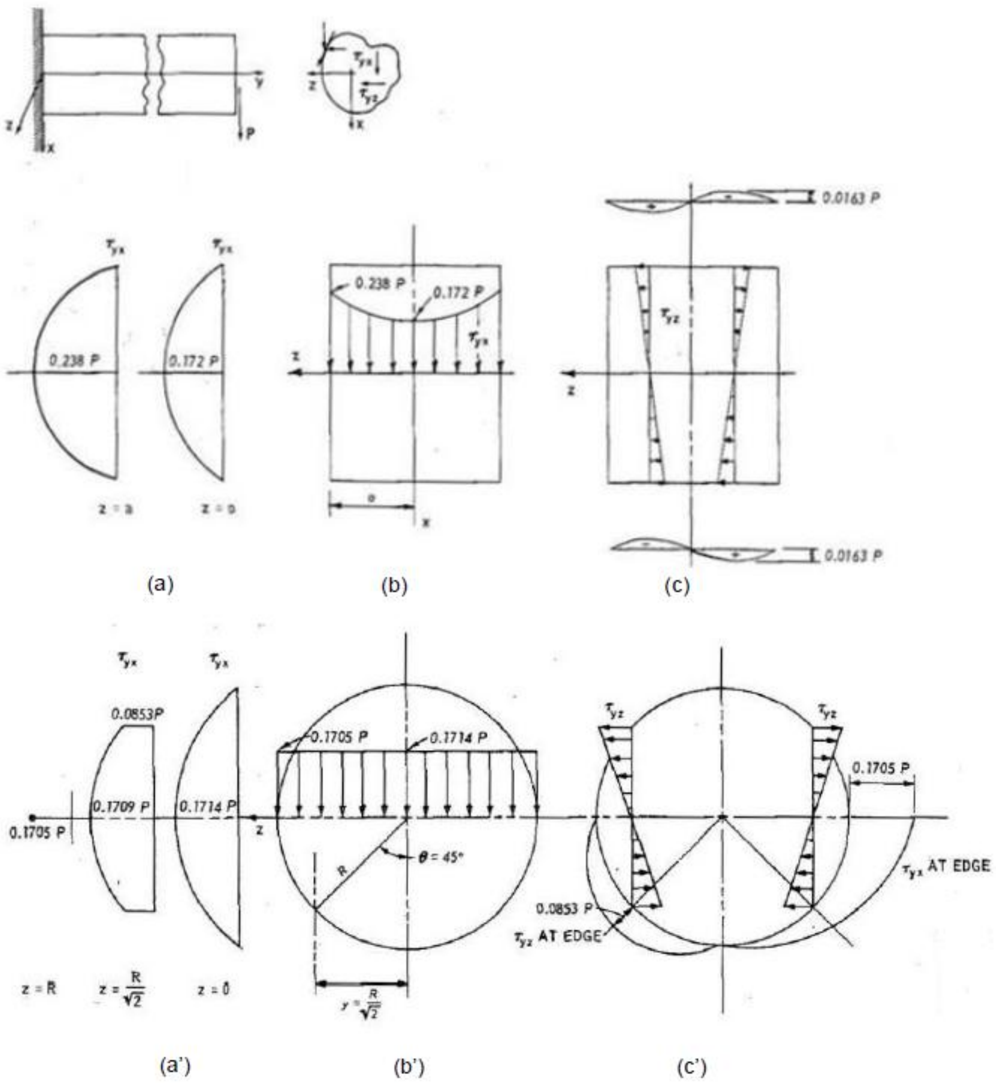

Figure 19: Distribution of the shear stresses in the rectangular cross section (top) and in the circular cross section (bottom) from the Saint Venant solution (Wright et al. 1978)

In order to examine experimentally the elastic stress distribution in simple shear models, the authors used the three dimensional photoelastic method. A transparent material is modelled in the form of a specimen and the adjacent platens stressed and subjected to cross-polarized light. The interferences created by the emerging light beams are registered with a polariscope and the stress state can be calculated since the index of refraction of the material changes in a manner directly proportional to the induced stresses. The photoelastic models used for both circular and square specimen as well as the axes considered are presented in figure 20. The resulting light field patterns of the central slices (z=0) are presented in figure 21. The results from the plane y=0 are not presented here. From the photoelastic measurements, the round model displays large variability of τ_{xy} in both shearing plane. One can note that the stress distribution is not symmetrical over x=0. For this reason, this result has been criticized (Christian 1982). Concerning the variation of transverse shear stresses (τ_{yz}), the experimental results were found to fit well with the theory. The authors observed higher transverse stresses near the boundaries and lower in the interior than expected. Finally, the variation of shear stress in the shearing direction (τ_{xy}) is significant for both square and circular specimen. The transverse shear stress (τ_{yz}) is significant for the circular specimen except in the vertical plane of symmetry. It can be neglected in case of a square specimen.

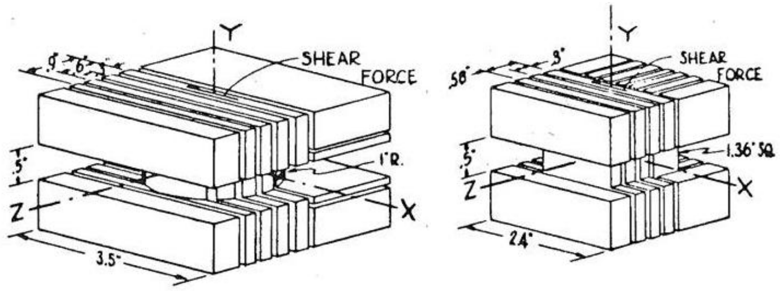

(a) (b)

Figure 20: Photoelastic models for circular sample (a) and rectangular sample (b)

This study has been used then to support the strong criticism of the direct simple shear device by Saada and Townsend (1981). According to them both Cambridge and NGI apparatuses “cannot claim to yield either reliable stress – strain relations or absolute failure values” and finally “simple shear tests are of no value for research purposes”.

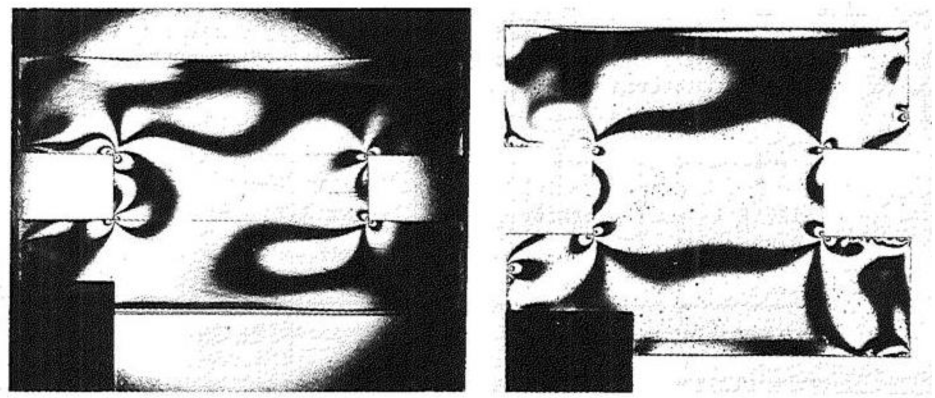

(a) (b)

Figure 21:Results of the photoelastic study on the central slices (z=0) for the circular specimen (a) and rectangular specimen (b)

1.6 PRACTICAL APPLICATIONS OF SIMPLE SHEAR TEST RESULTS

For some types of field loading conditions, direct simple shear tests provide a measure of shearing resistance which may be very useful for stability analyses. The most well known example is the building of an embankment and the assessment of potential circular failure of the soil under the embankment in response to the loading. The investigation of shear strength along the failure zone can be shared into three states: active (A), passive (P) and intermediary (D) as detailed in figure 22. The stress-strain condition in this intermediary zone is closely reproduced by the direct simple shear device whereas triaxial tests in compression and extension are used to model the conditions in the active and passive zones respectively. Furthermore, the results obtained from the direct simple shear test are considered to provide a conservative average of the shear strength of the soil for the total stability calculation.

A second example is the contribution of the direct simple shear test in understanding the failure mechanism of peat slopes and peat dykes which tend to fail along an horizontal plane (Pigott et al. 1992, Van Baars 2005, Boylan et al. 2008). More details are given in 1.7.

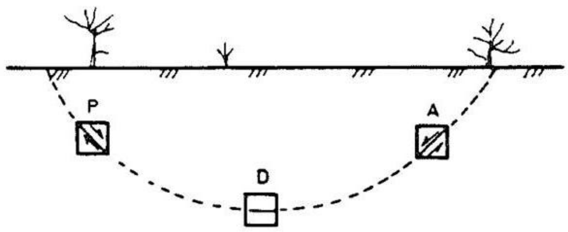

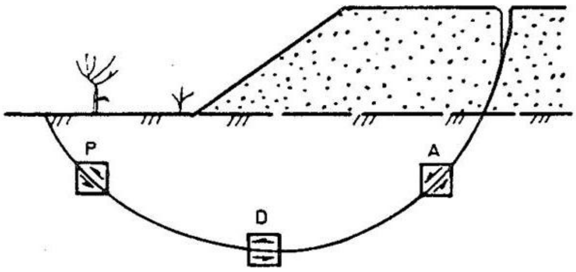

Figure 22: Shear stresses on a possible slip surface before and after the placing of a fill (Aas 1980)

The direct simple shear test can also be adapted in analyses of the stability of dykes under the loads imposed by fluid or hydraulic fill. The stability of the dyke therefore depends on the amount of shear stress τ_{xy} which can be surimposed on the initial stresses without causing failure of the soft soil as illustrated in figure 23. Since the Direct Simple Shear test provide conditions close to this case, the likelihood of horizontal sliding of the dyke can therefore be evaluated by comparing the maximum value of τ_{xy} measured in sample with the value imposed by the hydraulic field in situ.

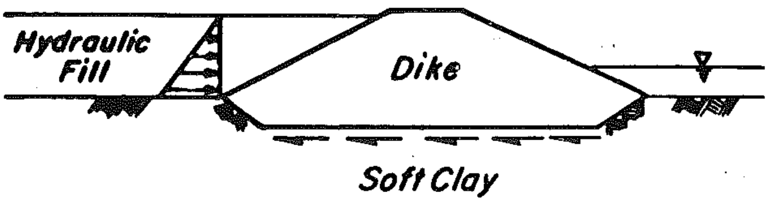

Figure 23: Loading of a dyke by imposing a hydraulic fill (Duncan and Dunlop 1969)

The behaviour of soils adjacent to a pile can be closely reproduced by simple shear since it allows the rotation of principal stresses. Cyclic Direct Simple Shear tests are also extensively used to determine the likelihood of liquefaction of sand during earthquakes or to simulate the soil behaviour beneath the foundation of an offshore platform.

1.7 INTEREST FOR PEAT TESTING AT LOW NORMAL STRESS

A renewed interest on direct simple shear has appeared during the last years especially for peat testing. This interest is due partially to the occurrence of peat slope failure (Boylan et al. 2008) and peat dyke failure (Pigott et al 1992, Van Baars 2005) but also to the necessity to build on peaty soils in various countries as Ireland, Canada or the Netherlands. For instance, recent developments of wind farms on peat slopes have been considered (Boylan et al. 2008).

Because of its anisotropy and its fibrosity, peat cannot be tested with all devices testing shear strength. In situ vane tests are limited since the interaction of the fibres and the vane creates uncertainties on the actual failure surface and compression of the peat ahead of the vane (Helenund 1967, Landva 1980). Peat tested in triaxial apparatus shows high values of friction angle due to the fibre reinforcing effect (Landva 1983). Direct shear testing is not recommended either, owing to the uncertain stress distribution and mode of deformation. Ring shear testing is only useful to eliminate the effect of fibres and study peat strength at large strain. The use of direct simple shear tests is routinely used (Farrell and Hebib 1998, Carlsten 2000) since its strong anisotropic structure gives it a disposition towards horizontal sliding. The Direct Simple Shear apparatus appears to be the most appropriate apparatus for obtaining undrained strength parameters for stability assessments.

However testing peat with simple shear apparatus properly remains a challenge for geotechnical engineers for various reasons.

First, to be representative of the in situ conditions, peat must be tested with very low vertical stresses. Indeed, if we consider that the peat density is very close to that of water, the apparent vertical effective stress is also very low (close to zero for an horizon only constituted of peat). Shearing the sample in such conditions becomes more complicated because slippage at the interface between the top (or bottom) cap and the specimen is more likely to occur and is further facilitated by the high water content of the specimen. As explained earlier, slippage increases stress inhomogeneities in the soil specimen and should be prevented.

Then, testing peat in simple shear demands much more accuracy than required with other (stiffer) soils. Since the peat strength measured at low vertical stress is often less than 10kPa, corrections related to apparatus compliance can form a large percentage of the measured strength. Then, the device needs to have the lowest friction possible in its carriage and measurements gauges and also the lowest resistance possible of the boundary enclosing the sample (membrane, rings).

Finally, Den Haan and Kruse (2007) pointed out the importance to enlarge the usual size of samples to take into account the influence of fibres.

The recent work of Boylan and Long (2009) has resulted in the development of the first direct simple shear apparatus adapted for peat testing. The device can apply vertical stresses as low as 3kPa (lower than 3 kPa is not feasible due to difficulties to maintain grip on the specimen during shearing) to a sample of square cross section of 70mm and with a varying height. A visual inspection, by mean of Particle Image Velocimetry of the specimen is possible during shearing to check if slippage occurs and to assess the uniformity of shear strain in the specimen. The horizontal compliance of the apparatus is between 1.5kPa and 2.25kPa whereas the sidewall friction is evaluated at about 0.5kPa.

2. DIRECT SIMPLE SHEAR TESTING OF PEAT WITH THE GEONOR DEVICE

The testing of peat in Direct Simple Shear device is detailed in this chapter. A description of peat parameters is given as well as the results obtained from a classical Direct Simple Shear device on a large number of tests. The final part of the chapter focuses on the comparison of two different boundary conditions used for cylindrical samples.

2.1 PRESENTATION

Deltares has been using the reinforced membrane (Bjerrum and Landva 1966) for all soils in direct simple shear tests. Recently, the system used initially by Kjellman (1951) with rings enclosing an unreinforced membrane has been gaining popularity and presents an interesting alternative to the NGI reinforced membrane. Indeed, it is much less fragile to manipulation and also much cheaper. It also presents a number of inconveniences as it will be detailed later. The two boundaries are presented in figures 24 and 25.

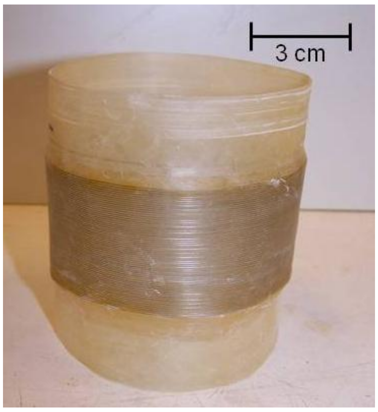

Figure 24: Reinforced membrane

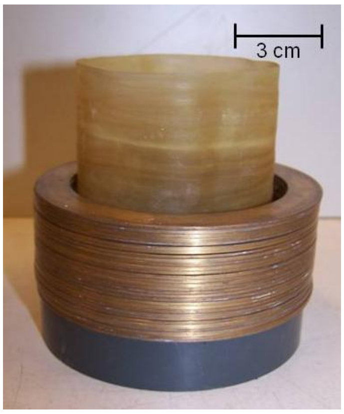

Figure 25: Unreinforced membrane enclosed by a stack of rings

The purpose of this chapter is to compare the effect of the two boundary conditions on the classical measurements obtained from Direct Simple Shear testing and on parameters determined from such a test. The limitations encountered by peat testing in classical simple shear devices are detailed. First, a description of the peat tested is given before presenting the characteristics of the Direct Simple Shear apparatus used and the results from compliance tests of the device. Finally, the results from the Direct Simple Shear tests on peat are presented and discussed.

2.2 DESCRIPTION OF THE PEAT TESTED

The most common characteristics of peat are detailed here. Den Haan and Kruse (2007) suggested for instance that simple description can rely on essential data such as bulk density, water content, main botanical type and degree of humification. Other characteristics like ignition loss, specific gravity, void ratio or degree of saturation are also presented.

2-1-1 Location, depth, in situ conditions

The samples tested come from a large block extracted from the IJKDijk project location (north of the Netherlands close to the German border). This project focused on large scale experiment to test dyke stability and to develop sensor network technologies. Large cubic blocks of 50cm large have been extracted with PVC sampler pushed inside the soil with a shovel. Some disturbance might have occurred due to the imperfect sampling method. No cracks or disturbance have been observed in the peat block.

The in situ conditions as evaluated from close samples located close to those considered are presented in the table 1.

Table 1 : In situ conditions of the peat samples

Depth (m) NAP	-3.261
Vertical stress (kPa)	23.4
Effective vertical stress (kPa)	12.1
OCR	1.93
POP (kPa)	11.30

2.2.1 CLASSIFICATION

As peat exists in different degrees of decomposition, several classifications can be considered. The term decomposition/humification defines the breakdown of the structure of plant material and its transformation into amorphous material. The most widely used method of Von Post (1922) focuses on the degree of humification of the sample (H1 no decomposition to H10 very decomposed peat) and on the botanical type of the constituents. This parameter can be obtained by squeezing the material by hand and evaluating the amount of peat which is able to extrude between fingers. This classification has been extended later with other characteristics of the peat such as water content, pH etc… A table describing the classification in more detail is given in appendix A. The present peat has been described roughly as a wood and sedge peat. Its degree of humification varies between H5 to H6.

For geotechnical purpose, Landva et al (1983) defined peat as a soil with an ash content lower than 20%. The Dutch classification also focus on this criteria (NEN-5104 1989).

The French geotechnical classification is based on the Von Post index for highly organic soils (OC>30%) but simplify it to three main categories (Magnan 1994). The present peat is a highly organic soil semi fibrous (tO_sf).

2.2.2 FIBRE CONTENT AND WOOD CONTENT

The fibre content can be determined in two ways. By removing all the fine material from the peat by sieving and by weighing the amount of fibres. Or by comparing the sample with a visual chart (TAW, 1996). A distinction is made between fibre with a diameter larger than 1mm (coarse) and smaller than 1mm (fine). The samples tested have a fibre content of about 15% of fine fibres and 10% of coarse fibres. The fibre content is believed to have a large influence on the peat behaviour. For instance, it is expected to have a reinforcing effect when the fibres are stretched (Landva and La Rochelle 1983). The influence of fibres remains difficult to quantify.

An significant amount of wood remnants is observed in the samples tested. Its proportion is determined by visual assessment. The wood percentage is detailed in appendix B for each sample, but no further investigation of the influence of these parameters has been performed.

Two pictures of samples during preparation are illustrated in figure 26 and figure 27. The sample a15 shows the presence of large wood remains which are cut during the sample preparation. The sample a17 presents a better homogeneity with thin fibres and remnants of leaves. The necessity to test peat at larger scale becomes more understandable when considering these pictures.

Figure 26: Sample a15 surmonted by the hand cutting ring

Figure 27: Sample a17 after cutting with the NGI cutting ring

2.2.3 WATER CONTENT

The water content is measured before (initial) and after the test (final). The water content is determined by drying the sample at an oven temperature of 105°C during 24 hours. It gives a simple and reliable characterisation of the peat. The water content for peat is very dependent on the different plant remains present in the sample and their ability to retain water. The water content is considered to be held in three states (1) free water in large cavities, (2) capillary water in narrow cavities within plant matter and (3) water adsorbed physically or chemically (MacFarlane and Radforth 1964). Water in states (1) and (2) is removed by consolidation. The initial water content of the peat tested is between 508% and 635%. According to Hobbs (1986), such a range of water content can be observed for a degree of humification varying between H3 to H7 in the Von Post classification. It corresponds to the water content of transition peat (between bog peat and fen peat).

The reduction of water content due to consolidation is about 5% for tests performed at a normal stress of 10kPa and 45% for tests performed at a normal stress of 120kPa (the reduction is expressed as a percentage of the initial water content).

2.2.4 BULK DENSITY

The bulk density is measured by weighing the sample and knowing its volume. The bulk density of the peat tested is between 0.89 t/m3 and 1.05 t/m3. A large majority of the sample have a bulk density lower than 1 and so would be buoyant under water. This is supposed to be due to the under-saturation of peat and to the presence of gas in the samples. The under-saturation may develop after sampling if large cavities and coarse fibres are present.

The relative small variation of both the water content and bulk density do not make possible any correlation between the two parameters. The values measured are close to the data gathered by den Haan and Kruse (2007) at HSL Rijpwetering and Polder Zegveld as illustrated in figure 28. the data corresponding to the peat tested are enclosed in the red rectangle.

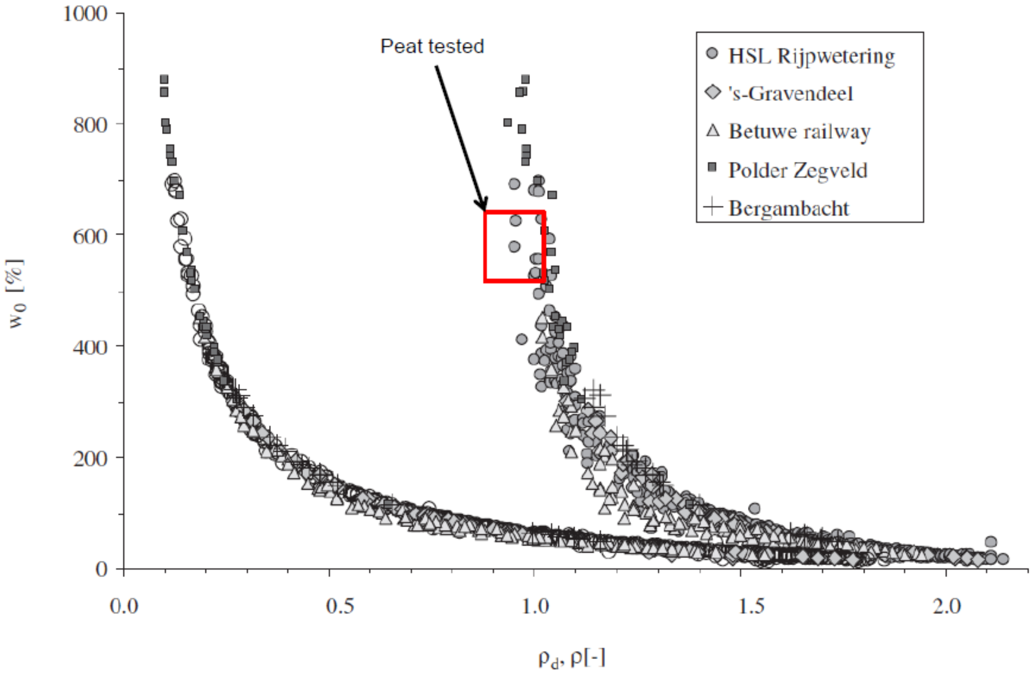

Figure 28: Correlation of wet and dry density of various dutch peat (den Haan and Kruse 2007)

2.2.5 IGNITION LOSS - ORGANIC CONTENT

An ignition loss test is performed on a sample which has been previously dried and consists in combusting the sample at 500°C during 4 hours.

The organic content is closely correlated to the loss on ignition. The correction proposed by Skempton et al. (1970) is presented in equation (5).

$$OC = 100 - 1.04 * (100 - N) \qquad (5)$$

This formula is only valid for more than 10% organic matter.

The results obtained are an average organic content of 73% (min=61%, max=85%).

2.2.6 SPECIFIC GRAVITY

The specific gravity of organic soils is largely influenced by the organic content. Skempton et al. (1970) produced a correlation between specific gravity of organic soils and ignition loss, assuming a specific gravity of 1.4 for organic fraction (cellulose) and of 2.7 for inorganic fraction. This correlation is expressed in equation (6).

$$\frac{1}{G_s} = \frac{1-1.04*(1-N)}{1.4} + \frac{1.04*(1-N)}{2.7} \qquad (6)$$

The specific gravity is calculated from this correlation. The average specific gravity for the 21 samples is 1.60 (min 1.51; max 1.70).

2.2.7 VOID RATIO AND DEGREE OF SATURATION

The void ratio and degree of saturation are determined from the parameters determined earlier, according to the equations (7) and (8).

$$e = G_s.(1 + w)\frac{\rho_w}{\rho} - 1 \qquad (7)$$

$$S_r = \frac{w * G_s}{e} \qquad (8)$$

The void ratio is particularly large for peat compared to other types of soils (average of 10.45).

The results show an average degree of saturation of 0.87 (min 0.80, max 0.97). The peat is not fully saturated. These data correspond to transition peat as described by Hobbs (1986). The reed, sedge and wood peats formed in the transition stage between submerged formation in nutrient-rich waters, and acid bog peats formed high above the groundwater table.The under saturation of peat has been also observed by den Haan and Kruse (2007) who observed gas bubbles trapped in the structure of peat. Some other reasons can be responsible of the undersaturation measured such as the migration of water after sampling from the top to the bottom of the block due to gravity forces.

2.2.8 SUMMARY OF THE PEAT CHARACTERISTICS

All the characteristics of the peat tested are summarized in the table 2. 21 samples have been tested in total. The standard deviation is especially large for the wood content.

Table 2: Summary of the index properties of the peat tested

	Average	Min	Max	Standard deviation
Bulk density (t/m3)	0.95	0.89	1.05	0.05
Water content (%)	567	509	635	36
Loss on ignition (%)	74	62	86	6
Organic content (%) (Skempton 1970)	73	61	85	6
Wood content (%) (Visual assessment)	22	5	50	14
Specific gravity (t/m3) (Skempton 1970)	1.60	1.51	1.70	0.05
Void ratio	10.45	9.08	12.07	0.68
Degree of saturation	0.87	0.80	0.97	0.04

The plasticity limits are not determined for the peat tested. Difficulties are encountered with classical methods due to the presence of fibres.

2.3 TEST PROCEDURE

2.3.1 CUTTING OF THE BLOCK

From the initial block, one slice of 4 cm thickness is cut with a cutting wire from the top. Then the top slice is cut in nine cubic samples of 8cm large. Each sample is then used to perform a direct simple shear test. In this way, the sample disturbance is expected to be small.

2.3.2 SAMPLE PREPARATION

The sample preparation is performed in accordance to NGI recommendations (Bjerrum and Landva 1966) with the reinforced membrane. An illustration of the preparation procedure is given in figure 29. The sample is placed on a steel plate covering the pedestal and is cut to the proper diameter with a cutting ring sliding on two vertical tubes (a and b). The bottom cap is screwed on the cutting ring (c) from above and then the cutting ring is removed from the guides with the sample still in it. The reinforced membrane is placed around the pedestal with a vacuum cylinder to slightly enlarge the diameter of the reinforced zone of the membrane (d). A talc powder is spread on the inside of the membrane to reduce the soil/membrane friction at the sides. Then the bottom cap is inverted and fixed on the pedestal and excess height of the sample is removed with a cutting wire (e). The top cap is applied with the help of a plunger (while giving a particular attention to the shearing direction) (f). Finally the cutting ring is removed and the membrane is put around the sample by cutting off the vacuum (g and h). The sample is now ready to be placed in the Direct Simple Shear device.

The second boundary used is an unreinforced membrane surrounding the specimen and enclosed in a stack of rings as detailed earlier. A similar preparation is performed for the stack of rings. The rings are placed one by one around the sample and rely on a PVC cylindrical pedestal. The height of rings used has to be larger than the height of the unconsolidated sample. A care is needed to avoid that the bottom of the vertical loading frame come in contact with the rings in case of large settlements. Otherwise, a vertical load is applied on the rings and the measured vertical load is highly over-estimated.

After preparation, the sample dimensions are 63mm diameter and 20mm height (30mm for tests at σ_V=120kPa to accommodate the larger compression).

Two rubber O'rings are used to clamp the membrane to the top and bottom cap to ensure constant volume during shearing. In the case of the stack of rings, they are placed during the sample preparation. In the case of the reinforced membrane, they are placed at the end of the consolidation phase. In this way, the deformation of the reinforced membrane due to large settlements is reduced and the membrane can be stretched before applying the O'rings in case it has folded.

2.3.1 THE GEONOR DEVICE

The Geonor direct simple shear apparatus was developed by the Norwegian Geotechnical Institute (Bjerrum and Landva 1966). The device used in this study is illustrated in figure 30. It presents many similarities with the original one.

The sample is placed on the bottom plate of the loading frame. The top cap is clamped to the specimen carriage, which guide the travel of the top cap and prevents it from tilting. The vertical load is applied with a lever arm which is connected to the vertical motor. The desired vertical load is obtained by entering the desired value in the amplifier (which is connected to the vertical motor). The vertical load is transferred to the top cap through the roller bearings. This bearing is restrained in horizontal direction with pins during the phase of consolidation. Once the pins are removed the bearing is able to slide horizontally during shearing. The horizontal load is applied to the top cap of the sample by a fork linked to the horizontal motor.

The vertical and horizontal loads are measured by load cells. The horizontal and vertical load cells have a similar capacity of 6.4MPa (20kN). The maximum absolute error is of 3Pa. The horizontal and vertical displacement are measured by two linear variable differential transformers (LVDT). The maximum absolute error is 0.032 mm and 0.074 mm respectively for the horizontal and vertical transformer.

Figure 29: Sample preparation procedure with the reinforced membrane for the Geonor device (Bjerrum and Landva 1966)

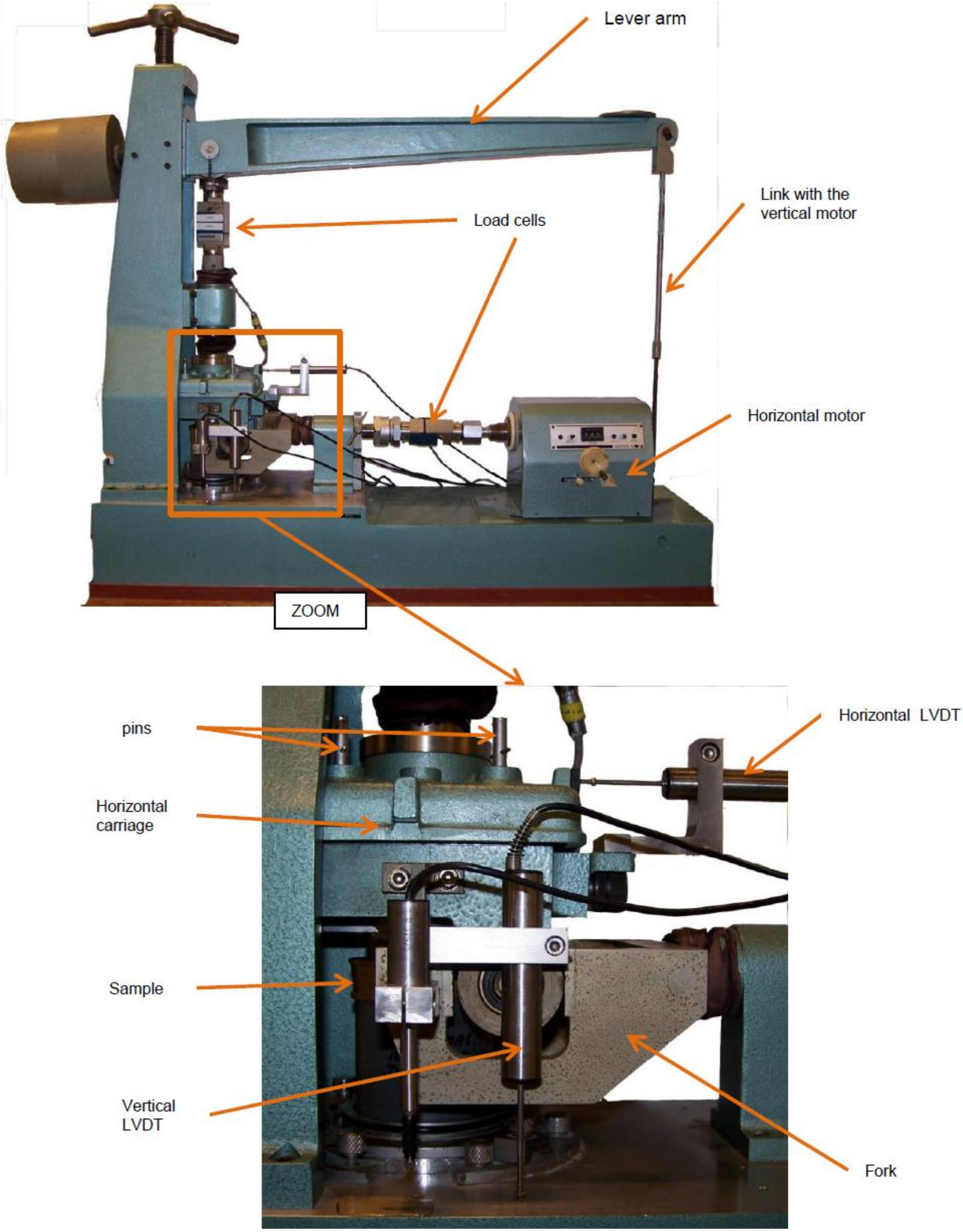

Figure 30: The Geonor device (top) and details of the sample surrounding (bottom)

In case of constant volume tests, the volume of the sample is kept constant by maintaining a constant height during the shearing phase. For this, two methods can be used. The first one is to mechanically lock the height at the vertical motor level and to measure the change in vertical load during shearing.

The second one consists in coordinating the vertical load and the vertical displacement with a feedback system (DeGroot et al. 1991). The vertical load is adapted to keep the vertical displacement constant equal to zero. The first solution has been applied in this study and gave satisfactory results. The change in height observed during shearing is always less than 0.05mm. A single test performed with active control with a vertical stress of 120kPa showed a larger variation.

2.3.2 TESTING PROGRAM

Each test has been repeated twice for both the reinforced membrane and the stack of rings associated with an unreinforced membrane at each vertical stress. The detail of the testing program is given in table 3. Tests have been performed at four different vertical stresses: 10kPa, 30kPa, 60kPa and 120kPa. The sample numbering (from a3 to a24) has no relation with the vertical stress applied. The samples are consolidated in one step of 4 hours for a final vertical stress of 10kPa and 30kPa. Two steps of 4 hours and an extra step of 14 hours are applied respectively for tests at a final vertical stress of 60kPa and 120kPa. The initial height has been adapted in order to obtain a similar height of the sample at the end of consolidation for each consolidation stress. The initial height used is 20mm for vertical stress between 10 and 60kPa and 30mm for 120kPa.

The shearing is applied with a speed of 1mm/hour, which represents between 5 and 8 percent of the height per hour. This shearing speed is supposed to be small enough to prevent generation of excess pore pressure internally by allowing time for equalisation.

Table 3: Details of the testing program

Sample numbers	**Vertical stress (kPa)**	**Initial height (mm)**	**Total time of consolidation (h)**	**Time of consolidation per step (h)**		
a8-a9-a10-a11	10	20	4	4	-	-
a3-a5-a6-a7	30	20	4	4	-	-
a13-a15-a16-a17	60	20	8	4 (30kPa)	4	-
a21-a22-a23-a24	120	30	22	4 (30kPa)	4 (60kPa)	14

The sample are all sheared in a chosen direction (parallel to the large fibre/wood orientation) determined by placing pins during the sample cutting from the large peat block.

2.4 COMPLIANCE TESTS

2.4.1 VERTICAL COMPLIANCE

Vertical compliance tests have been performed to assess the vertical deformation of the apparatus in function of the load applied. The compliance test is performed by placing a steel specimen between the top and bottom cap. The steel specimen is assumed not to deform during the test.

The load unload loop is fitted by a single curve of equation (9).

$$y = 0{,}0263.\,ln(3{,}147.\,x) + 0{,}0369 \qquad (9)$$

y is the vertical displacement
x is the vertical load in kPa

For instance, a vertical load of 120kPa will lead to a vertical deformation of 0.19mm. This correction is applied for all the tests presented.

2.4.2 HORIZONTAL COMPLIANCE TEST PROCEDURE

Calibration tests have been performed to know the resistance of the carriage, bearing and reinforced membrane or unreinforced membrane associated with the stack of rings. Since the point of this study is to compare the effect of the two boundary conditions, the calibration of each boundary condition is of great significance and might largely influence the results obtained from the tests.

The horizontal load due to the carriage, bearings and displacement transducers of the Geonor device has been presented in an ancient report (den Haan 1987). They have been obtained by applying the shearing by the horizontal motor without any sample inside the device. The results show a horizontal load equivalent to about 0.4kPa for the carriage and bearing and 0.7kPa if the displacement transducers are taken into account.

The additional horizontal load due to the resistance of the boundaries conditions has been investigated by filling the membrane with water and shearing the sample assuming that water has no shear resistance. Two heights of sample have been tested (13mm for higher pressures and 20mm for lower pressures) since the height of the peat samples at the end of consolidation vary in function of the vertical load applied. The water pressure has been varied between 3kPa and 40kPa, considering that the water pressure have an influence on the resistance of the membrane. Higher water pressure is difficult to obtain considering the difficulty of avoiding leakage during shearing. The sample is filled in from two holes in the bottom platen until the major part of the air has left the sample. An extra pressure is applied by hand at the top of the sample to make any remaining air leave the system. Finally, the top tubes are clamped before starting the shearing. For low water pressure (up to 10kPa), the pressure has been applied with a constant water head so the tubes remains open. For high water pressure, the pressure is applied from the vertical motor (as for a regular test) and the sample is prepared underwater in order to avoid the presence of air bubbles in the system. The entry and exit usually used to fill in the sample were closed by a joint and a screw.

The water pressure is measured by the vertical load transducer. A special attention has been given to the eventual leakage which could occur at the O'ring level or connection with the tubes, since the loss of one single drop of water can cause the complete loss of pressure (especially at the highest pressures).

The calibration tests are performed in constant volume conditions (by maintaining the height constant mechanically). The maximum change in height measured is 0.04mm (0.3% of the height for a 13mm sample).

The shearing speed for calibration tests is 2mm/h, which is the double of the shearing speed used for testing peat samples. The difference of resistance due to the shearing speed is assumed to be negligible within the range of horizontal displacement considered.

2.4.3 HORIZONTAL COMPLIANCE TEST RESULTS

The results from the horizontal test compliance are shown in figure 35. The height of sample and the vertical stress is given in the name of each curve. The horizontal shear stress (τ_{xy}) is plotted against the horizontal displacement. The results from calibration tests show a linear increase of the membrane resistance with the horizontal displacement for both boundaries, due to the stretching of the membrane during shearing.

The reinforced membrane resistance decreases as the water pressure increases. A clear difference is observed between a water pressure of 3kPa and 10kPa for 20mm height samples. This reduction of resistance is also observed with shorter specimens and higher water pressures. The correction curve used in Deltares until now is plotted as a comparison. It is very close to the curve obtained with a water pressure of 3kPa and a height of 20mm.

For 20mm height samples, the results obtained from the stack of rings show a very light variation with water pressures varying from 3kPa to 10kPa. The three curves are assumed to be close enough to be approximated by a single linear curve. For samples of lower height with higher water pressure, the resistance variation is opposite to the one observed for the reinforced membrane.

These unexpected results are supposed to be due to a limitation of the stack of rings. A swelling of the membrane appears between the top ring and the top O'ring due to the increase of water pressure in the specimen as illustrated in figure 31. This swelling is applying an extra vertical load on the rings and causes an overestimation of the friction of the stack of rings. This effect is observed due to the slight difference of diameter between the rings and the top cap. This difference is anyway necessary to allow the top cap to slide between the rings during consolidation. Since this swelling is not encountered during soil testing, the results from horizontal compliance tests of the stack of rings cannot be used. An appropriate calibration is needed in order to gain more accuracy but cannot be performed in the actual configuration. The influence of the calibration results on test results is discussed in the next section.

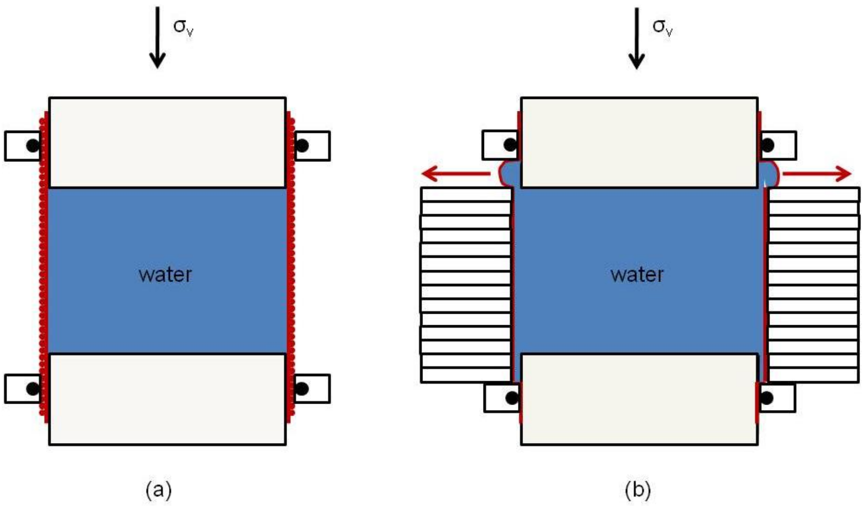

Figure 31 : Different behaviour of the reinforced membrane (a) and stack of rings (b) during calibration tests

2.4.4 EFFECT OF HORIZONTAL COMPLIANCE ON TEST RESULTS

Three correction methods to account for the boundary stiffness in test results have been investigated. These correction methods assume that the measurement of the vertical load is equal to the water pressure inside of the cell. The water pressure is then considered as equivalent to the horizontal stress applied on the membrane during a test with peat inside of the specimen. The corrections considered are detailed below:

(1) Applying a single linear correction independent on the vertical load applied for all the tests performed. Only the curve obtained at low water pressure (3kPa) is used. This correction has been used by Deltares engineers so far.

(2) Applying a linear correction dependent on the vertical load applied. The linear correction is chosen in function of the initial horizontal stress applied on the membrane (at the end of consolidation) and taken equal to $K_0.\sigma_v$. For instance, consider a test performed at a vertical stress of 60kPa and a K_0 value of 0.3. The correction curve used will be the one obtained at a

water pressure of $K_0.\sigma_v$=20kPa. With this calibration, it is supposed that the horizontal stress applied on the membrane is constant during shearing. This is certainly not likely to be the case considering the variation of K_0 in the over-consolidated region, the effect of shear stress and the rotation of the stresses occurring during simple shear. Nevertheless, this correction provides more accuracy than the correction (1).

(3) Applying a nonlinear correction dependent both on the vertical load applied and on the horizontal displacement. Since the horizontal stress applied by the soil on the membrane during shearing is varying, the horizontal load due to the membrane resistance will also vary in function of the horizontal displacement. So if the evolution of the horizontal stresses in function of the horizontal displacement is known, the correction chosen is obtained by jumping between the different linear curves of constant water pressure. Since no proper measurement of the horizontal stresses is possible in simple shear, a finite element simulation can be used.

The three methods of correction are illustrated in figure 32.

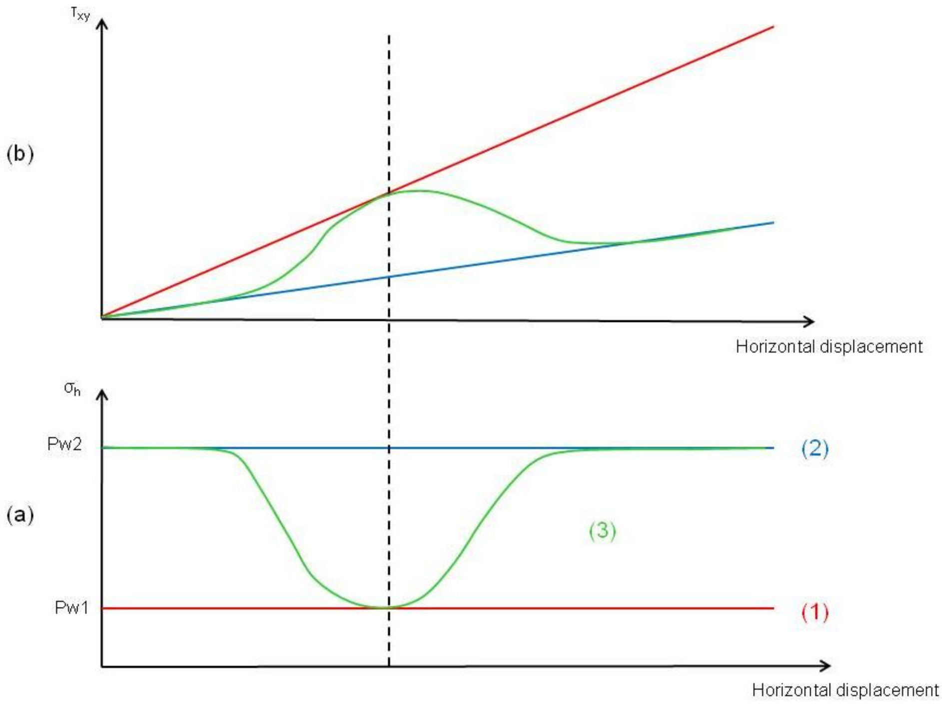

Figure 32: Three methods of calibration with the evolution of the horizontal stress (a) and corresponding evolution of shear stress of the membrane (b) versus the horizontal displacement

Considering the effect of calibration on the test results is the most effective means of evaluation. The difference between the two correction methods (1) and (2) has been investigated on two typical results obtained at normal stresses of 30kPa and 120kPa with the reinforced membrane. The effect of the correction (3) has been investigated on one set of results obtained at a vertical stress of 120kPa.

The evolution of the horizontal stress has been estimated by one finite element modelling (with Plaxis 2D v10) of the Direct Simple Shear test in the Geonor device. The details of this study are given in appendix E. The difference between the three correction methods on the stress strain curves is illustrated on the figure 33.

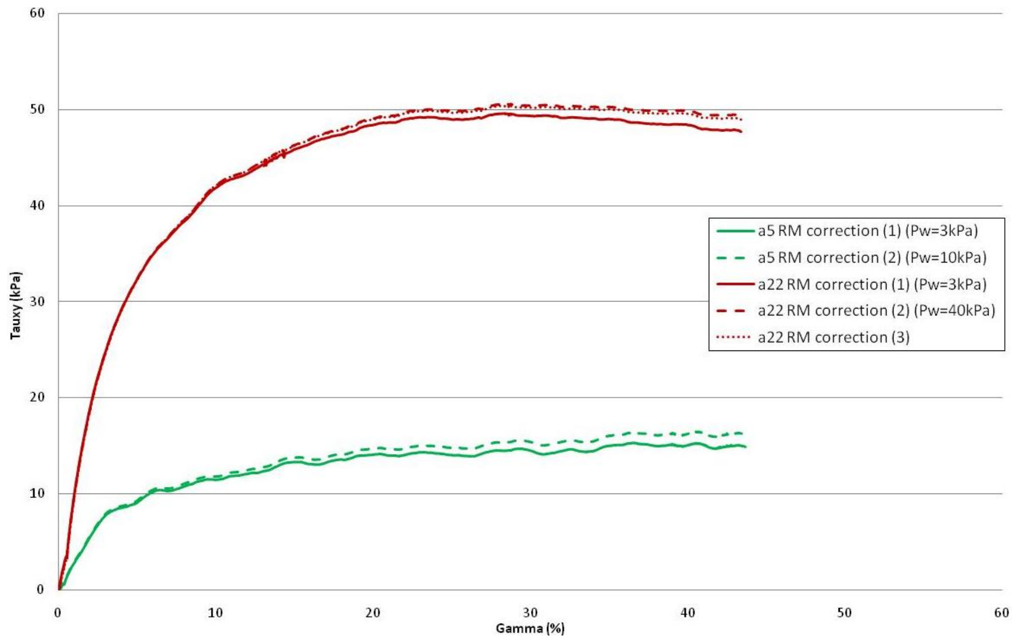

Figure 33: Influence of the correction method on the stress strain curves obtained at different normal load

The difference on the test results between the three methods is logically increasing with the horizontal displacement. Considering the horizontal shear stress at 40% shear strain, the difference between results obtained from method (1) and methods (2) and (3) is about 8% for tests at sv=30kPa and 6% for tests at sv=120kPa. Considering the determination of the cohesion and friction angle, the results from both methods are providing very close results.

Correction methods (2) and (3) are giving very similar results for a test performed at a vertical stress of 120kPa. The method (3) is tedious and of small improvement compared to the method (2). The utility of considering the method (2) instead of the method (1) is disputable and depends on the accuracy desired. Using it at low vertical stress (10kPa for instance) becomes pointless considering the small differences of membrane stiffness. One should note that the correction (1) is always providing conservative results compared to the two others.

Considering the physical limitation of calibration encountered with the stack of rings, the correction (1) is used for all the results with a water pressure of 3kPa. The difference between this correction and the second more accurate one is small (less than 8% for any normal stress) and will have only a small influence on the determination of usual Mohr Coulomb parameters.

The correction used is very similar for both boundary configurations, even if the slope of the reinforced membrane correction is lightly higher as detailed in table 4.

Table 4: Equations of the correction used in horizontal compliance

Boundary	**Correction equation**	
Reinforced membrane	$\tau_{xy} = 0.4624d + 0.5390$	(10)
Stack of rings	$\tau_{xy} = 0.4022d + 0.5142$	(11)

The effect of horizontal compliance is especially significant for test results at low vertical stress. For a normal load of 10kPa, the horizontal resistance is around 30% of the measured value of horizontal shear stress as illustrated in figure 34. The proportion of the shear stress due to the membrane stiffness in the measured value is reduced when the normal load is increased.

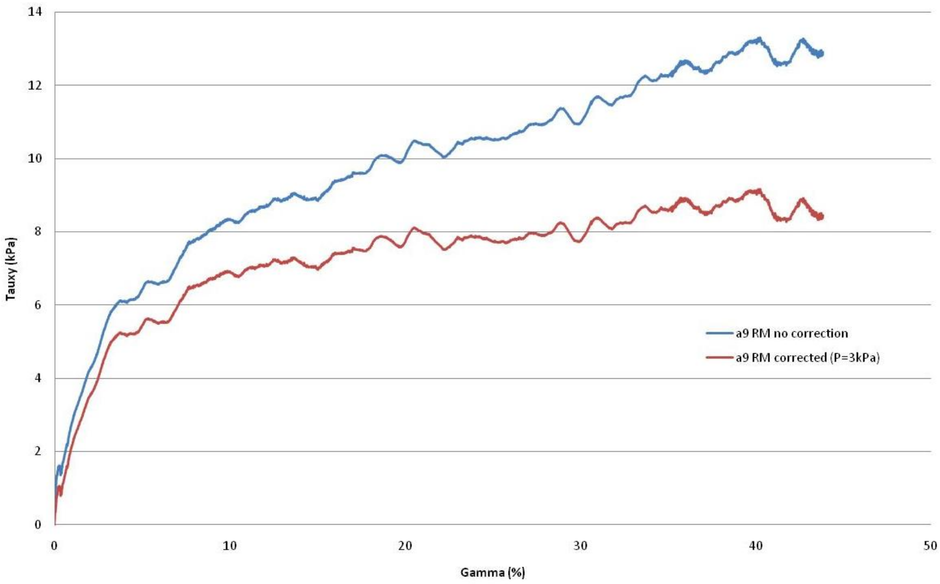

Figure 34: Importance of the correction for tests at low vertical stress

2.5 CONSOLIDATION RESULTS

The settlement due to consolidation is about 1mm for tests at a vertical stress of 10kPa and about 15mm for tests at a vertical stress of 120kPa. The determination of the consolidation parameters is not detailed here. The curves of settlement over time are detailed in appendix C.

2.6 SIMPLE SHEAR RESULTS

In this section, a comparison is presented of the effect of the boundary conditions on typical results obtained from simple shear tests such as the shear stress or the change in vertical stress. The shear modulus and the Mohr Coulomb parameters are also discussed. The comparison is done between samples tested at a similar normal stress, but it is noted that a maximum inaccuracy of 8% is observed in the vertical stress as applied by the motor. The sample numbering is detailed in table 3.

2.6.1 STRESS-STRAIN CURVES

For all the results from the direct simple shear tests, the correction (1) is applied (see 1.4.4). In figures 36 to 39 the stress-strain curves are presented through the evolution of the shear stress τ_{xy} (a) and the evolution of the vertical stress σ_v (b) in function of the shear strain (γ). The stress-strain behaviour of the peat tested does not show any strain softening even with high vertical stresses (σ_v=120kPa). In some cases, the shear stress continues increasing even after very large strain (γ>40%). This behaviour is quite different from other types of soils which usually show a clear peak in the stress-strain curve. The largest variability is observed at low normal stress, probably because the effect of the peat structure disappears at higher normal stress.

Considering the four tests performed at a vertical stress of 10kPa, the results from tests a8 and a9 show a very good correspondence whereas the results from the test a10 shows a much steeper curve at small strain and an significant strain hardening is observed for the test a11.

The evolution of the normal stress is different at a normal stress of 10kPa compared to higher normal stresses. Indeed, after an initial reduction, the normal stress increases after a certain shear strain. It always reduces at higher vertical stresses (>30kPa). This behaviour is due to the over consolidation of the specimens. An initial tendency of dilatancy occurs after a tendency of contractancy.

For the series of tests performed at a vertical stress of 30kPa, the very good agreement of the four stress-strain curves is remarkable. The results obtained at higher vertical stresses also show a good correspondence between each tests.

No difference can be ascribed to the different boundaries in the stress strain curves since all the results show a good repeatability. At a shear strain of 40%, the highest variability of the shear stress (on four sample) is 22% (at σ_v=10kPa) and the lowest is 9% (at σ_v=30kPa). This variability is most probably due to the material and it can be concluded that any difference in boundary conditions is small relative to the material variability.

2.6.2 STRESS PATH

The ratio of the shear stress over the normal stress in function of the shear strain is presented in the subfigures (c) of figures 36 to 39 while shear stress is plotted in function of the vertical stress in subfigures (d). In the latter, the shear stress and normal stress are normalized with the initial vertical stress. All curves starts from a normalized vertical stress equal to unity. It should be noted that the normalizing normal stress varies from test to test, however by an amount less than 8%. All the curves are not normalized by the same value since the vertical stress applied differs slightly for each test (of less than 8%).

A tendency is observed for a stronger reduction of the vertical stress for the reinforced membrane compared to the stack of rings. This observation is particularly obvious at a vertical stress of 30kPa. The tendency is less strong at vertical stresses of 10kPa. For higher vertical stresses (σ_v=60kPa and σ_v=120kPa), a similar evolution is observed for only one of the two curves. At σ_v=120kPa, all the curves show a remarkable correspondence. Furthermore, the reduction of normal stress is more significant at large shear strain and influences the end of the stress path.

The observation of the simple shear results at a vertical stress of 30kPa should be also linked with the consolidation curves presented in appendix C. It should be noted that the settlements of the samples tested with the reinforced membrane are more important than the one tested with a stack of rings at this specific stress level. The change in vertical stress during shearing is obviously influenced by the amount of settlement which occurs during consolidation. The reason of these large settlements has not been investigated.

In conclusion, it seems that the results obtained with a reinforced membrane show a greater reduction in the vertical stress during shearing. Consequently, the stress path obtained with the reinforced membrane tends to be always more on the left than the one obtained with the stack of rings. Considering the τ_{xy}/σ_v curves, this observation results in a stronger slope of the curves. Then the ratio τ_{xy}/σ_v is larger at large strain with the reinforced membrane.

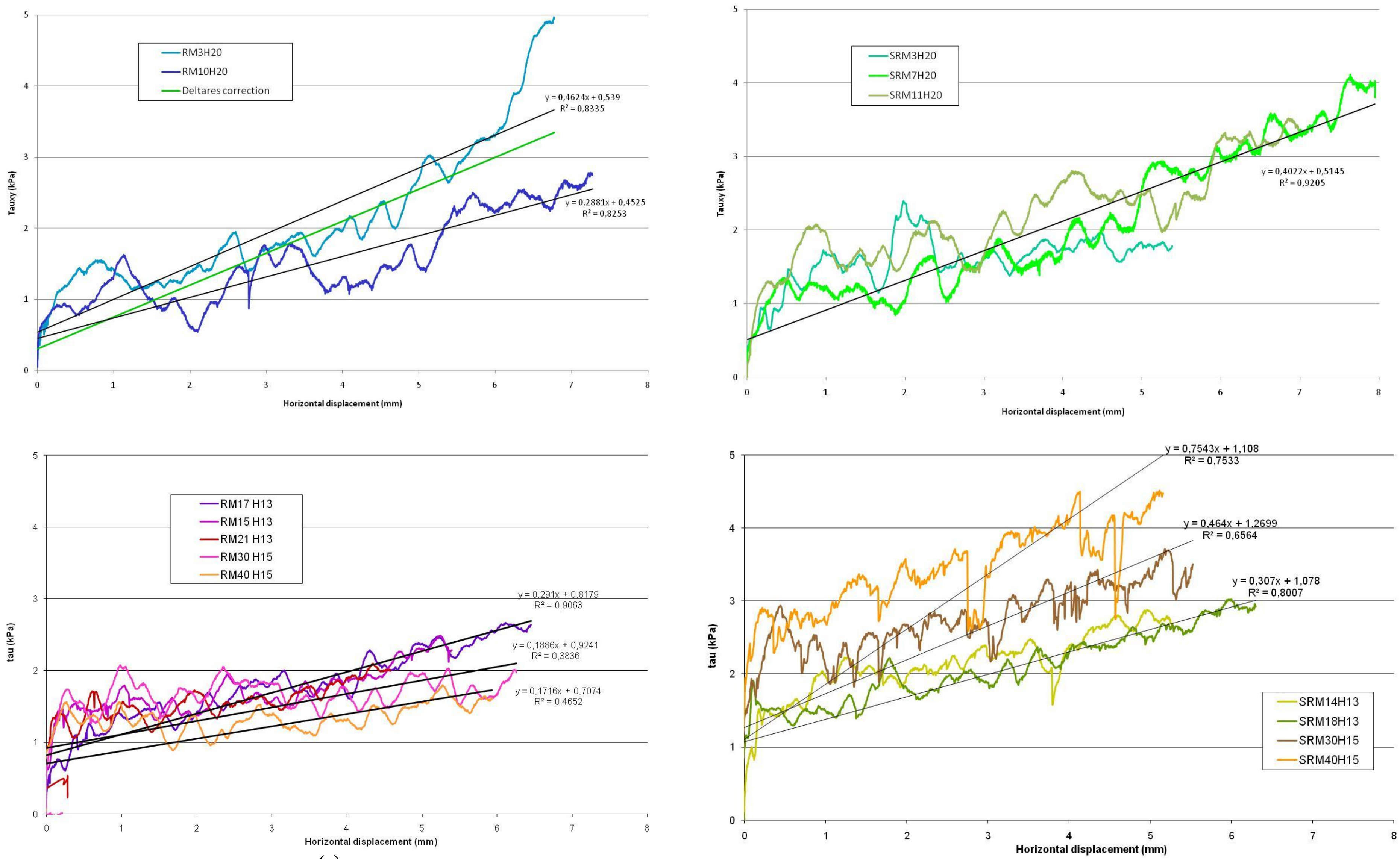

(a) (b)

Figure 35 : Results of compliance tests for the reinforced membrane (a) and stack of rings (b)

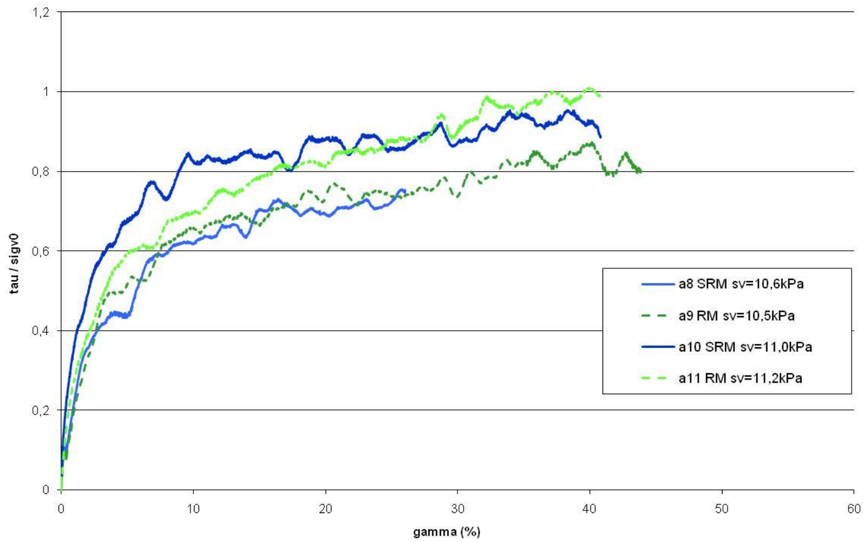

(a)

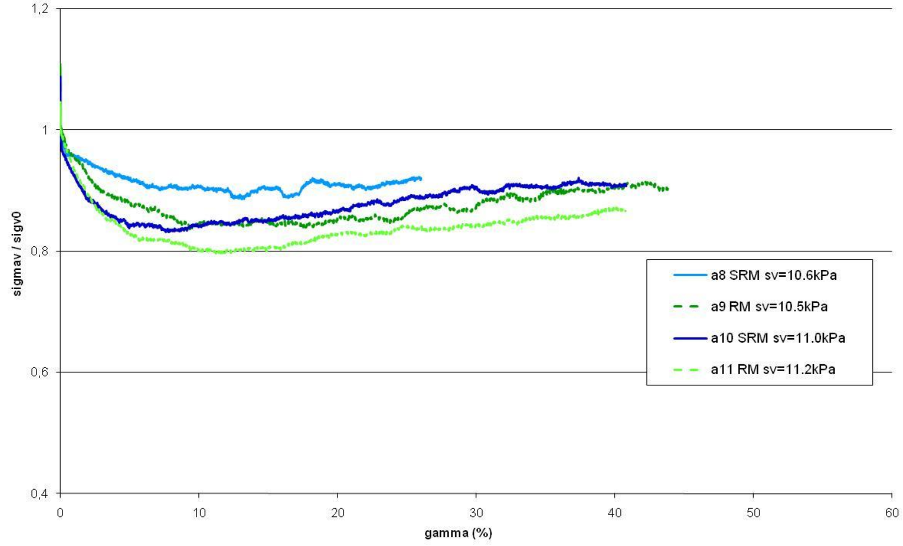

(b)

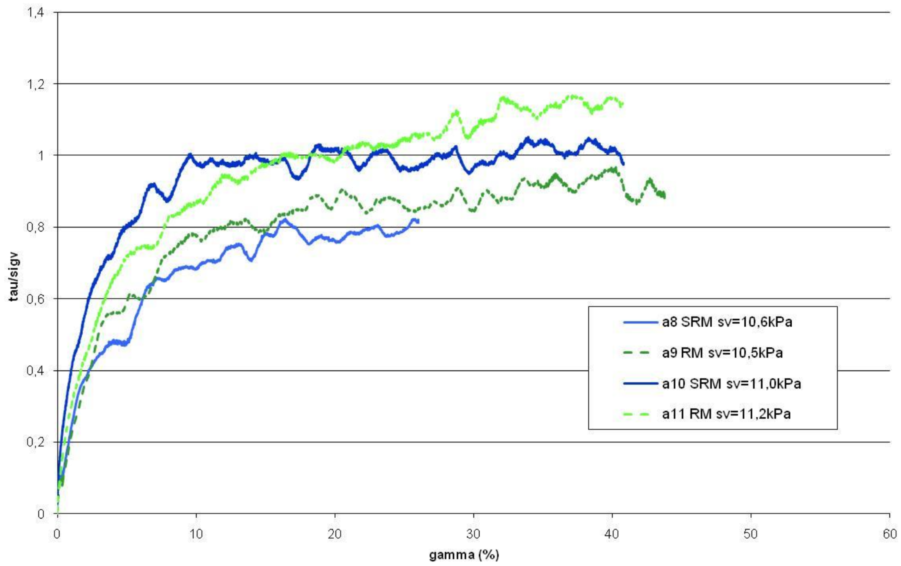

(c)

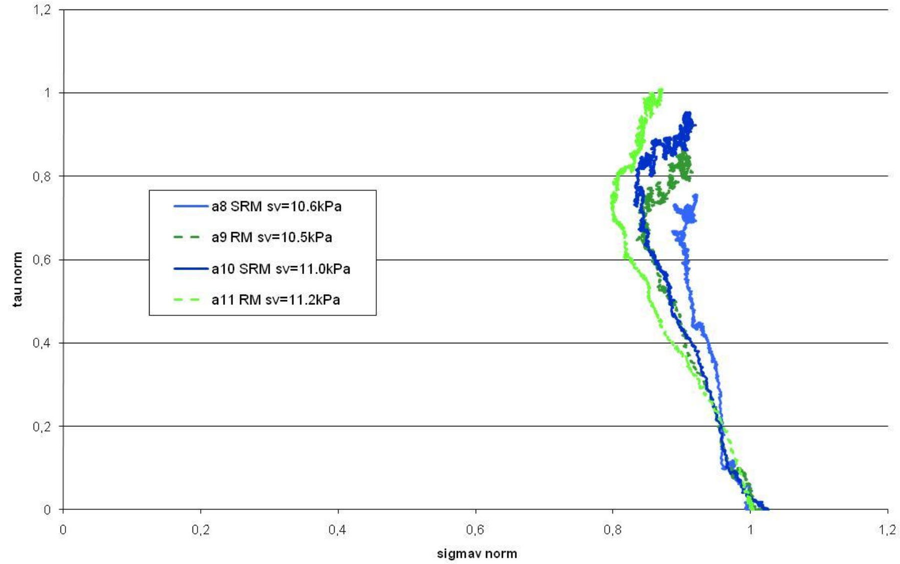

(d)

Figure 36: Test results at vertical stress of 10kPa

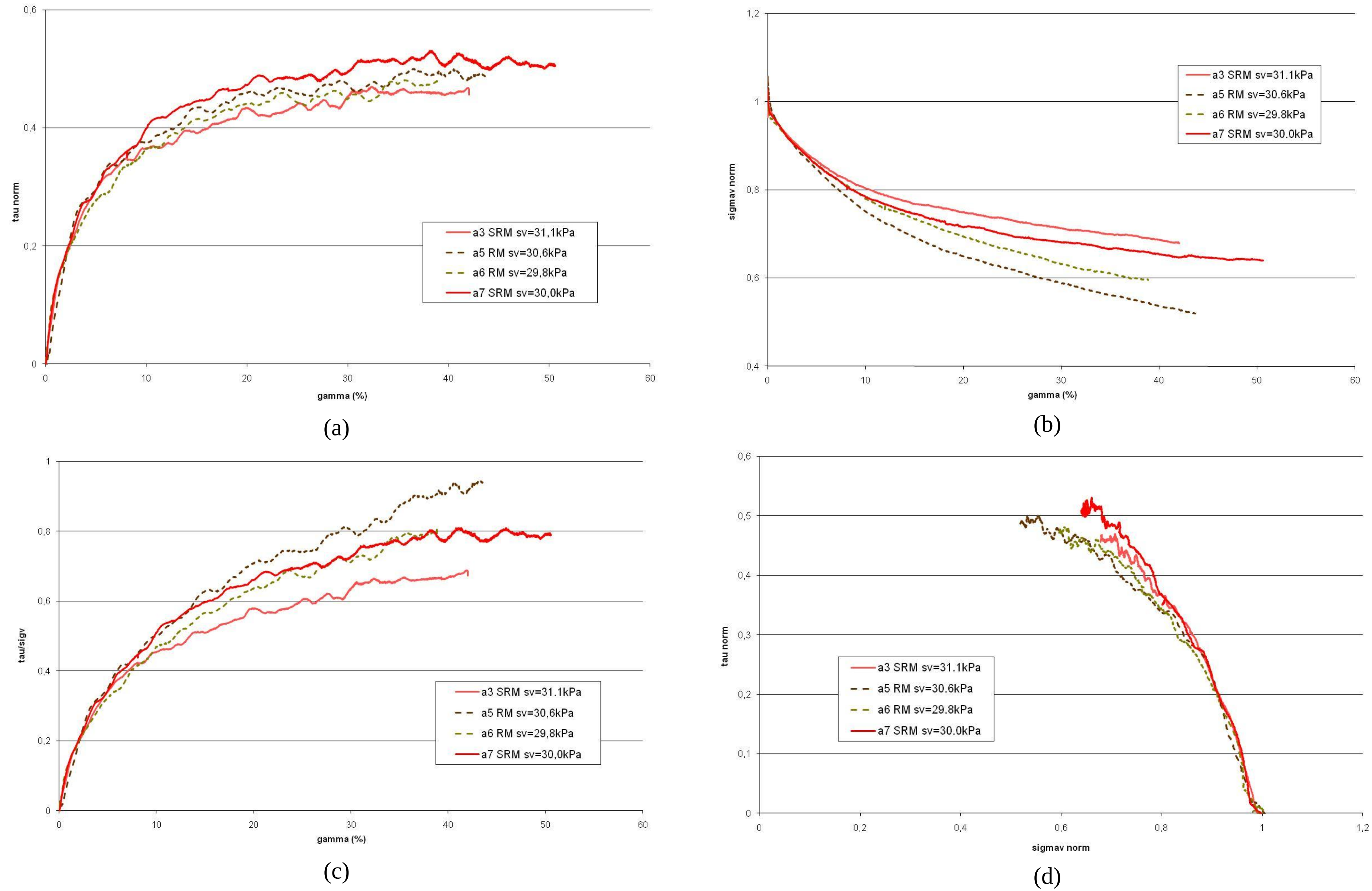

Figure 37: Test results at vertical stress of 30kPa

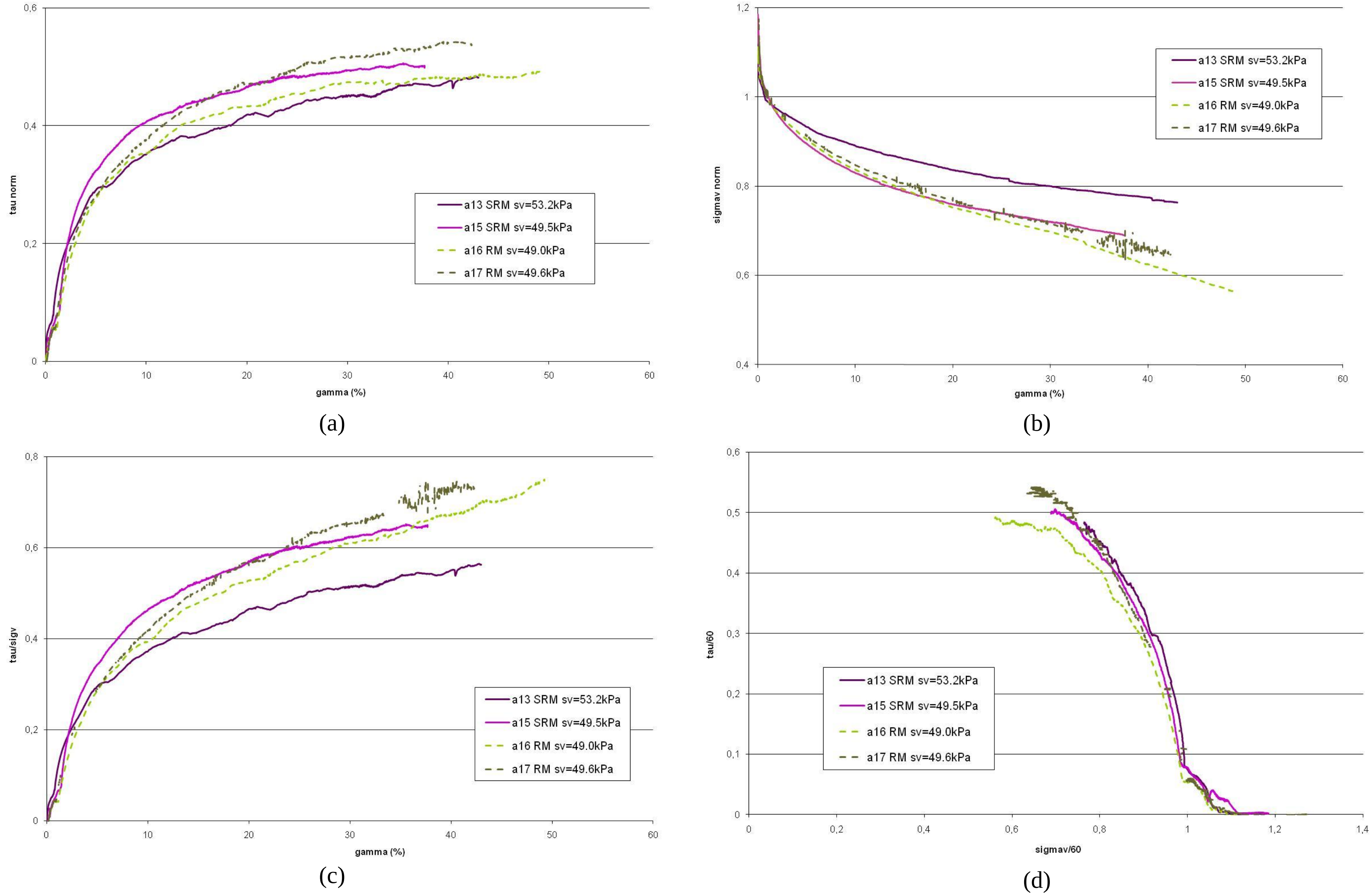

Figure 38: Test results at vertical stress of 60kPa

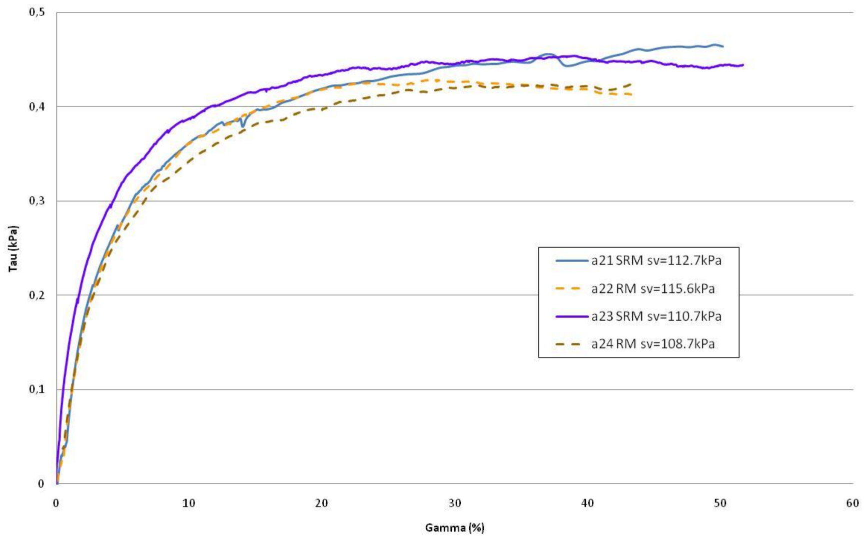

(a)

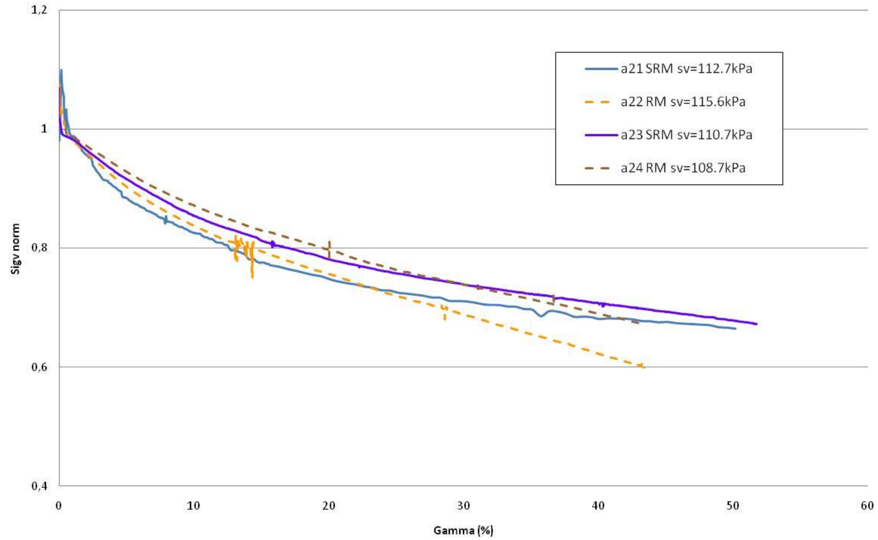

(b)

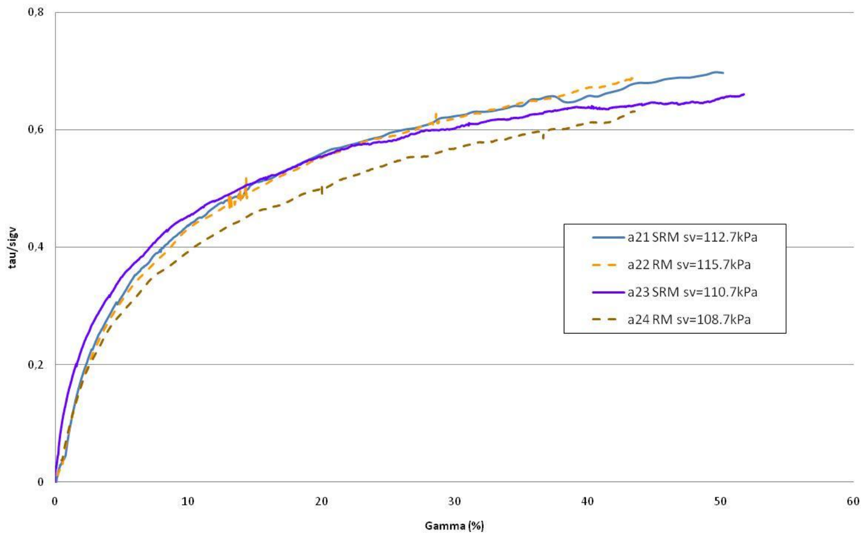

(c)

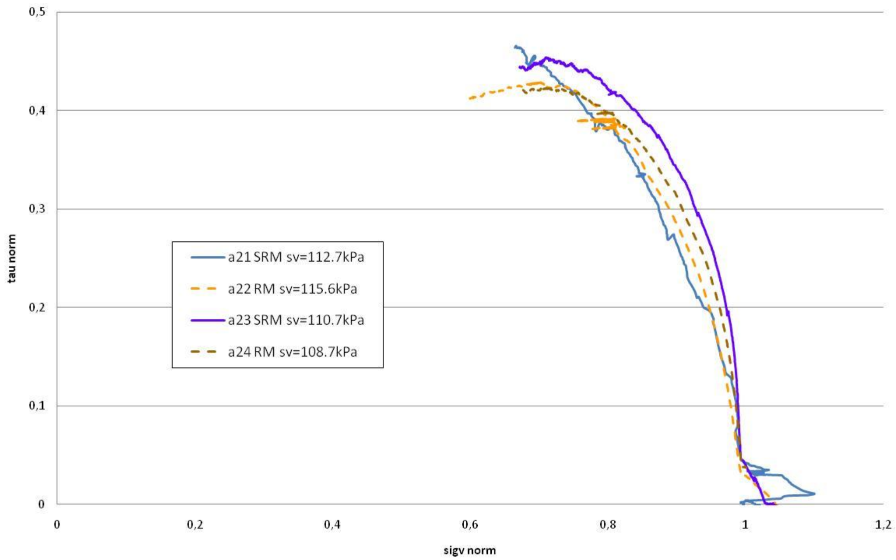

(d)

Figure 39: Test results at vertical stress of 120kPa

2.6.3 COHESION AND FRICTION ANGLE

The Mohr Coulomb drained parameters are determined using the classical method, assuming that the horizontal plane is a plane of maximum stress obliquity. For this assumption, the cohesion and friction angle are determined with the equation (1).

Table 5: Values of drained and undrained Mohr Coulomb parameters determined with the two boundaries

	Reinforced membrane	**Stack of rings**
γ=10%	φ' = 20,7 °; c' = 2,7 kPa φ_u = 18,1 °; c_u = 2,3 kPa	φ' = 21,9° ; c' = 2,8 kPa φ_u = 18,8 °; c_u = 2,7 kPa
γ=40%	φ' = 30,0°; c' = 4,5 kPa φ_u = 20,6 °; c_u = 4,5 kPa	φ' = 30,9°; c' = 2,5 kPa φ_u = 22,3 °; c_u = 3,4 kPa

The cohesion and friction angle are determined at 10% shear strain for the serviceability limit state (TAW, 1996). In lieu of a peak shear stress, the ultimate limit state is supposed to be reached at 40% shear strain and so cohesion and friction angle can be calculated at this level of shear strain. The failure criterions obtained are plotted in figure 40 and figure 41 for the drained parameters. The values of cohesion and friction angle obtained are summarized in table 5. The two boundaries are providing quite similar results at both 10% and 40% shear strain in drained and undrained conditions. The stack of rings provides an augmentation of drained friction angle of about 1° at both a shear strain of 10% and 40%. The difference between the two boundaries decreases to 0.7° at 10% shear strain and increases to 1.7° if the undrained friction angle is considered at 40% shear strain.

Other methods of interpretation (sinus or de Josselin de Jong assumption) are believed to give also quite similar results.

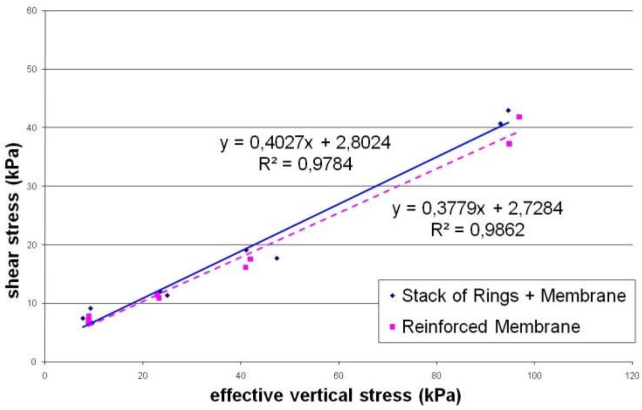

Figure 40: Mohr Coulomb failure envelope at 10% shear strain (drained parameters)

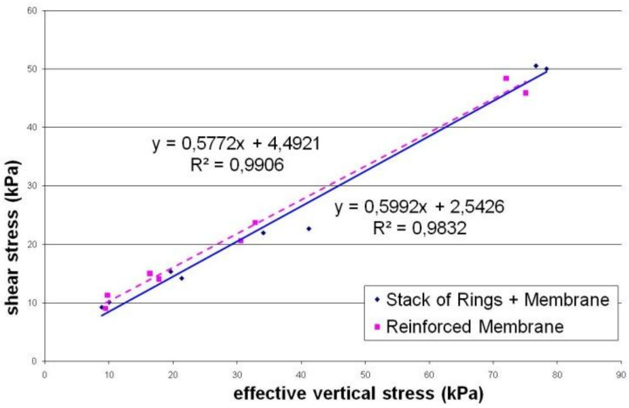

Figure 41: Mohr Coulomb failure envelope at 40% shear strain (drained parameters)

2.6.4 INITIAL SHEAR MODULUS

The method used to determine the initial shear modulus assumes an hyperbolic stress-strain relation (Kondner 1963). It is remarked that this hyperbola was already used by Professor Keverling Buisman since 1948. The principle of this method is presented in figure 42. The τ_{xy}–γ curve is approximated by the equation (12).

$$\tau_{xy} = \frac{\gamma}{(a+b.\gamma)} \qquad (12)$$

This hyperbola is transformed to a linear function between the ratio of shear strain over shear stress and the shear strain. The b parameter is the slope of this line and the a parameter is the intersection with the zero shear strain line. A correction is needed in case the line is horizontal at small strain. Some compliance is accounted for by taking the a parameter at the intercept with the horizontal line AB as illustrated in figure 42 (c).

The ultimate value of shear stresses can be obtained by taking the limit of equation (13) as gamma becomes very large.

$$\tau_{xy-ult} = lim_{\gamma\rightarrow\infty}\, \tau_{xy} = 1/b \qquad (13)$$

The initial tangent modulus is given by evaluating the value of the derivative with respect to the shear strain of equation (12) at shear strain equal zero.

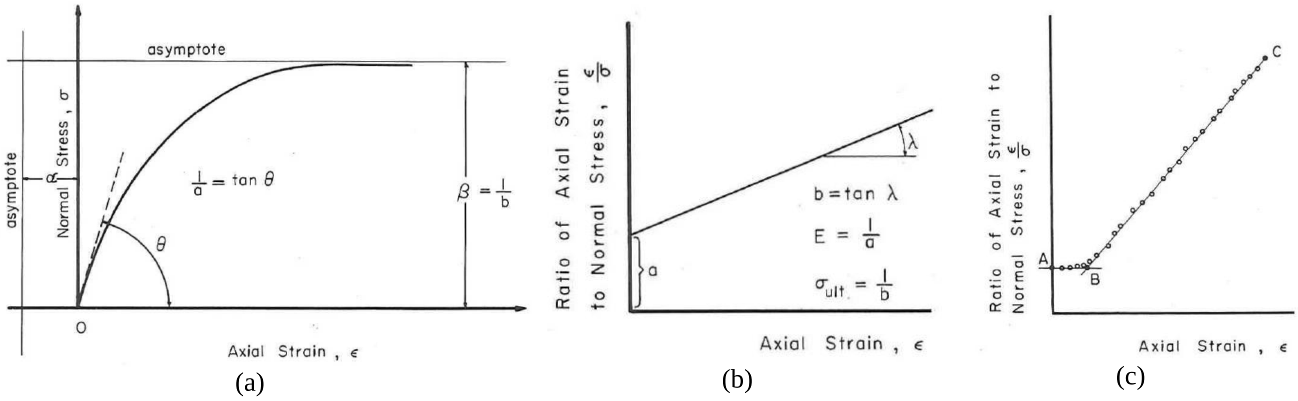

Figure 42: Kondner method, (a) rectangular hyperbolic representation of stress train, (b) transformed hyperbolic representation of stress strain, (c) composite response in transformed hyperbolic form

A example of the application of this method to the test results is presented in figure 43. Further details about the determination of the parameters obtained are given in appendix D. It should be noted that a very good correspondence of the stress strain curve can be obtained with this method (R2>0.99 for all the curves). Points varying a lot from the line are observed at small strain, due to a delay in the increasing of the shear stress. It can be explained by the imperfect contact with the sample at the beginning of shearing.

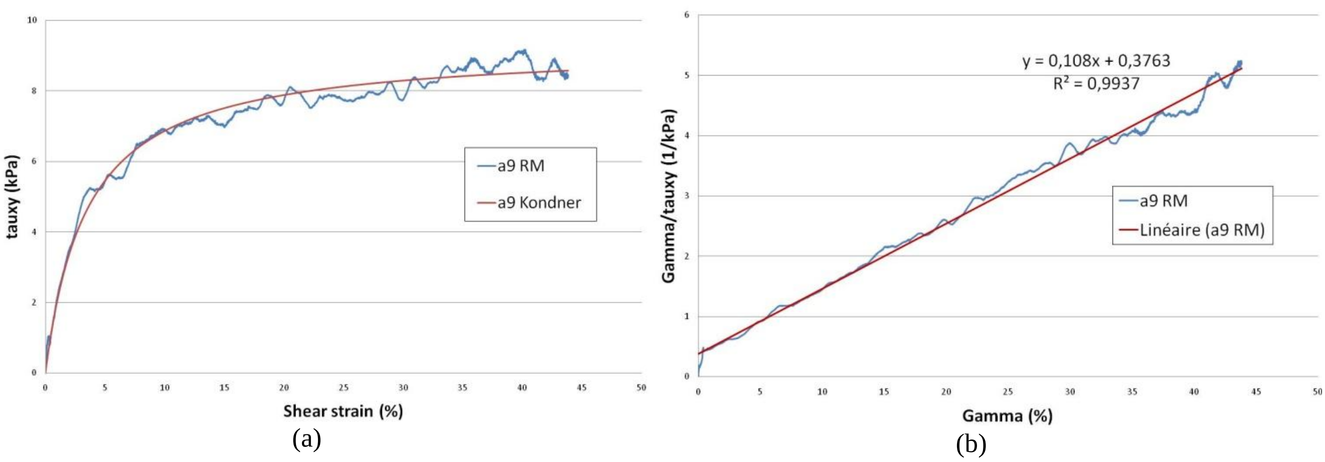

Figure 43: Application of the Kondner method to one test result (a9) with stress strain curve (a) and transformed hyperbolic representation (b)

The results of initial tangent modulus obtained with the Kondner method are given in figure 44. The initial shear modulus is plotted in function of the initial vertical stress. One point obtained with the stack of rings give a notably higher value than for other tests performed at a vertical stress of 120kPa. The results obtained with the stack of rings provide higher values of initial shear modulus

(+40% in average) at low vertical stresses than results obtained with the reinforced membrane. The number of tests remains limited and a high variability is certainly due to the material rather than to the boundary itself.

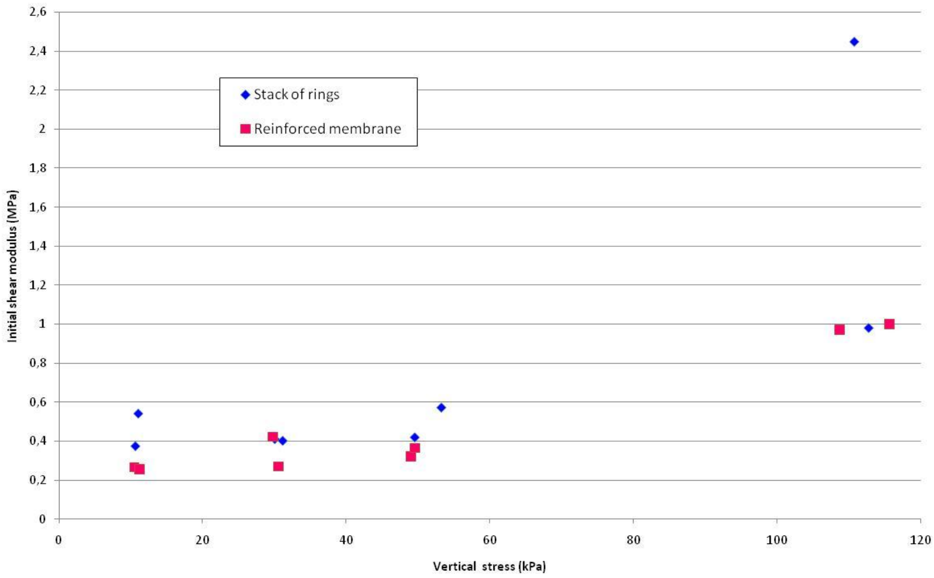

Figure 44: Results of initial shear modulus for the two boundaries

2.7 CONCLUING REMARKS

No significant difference due to the boundaries is observed in the stress strain behaviour. The variation of the results is much more due to the variability of the material than to the boundary considered. Results at low vertical stress show a much larger variability which is most probably due to the significance of the peat structure (which disappears at higher normal stress).

The reduction of vertical stress during shearing is in general more significant with the reinforced membrane than with the stack of rings. It directly influences the stress path curves obtained with the reinforced membrane:

- the τ_{xy} vs σ_v curves are more on the side of a reduction of vertical stress
- the τ_{xy}/σ_v vs γ curves show a steeper slopes and higher values at large shear strain.

Several reasons can be responsible for this observation, but the most reliable ones concerns the assumption of constant volume.

The volume of the sample chamber tends to decrease during shearing with the stack of rings as pointed out de Jong (2007). The rings slide over each other and create a series of steps on both sides of the sample in the shearing direction. The membrane between the sample and the rings is stretched but cannot fit exactly to the steps. In this way the volume slightly decreases during shearing. A representation of this phenomenon is proposed in figure 45, the shear strain applied is exaggerated for a clearer view. Anyway, the volume reduction is expected to be small, in the order of 1% of volume at 40% shear strain. This phenomenon might have more significance at low normal stress, where small stress is applied on the boundaries.

The constant volume assumption with the stack of rings can also be criticized considering the light difference in diameter between the top cap and the rings. As explained in the compliance section, water can flow between the top ring and the O'ring and the same phenomenon can also develop for soils, especially in zones of stress concentration at the top of the sample.

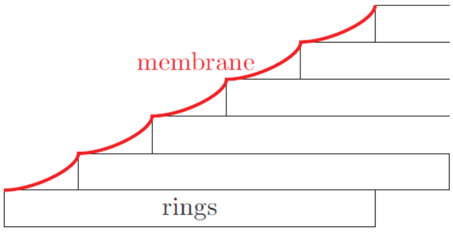

Figure 45: Streching of the membrane enclosed by a stack of rings (exagerated strain) (de Jong 2007)

The reinforced membrane cannot ensure a more constant volume since there is no guarantee of constant cross section at all. The cross section can even change over the thickness. Furthermore, the behaviour of the reinforced membrane depends a lot on the accuracy with which it is placed around the sample and on the quality of the membrane (the reinforced membrane is easily damaged).

Considering the Mohr Coulomb parameters (cohesion and friction angle) determined at 10% and 40% shear strain, the differences between the two boundaries are relatively small. At 40% shear strain, the drained and undrained friction angle increase respectively of 3% and 8% with the stack of rings.

The initial shear modulus (determined with the Kondner method) is higher at low vertical stresses with the stack of rings with an increase of about 40%. The number of tests considered remains limited and shows large variability of the measured initial shear modulus.

The stack of rings associated with an unreinforced membrane can therefore be used with a good confidence.

These conclusions are valid for peat with similar characteristics to the one tested and in the range of normal stress considered in this study. Further tests should be done for clay or sand.

The comparison presented here is limited since:

- The calibration performed to measure resistance of the boundaries is limited. This calibration should be improved to know the resistance of the stack of rings at higher water pressure.
- The material tested is highly variable (fibre orientation, wood content) and might not make possible more accurate comparisons, even if the calibration of the apparatus is more accurate. Another more homogenous material (clay) could also be used to support (or dismiss) the pervious conclusions.
- The device (vertical motor and amplifier) applying the vertical stress is inaccurate within 8% around the desired normal stress. The initial normal stress applied is then having an influence on the shear stress measured. The initial normal stresses are normalized to unity and make this inaccuracy disappear in the test results as presented here. It would be desirable to reduce this inaccuracy, especially at low normal stress. It is certainly possible by using a more modern (and more accurate) amplifier.
- The height over diameter ratio is varies between 0.20 and 0.31 in function of the normal stress applied. This is not influencing the comparison for tests performed at the same normal stress but it can influence the determination of the Mohr Coulomb parameters. As explained in chapter 1, the higher the H/D ratio, the larger the influence of the inhomogeneities inside the sample (and the larger the difference with the pure shear state of stress conditions). The average measurement of the different values depends a lot on the significance of these inhomogeneities. Vucetic and Lacasse (1982), observed experimentally that in this range of H/D ratio, the results from simple shear tests can be considered as similar. However, this

conclusion is only valid for laminated saturated clay and is not necessarily true for the unsaturated peat tested here.

2.8 LIMITATIONS OF THE GEONOR DEVICE FOR PEAT TESTING

2.8.1 ASSUMPTION OF SIMPLE SHEAR STATE

Neither of the two boundaries can ensure a true simple shear state since the rings (or reinforced membrane) are following the movement of the soil but do not impose any displacement from the sides (as Cambridge stiff straight boundaries do for instance). Only a small displacement might be imposed at the sides by the stretching of the membrane.

2.8.2 PROBLEMS DUE TO LARGE SETTLEMENTS

When large settlements are occurring, in particular with very compressible material such as peat, problems relative to the deformation of the boundaries can appear. The reinforced membrane which is very tightly enclosing the sample tends to deform and to fold because of the large settlements. It is supposed to apply significant disturbance at the sides of the sample during consolidation. If the reinforced membrane is not stretched to recover a straight initial shape, it will provide a large overestimation of the shear stress measured. So this action is done at the end of each step of consolidation applied. This point is detailed in figure 46. A test has been performed with keeping the membrane folded. A large increase in the shear stress is observed due to an extra resistance of the folded membrane. The normal stress applied to the sample is certainly influenced as well since a part of it is kept by the membrane.

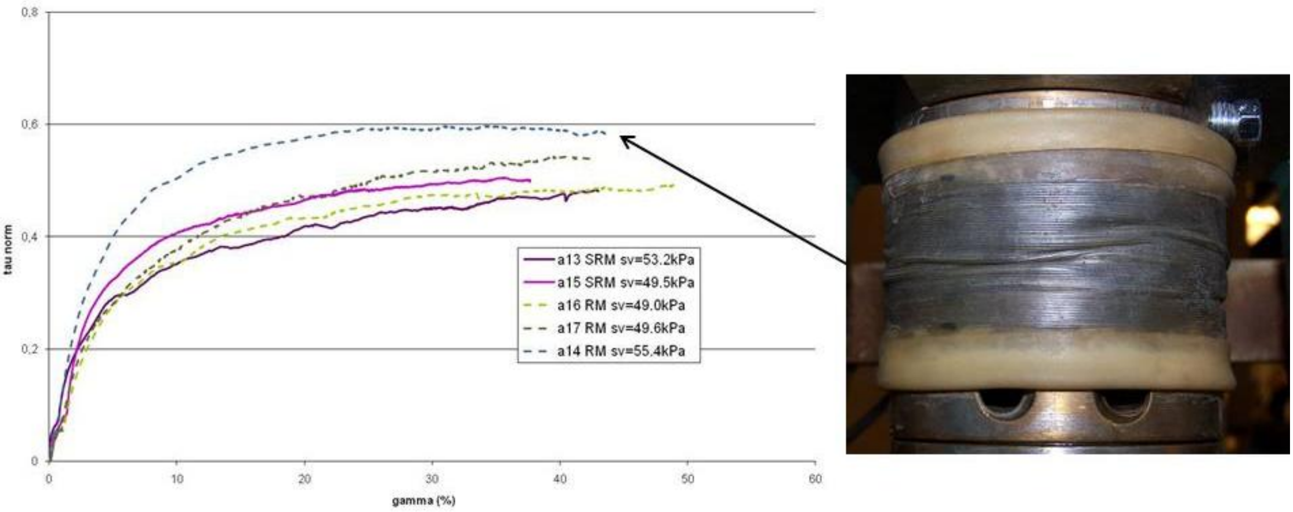

Figure 46: Effect of the folding of the reinforced membrane on the stress-strain curve with large settlement

To reduce the folding during consolidation, the reinforced membrane is put around the sample but without O'ring at the top and bottom. In this way, the reinforced membrane can slide "better" along the top and bottom cap during consolidation. The O'rings are installed after having stretched the reinforced membrane. A similar folding of the membrane is certainly occurring with the stack of rings but its effect on test results must be small. This effect is also small at low vertical stress (small settlements).

2.8.3 PROBLEMS WITH TESTS AT LOW VERTICAL STRESS

The Geonor apparatus used for this study is unable to apply vertical stresses lower than 10kPa. In situ vertical stress of some peat is often lower than this, and it is desirable to obtain characteristics of the soil with stress levels similar to in situ conditions. A system of dead weight instead of the vertical motor can perhaps help to reach lower normal stresses. A better accuracy of the amplifier is also needed. As a comparison, the device developed in Trinity College (Boylan and Long, 2009) is able to reach vertical stresses up to 3kPa. Lower stresses is unrealistic since slippage develop between the top (or bottom) cap and the sample and gives unreliable results. In this case, the shear stress measured is not anymore representative of the shear strength of the soil but of the discontinuity where the slippage occurs. One can note that in the Geonor device, no visualisation of the sample is possible during shearing to check if slippage occurs or not. A visual check of the sample deformation should be preferred for tests at low vertical stresses.

At low vertical stress, the values of shear stresses are low, often lower than 10kPa. In consequence, the significance of the horizontal stress due of the device itself (bearing, transducer, membrane) should be as low as possible to ensure reliable measurements. In the case of the Geonor apparatus, the horizontal stress due to the bearing, transducer and membrane is about one third of the shear stress measured and increases up to the half of it at large shear strain due to the membrane stretching. Removing the membrane and keep only the aluminium rings would have the advantage to reduce significantly the resistance of the boundaries. This modification would need an adaptation of the whole setup and a study of the effect of the new boundaries. This point is studied in more detail in chapter 3.

The curves obtained at low stresses are much less smooth than the one obtained at high stresses. Each detail or imperfection of the device or of the boundary can have an effect on the results obtained at low normal stresses. A particular care has to be given to the possible sources of disturbance. The reproducibility of the results also reduces when the normal stress is reduced since the effect of peat structure (fibres, wood remains) becomes more significant.

The load cells should be chosen with low capacities to maximize the accuracy and resolution of measurements. The one used in this study have a capacity of 20kN but a good accuracy so it should not be a significant problem. As a comparison, Boylan and Long (2009) used load cells of 0.5kN and 1.25kN respectively in horizontal and vertical stress measurements but no information is available concerning the maximum random error.

3. DEVELOPMENT OF AN EXPERIMENTAL DIRECT SIMPLE SHEAR DEVICE

A prototype device has been developed in order to test soil samples at low normal stress. The point of the study is to investigate the effect of the side boundaries to the stress/strain homogeneity. Two innovative boundaries are studied. The strain distribution has been investigated by performing a simple visual assessment associated with Particle Image Velocimetry analysis of the sample during a test. The stress-strain distribution has been investigated by Finite Element Modelling using several models with Plaxis 2D.

3.1 ABOUT THE ADVANTAGE OF ROUGH BOUNDARIES IN SIMPLE SHEAR

As explained in 1.5.1, the simple shear conditions are different from the pure shear conditions, notably due to the absence of additional shear stresses at the front and back sides. In both apparatus testing square or circular cross section samples, the lateral boundaries are made as smooth as possible to avoid any side friction which would influence the stress/strain homogeneity inside of the specimen. Furthermore, the H/D ratio is taken small (generally between 0.2 and 0.3) to limit the inhomogeneities at the sides and leave the major part of the sample free of the side effects. For this reason, the size of most samples tested in classical Direct Simple Shear devices are small (80*20mm in case of the Geonor for instance, adapted in the Deltares Geonor device to 63*20mm). In the case of peat, these small dimensions tend to cut the fibres and limit their effect on test results. In this way, the results obtained from usual Direct Simple Shear tests may be misleading for a proper understanding of the behaviour of peat and the influence of its structure. Larger samples with also larger H/D ratio are desired in the case of testing peat in simple shear conditions (Den Haan and Kruse 2007, Boylan and Long 2009).

Roscoe (1953) showed that at low normal stresses, the non homogeneities of strain are significant with straight boundaries as illustrated in figure 47. Especially at the front and back sides, the plane strain deformation is not ensured due to the moment of forces developing in the soil sample. In particular, a separation was observed in the acute corners (where tension is occurring). The sides were made as smooth as possible to limit the effect of edges but are insufficient to make the sample deform as a true parallelogram.

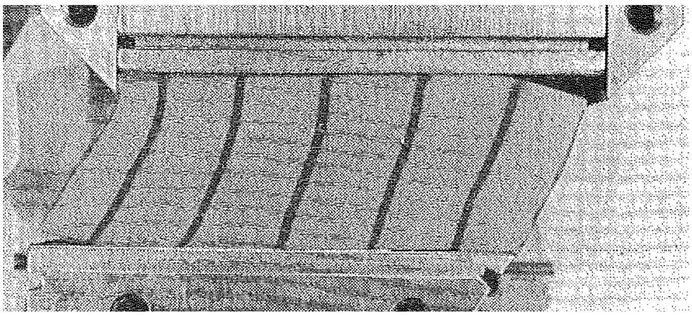

Figure 47: Side view of a plasticine sample after shearing with a vertical stress of 12kPa (Roscoe 1953)

The purpose of this study is to investigate the effect of innovative rough boundary conditions on the stress/strain distribution in the sample at low vertical stress. These boundaries are made of a serie of about 20 strips on each side of the sample. During shearing the strips slide on top of each other and form a serie of incremental steps. With such boundary, the strain homogeneity is hopefully improved and in particular the separation in the acute angle might be reduced. In the bottom acute angle, the steps are avoiding the tilting and at the top acute angle, they provide a better support to face the moment developing due to the eccentricity of the forces applied at the top and bottom side. A third boundary with vanes intruding inside the sample of few millimetres is expected to improve further the homogeneity by increasing the number of corners along the boundaries. The figure 48 illustrates the three boundaries on the front side considered in this study. The plate is not present at the back sides and the strips are moving with a system of rod (see 3.2).

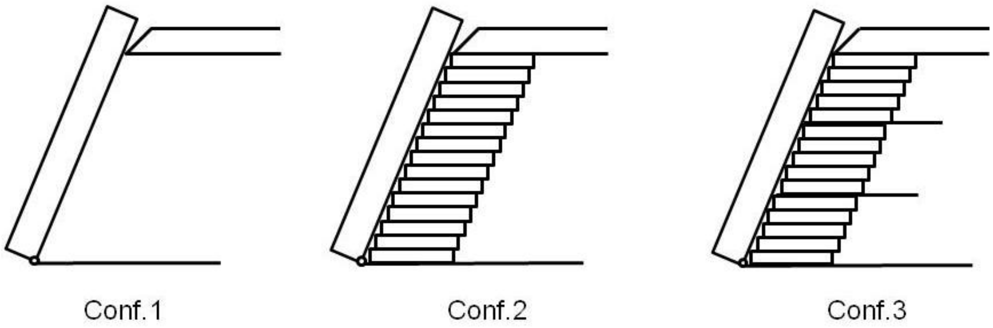

Figure 48: Boundaries considered for the front side

The configuration with strips can be compared with the new configuration used with the Geonor device (stack of rings) with removing the membrane between the soil sample and the rings. The sample tested is cubical rather than cylindrical in this study. Some Japanese authors used similar boundaries in simple shear testing to investigate the frictional resistance between sand and steel or to test reinforced sand (Uesugi and Kishida 1986, Hayashi et al 1988). Square cross section samples were used and a membrane was also inserted between the soil sample and the strips. No investigation of the effect of these boundaries on the stress/strain repartition inside of the sample has been performed until now. Furthermore, a difference should be made between an apparatus were the shearing is applied only from the top and an apparatus where the shearing is also applied from the sides. The shearing is applied both from the sides and the top in the prototype described here..For more convenience, the different configurations described are named as in figure 48 in the rest of the report.

3.2 DESCRIPTION OF THE PROTOTYPE

A picture of the prototype is detailed in figure 49. The prototype is designed for rectangular cross section samples. The two sides (front and back) are linked to the base by hinges (conf.1) or rods rotating around screws in the base (conf.2 and conf.3). The top plate of the apparatus is linked by four screws with a rail at the top and slides along it during the shearing. The top plate is directly pushed by the front side. The two sidewalls of the apparatus are closed by transparent (Perspex) plates in order to observe the deformations of the soil sample during the test. The shearing is applied with a motor pushing the front side of the apparatus with a constant shearing rate of 5% of the height per hour. The shearing rate is supposed to be small enough to prevent generation of excess pore pressure internally by allowing time for equalisation.

The first boundary condition is a “classical” straight boundary. Two PVC plates are enclosing the soil specimen at the front and back, both linked to the base by hinges. Silicon oil is applied on the front and back plates to reduce the friction on the soil. Two steel rod link the top of the two plates in order to ensure that both plates are rotating of the same amount. A special care has been brought to the hinges position to guarantee that the initial rectangle deforms as a parallelogram and that the volume is kept constant.

The second boundary is composed of strips sliding on top of each other. On the front, twenty one strips are placed in contact of the front plate where the motor is applying the shearing (the front plate is the one used for conf.1). On the back side, the same amount of strips are moving along two vertical steel rods at the sides of the strips and linked with the front plate at the top also by a steel rod. Special care was taken to have a similar displacement of the strips at the front and back side to guarantee a constant volume during the test. During the development of the prototype, some difficulties have been encountered to obtain the sliding of the strips on top of each other. Indeed, the strips tend to rotate if their width is not large enough. The strips dimensions are 3*30mm at the front side and 3*40mm at the back side.

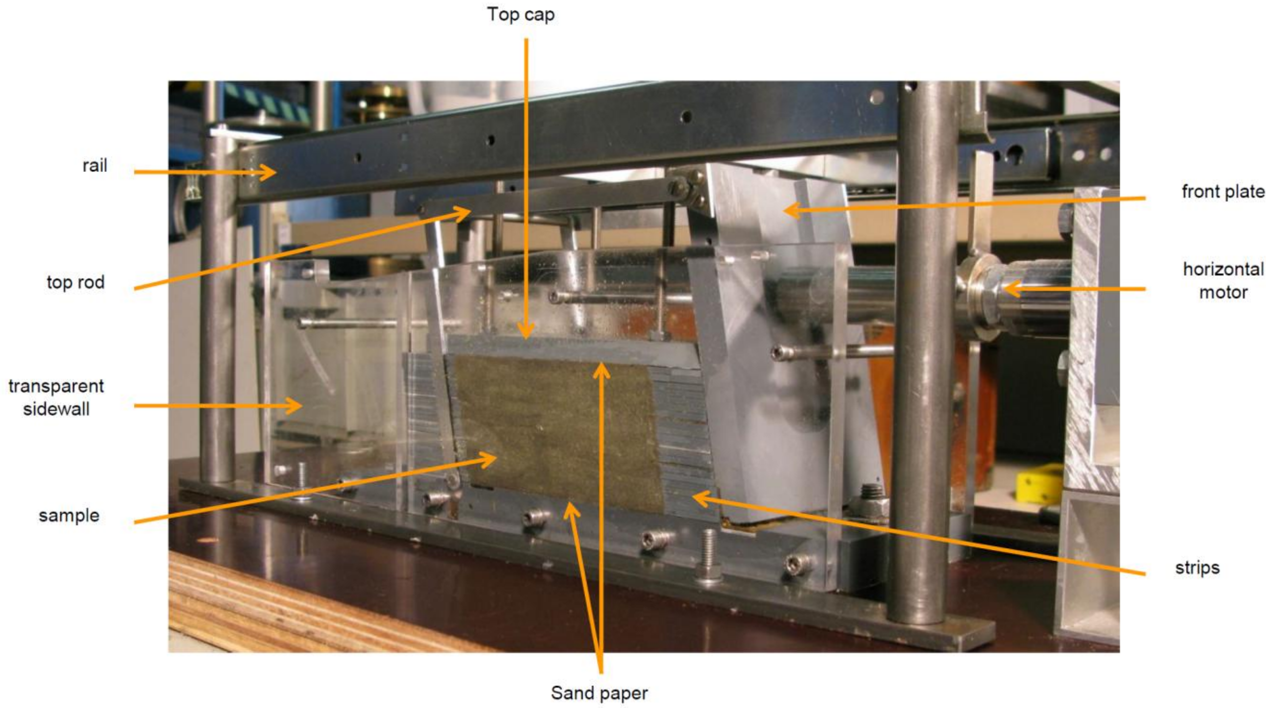

Figure 49: Direct simple shear prototype

The third configuration is similar to the second one, except that four thin (about 1mm large) steel plates longer of 6mm than the PVC strips are intercalated between the seventh and eighth strips and between the fourteenth and fifteenth strip.

The top and bottom of the apparatus is equipped with 00 sand paper in order to avoid slippage of the soil at the interface with the apparatus.

For practical reasons, the sample size (141*72*100mm) for the configuration 1 is slightly larger than for configuration 2 and configuration 3 (124*65*100mm). The height over length ratio (H/D) is similar for the three configurations, and is equal to 0.51. This ratio is taken larger compared to usual Direct Simple Shear configurations in order to make possible the observation of strain inhomogeneities at the sides of the sample. Furthermore, it corresponds to the geometry desired to test peat with larger samples.

The prototype is not equipped with load cells and make impossible any measurement of stresses at the sides of the specimen.

The development of the present prototype has been inspired by the work of Hervé van Baelen who designed a “rod” direct simple shear model at the University of Leuven. The use of simple shear is also of large interest in geology, in particular to understand the development of geological unconformities (Van Baelen and Sintubin 2008, Sintubin at al. 2009).

3.3 PARTICLE IMAGE VELOCIMETRY

3.3.1 PRESENTATION

The deformation of the soil is measured through the transparent sidewalls by image processing analysis. The method, originally used in fluid mechanics has been adapted to geotechnical purpose by White et al (2003). The point is to follow the soil deformation on a certain number of pictures taken by a camera at a fixed interval of time. It is based on a software called GeoPIV which is implemented in Matlab.

A mesh constituted of a certain number of given size patches is created on the initial pictures. If (u_1,v_1) are the coordinates of one patch in the first picture taken at a time t_1, the software searches for the best correlation in a given area of the second picture taken at a time t_2 and determine the position (u_2,v_2) of the updated patch. Each patch is characterised by its intensity I(U). The best correlation is searched in a given area characterized by s which is the distance of how much each patch is increased. This process is repeated for each patch and for all the pictures to give the deformation of the soil at a desired moment of the test. A displacement field is created on the basis of the displacement of each patch. The principle is detailed in figure 50.

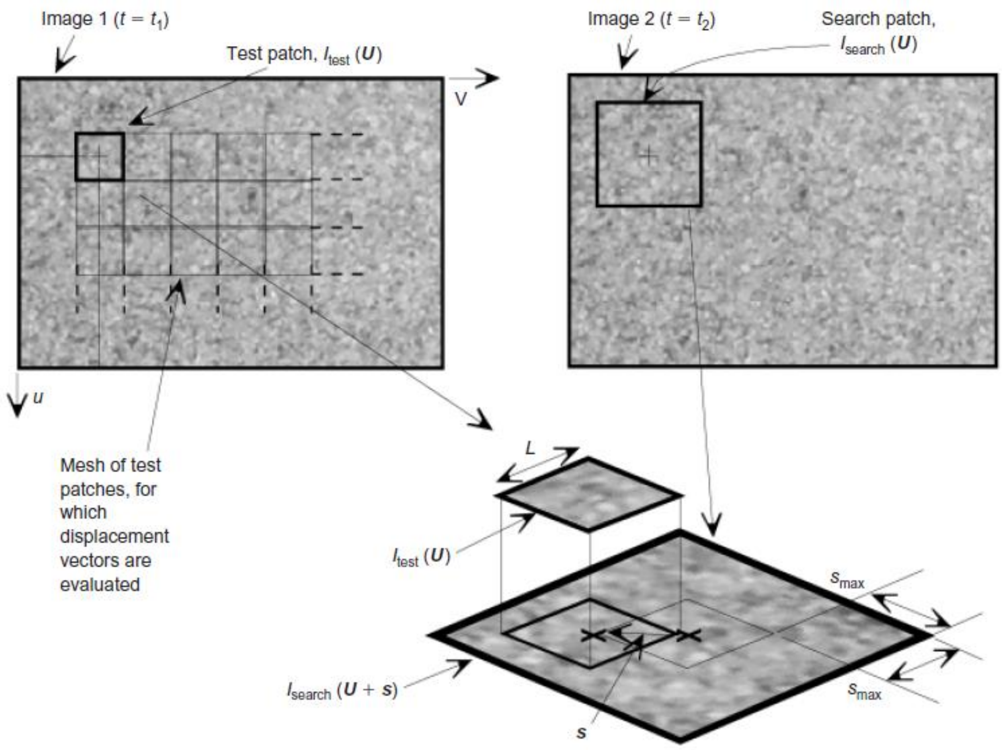

Figure 50: Principle of a Particle Image Velocimetry analysis (White et al. 2003)

3.3.2 PARAMETERS OF THE PIV ANALYSIS

The different parameters of importance in PIV measurements are listed below:

- <u>Size of the pictures:</u> The larger the pictures, the more patches of a given size that can be drawn on the initial picture and the more information that will be available. The images analysed in this study were captured using a Canon Powershot G9, which has an image resolution of 12 million pixels. The area occupied by the sample on the picture is about half of the total picture.

- Contrast: The ability of the software to follow the soil deformation is strongly dependent on the contrast of the sample. The more contrast that is brought to the sample, the more easily the software can follow one patch along several pictures. Since the clay used is dark brown and provide a poor contrast, a light green "flock" material is added on the surface of the sample. It is supposed to follow the same deformations as the clay.
- Patchsize: Experiments performed on a planar translation of a rigid body (White et al, 2003) showed that the precision of PIV analysis is a strong function of patch size L. The random error due to patch size is expressed in equation (14). It increases quickly with decreasing the patch size.

$$\rho_{pixel} = \frac{0{,}6}{L} + \frac{150\ 000}{L^8} \quad (14)$$

The selection of patch size has to be a compromise between the accuracy and the number of patches needed. Larger patch size provides improved precision whereas smaller patches allow the image to contain a greater number of measurement points. In the case of this experiment, the patch size has been chosen in function of the size of the flock used. The patches have to be large enough to contain several different "flocks" instead of one or only a part of one. In this way, each patch has a more recognisable intensity compared to the other patches in the searchzone. The patch size chosen is 45 pixels. The number of patches, about 1700 in one picture, is large enough to provide enough information in case of large strain gradient (along a failure surface for instance).

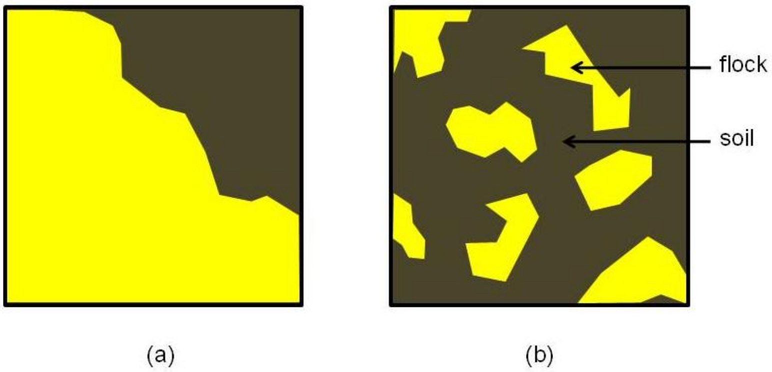

Figure 51: Choice of patch size depending on the flock size : (a) poor and (b) acceptable

- Search pixel zone: It is the largest displacement vector which GeoPIV will search for, defined as s in figure 50. The search pixel zone must be set higher than the maximum displacement of a soil particle between two pictures. It can be easily determined by inspection of two successive pictures. This parameter depends on the leapfrog parameter as well.
- Leapfrog: This parameter indicate how often the first image is updated. If the leapfrog is low (1 for instance), GeoPIV compares 1 and 2, then 2 and 3, 3 and 4 etc. The patches are easily identifiable but the measurement precision is low (since the measurement error is summed as a random walk). If the leapfrog is set higher (10 for instance), GeoPIV compares 1 and 2, 1 and 3 up to 1 and 10 and then 10 and 11, 10 and 12 etc. The measurement precision is increased but the chance of getting more wild displacement vectors is increased as well. In this case, the leapfrog is set to 10 this value is high and does not create too much wild vectors.

A light projector is providing a constant light during the entire test to avoid any inaccuracy due to change in lighting.

No correction for the picture distortion was applied since it was observed to be negligible on pictures taken replacing the sample by a millimetric paper sheet.

3.4 PREPARATION OF THE CLAY SAMPLES

For reasons of convenience, the material used in these experiments is clay. It was extracted from the Oostvaardersplassen (OVP) area on the shore of the Markermeer in the North East of Amsterdam. Then the samples have been remolded and stored with a wax envelope to preserve the water content.

The samples are cut with precision to the desired dimensions with a cutting wire. Then the sample is cut in two halves in the length side. Light green “Flocks” are spread on one side of the sample to improve the contrast for PIV measurements. A grid (1cm spacing) is drawn on the sides of the two halves with a permanent ink pen. It allows for a visual assessment of the soil deformation and brings complementary results to PIV image processing. The two halves are gathered with one grid outside (transparent sidewall – soil interface) and one grid inside (soil - soil interface). Since friction will certainly occur along the transparent sidewall, it is also desirable to have results from the inside of the sample. Morgenstern and Tchalenko (1967) used the same technique for tests performed in direct shear device with Kaolin. This technique makes possible to evaluate the significance of the sidewall friction by comparing the two grids at the end of the tests. At the sidewall interface, the grid is extended on the top plate and on the base to assess the occurrence of slippage.

3.5 EXPERIMENTAL RESULTS

3.5.1 VISUAL ASSESSMENT

The results obtained at the end of the three tests (γ=20%) both at the sidewall interface and at the middle vertical plane, are detailed in figure 52 (a) and (b) respectively. A clear failure principal plane is observed in the three specimens. For configuration 1 and 2, it is located in the shortening diagonal (linking the two obtuse angles). The failure in configuration 3 is different since it links the top front vane and the bottom back vane. The angle between the horizontal plane and the principal plane of failure is about 22° for conf.1 and conf.2 and reduce to 10° for conf3. The presence of vanes clearly influences the primary failure pattern. Secondary failures are observed in conf.1 locally with a reduced angle with the horizontal in the bottom front part. Secondary failures are also observed and form after the creation of the primary failure. With conf.1, two kinds can be differenced, one more horizontal and another almost vertical. The amount of observed secondary failures is much reduced with conf.2 and conf.3. Since failures would develop in consequence of stress inhomogeneities, it seems that the stress homogeneity is improved with conf.2 and cong.3.

Small differences are observed in comparison of the sidewall plane and the middle transverse plane. Two differences should be noted though. The pattern of the primary failure is regular at the soil sidewall interface whereas it is separated in several small failures parallel to each other on the middle transverse plane, especially observable with conf.2 and conf.3. Observed secondary failures are more numerous and more diversified at the sidewall, certainly due to the friction between the soil and the transparent sidewall. The general pattern remains very similar on the two planes and gives good confidence in the observation through the sidewall.

For all the tests, a clear failure occurs at about 7-8% external shear strain. So the homogeneity in displacement of the soil should be assessed before this limit. Nonetheless, differences are visually more obvious at large shear strain. The strain homogeneity can be assessed by the amount of vertical displacement and the significance of the separation of the soil from the boundaries as a consequence of tensile forces developing in these zones. With conf.1, the vertical displacement is significant at the sides: upward along the front side and downward along the back side. This observation is consistent with the mathematical analysis of Roscoe (1953) and is a direct consequence of the stress non-uniformities (tension and compression) which develop in the sample. In the top acute angle, a clear separation appears between the soil and the top cap. Roscoe (1953) also observed this separation in the two acute corners (top and bottom) with true frictionless sides (the pictures of his results are presented at much higher shear strain than here). In our case, the separation at the bottom is less obvious. The separation in the top acute corner is greatly reduced with conf.2 and conf.3, so the tensile forces must be reduced as well there. The vertical displacement at the sides is reduced in conf.2 and almost disappears in conf.3. For instance, the horizontal lines along the top and bottom of the sample are almost not deformed from the front to the back sides.

Slippage can be observed in the three cases at the top of the sample. Especially in conf.1, a thin highly disturbed zone is observed just underneath the top plate. Slippage should be avoided since it greatly increases stress inhomogeneities in the sample (Prevost et Hoeg 1976).

Finally, the innovative rough boundaries are showing better results than the classical straight boundaries considering the strain homogeneity. The strips and especially the vanes pushed deeper inside of the sample are forcing more homogenous deformation and reduce the side effect observed with classical straight boundary. These results should be considered with caution since slippage is occurring between the top of the sample and the top cap in the three tests. Furthermore, the friction at the sides of straight boundaries may be more significant than in classical frictionless side apparatus. In this case, the vertical displacement of the soil along the boundaries might be underestimated as well as the separation in tensile zones.

3.5.2 RESULTS FROM THE PIV ANALYSIS

The results from PIV analysis are presented in figure 53 and figure 54 at 4% external shear strain and 8% external shear strain respectively. Three set of results are given:

- The cumulative engineering shear strain (a): that is the maximum cumulative engineering shear strain in the horizontal plane (γ_{xy})
- The maximum incremental shear strain (b): calculated from the difference between the incremental shear strain from two successive images according to equation (16).

$$\gamma_{inc-max} = \varepsilon_{1-inc} - \varepsilon_{2-inc} \tag{15}$$

- The volumetric strain (c): calculated as the sum of the strain in the x and y direction according to equation 15.

$$\varepsilon_{vol} = \varepsilon_x + \varepsilon_y \tag{16}$$

Considering the results at 4% external shear strain, no failure has been reached yet for the tests considered. The shear strain is low in all cases at the bottom of the sample. It may result from some adhesion of the soil to the sidewall. The shear strain is concentrated in the central part of the sample and also extends to the bottom obtuse angle in conf.1. The soil close to the front and back sides are clearly sheared in a smaller amount than in the central part. The results from conf.2 and conf.3 show a better homogeneity of the shear strain throughout the sample and especially at the sides. In case of conf.3, the high strain at the sides are supposed to be due to the squeezing of soil between the Perspex sidewall and the strips or vanes and so lead to unrealistic strain measurements. It should be ignored. The maximum incremental shear strain is developing locally in various area of the sample. The volumetric strain is positive in the top obtuse angle (especially for conf.2 and conf.3) which is the sign of compression in this area. At the opposite, negative volumetric strain (extension) develops at the top acute angle. Compression is expected in the two obtuse angles with about the same amount. In this case, significant compression which only occurs at one side is certainly due to slippage occurring at the top of the sample. This observation corroborates the results from the visual assessment. High volumetric strain concentration at the bottom of the sample is due to scratches on the transparent sidewall which disturb the displacement field established by the software (fuzzy zones).

At 8% external shear strain, failure is clearly reached in conf.1 with two failure surfaces but ntot yet with conf.2 and conf.3. The shear strain homogeneity is improved with conf.2 and conf.3, especially at the front and back sides. In particular, the area of low shear strain corresponding to the tension zones in the top acute corner is greatly reduced in conf.2 and conf.3. The volumetric strains show compression at the front sides for all the configurations.

Finally, the PIV results show an improvement of the shear strain homogeneity in conf.2 and conf.3 compared to conf.1. This is especially visible at the back of the sample where the tension (not sheared) zones are reduced. Failure is occurring earlier with conf.1, which can be a consequence of the more important nonuniformities developing. It is consistent with the results from the visual assessment of the sample, and the reduced number of secondary failures with conf.2 and conf.3. Compression is observed systematically at the top obtuse angle and is synonym of slippage at the top of the sample. Slippage was also observed with the visual assessment of the sample deformation.

3.5.3 CONCLUING REMARKS

The grid deformation and the PIV image processing provide valuable and complementary information considering the strain homogeneity in the sample.

The results obtained from the tests performed with the Direct Simple Shear prototype are encouraging but limited. The simple shear deformation of the soil is improved by the new boundaries. Several observations support this argument: the vertical displacement is reduced along the sides, the separation of the soil from the top cap is reduced (so should be tensile forces), the homogeneity of shear strain is notably improved in the sample and finally primary and secondary failures are retarded. The initial goals of improving the simple shear deformation and increasing the strain homogeneity in the sample is reached. Unfortunately, slippage at the top of the sample could not be avoided with sand paper at the low stresses applied. Teeth or pins (as used in the Geonor device) should manage to provide an acceptable grip of the sample. A visual assessment of the soil deformation is necessary at low stresses to check if slippage is occurring or not, it can be observed by large compression along the front side.

The normal stress applied at the top of the sample should be checked for an accurate comparison of the effect of boundaries. In the present tests, the normal stress is small (and supposed similar in the three experiments) but could not be measured. A minimum normal stress is necessary to avoid slippage at the top, for instance Boylan and Long (2009) observed that loads lower than 3kPa could not be applied without getting slippage. Vertical load cells are needed to apply a repeatable vertical load at the top of the sample. Then horizontal load cells would make possible to measure the shear stress and so produce classical results from Direct Simple Shear tests. Stress-strain curves would be of great value to complete the comparison. For instance, the different time when failure is reached should have an influence on the shape of the curves.

Applying the shearing from the bottom plate instead of the top might improve the conditions and reduce the risks of slippage since the weight of the soil is also taken into account.

Further tests on clay are needed to comfort the conclusions of this first series of tests. Tests on peat should be also performed since the prototype has been designed for this material. Peat might present other problems like inaccurate cutting of the sample and difficult manipulation during preparation. Larger patches in PIV measurements might also be necessary, depending on the natural contrast of the material.

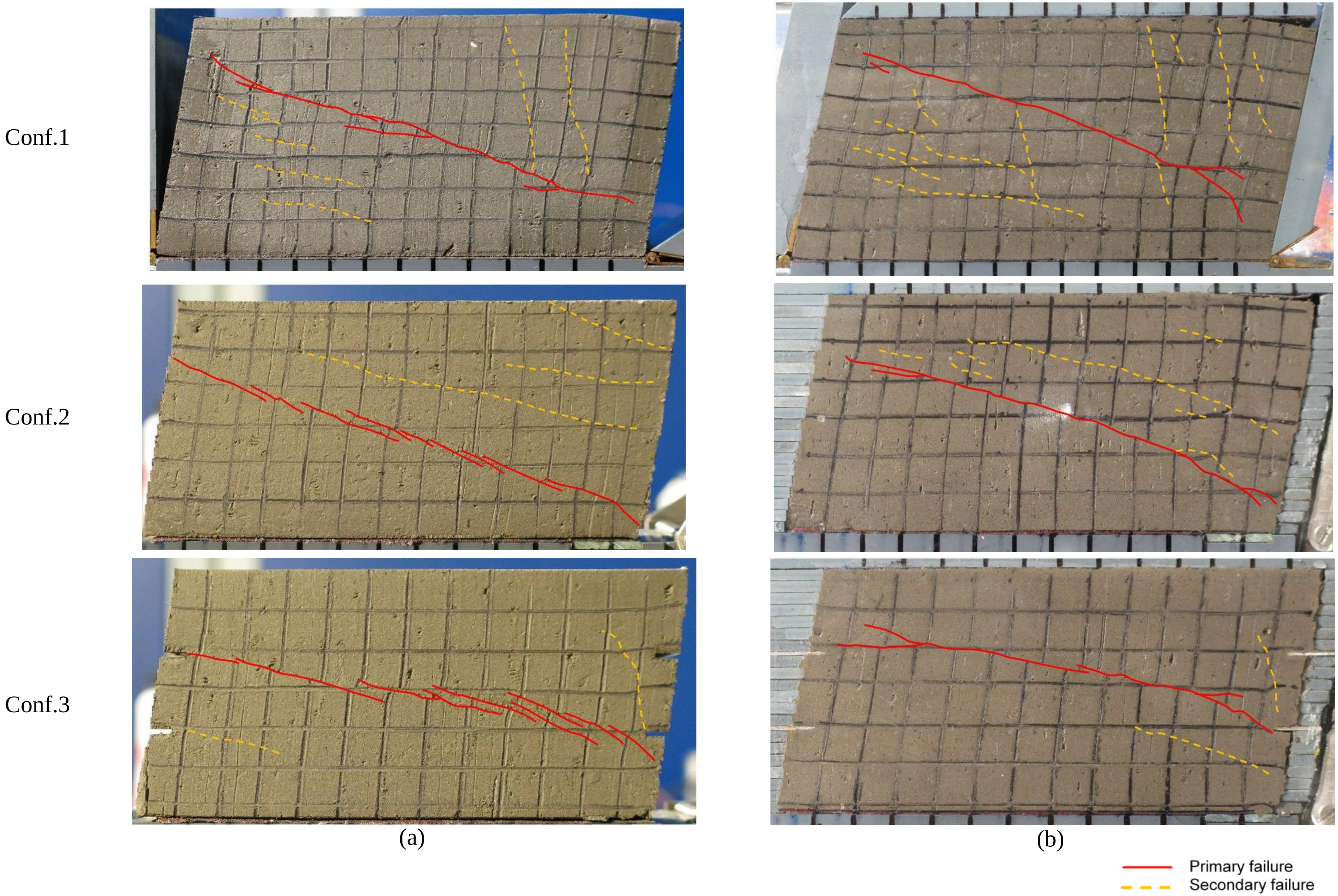

Figure 52: Results from the prototype tests on clay samples (γ=20%): the middle vertical plane (a) and through the transparent sidewall (b)

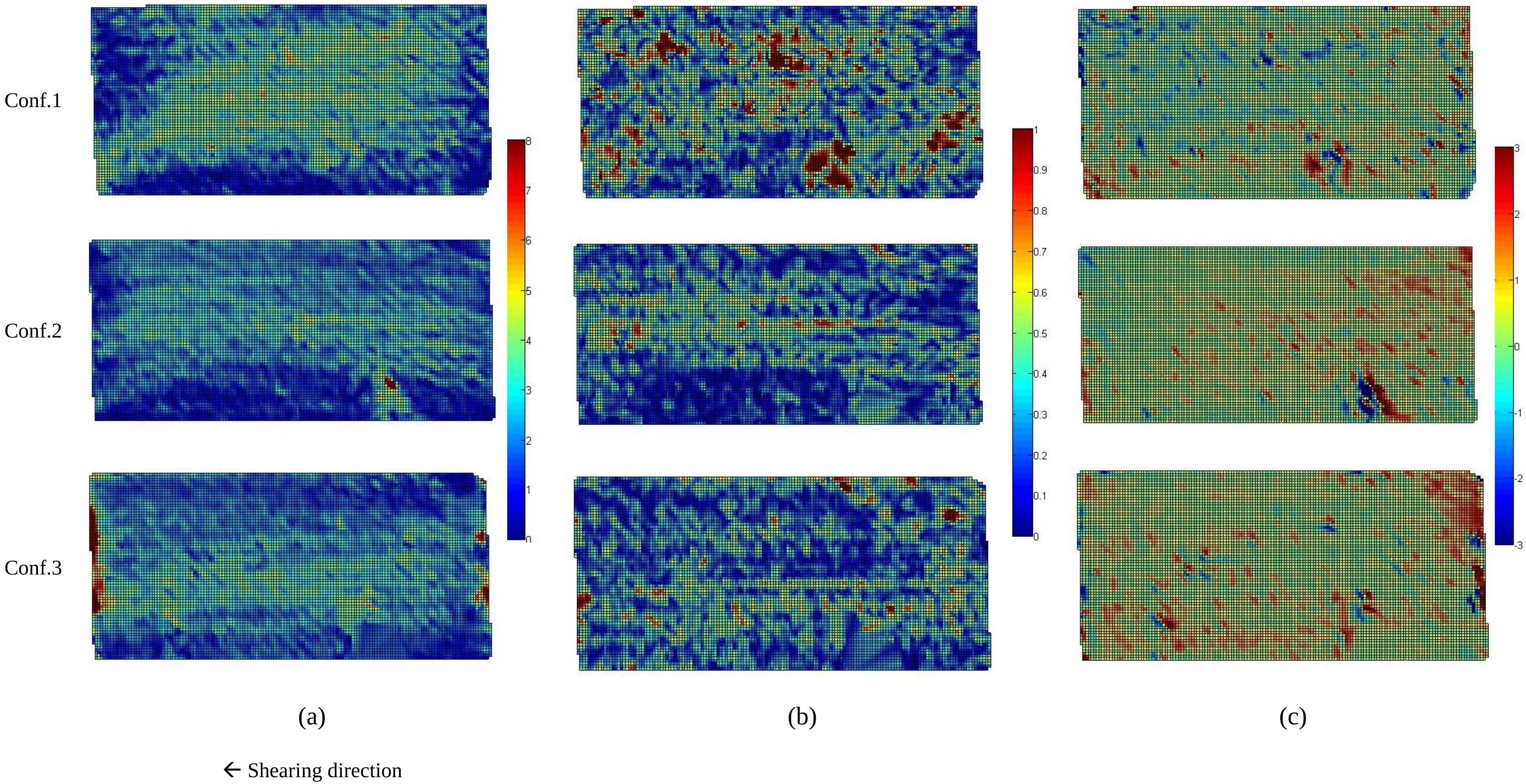

Figure 53 : Results from PIV analysis (γ=4%), (a) cumulative engineering shear strain, (b) maximum incremental shear strain and (c) volumetric strain

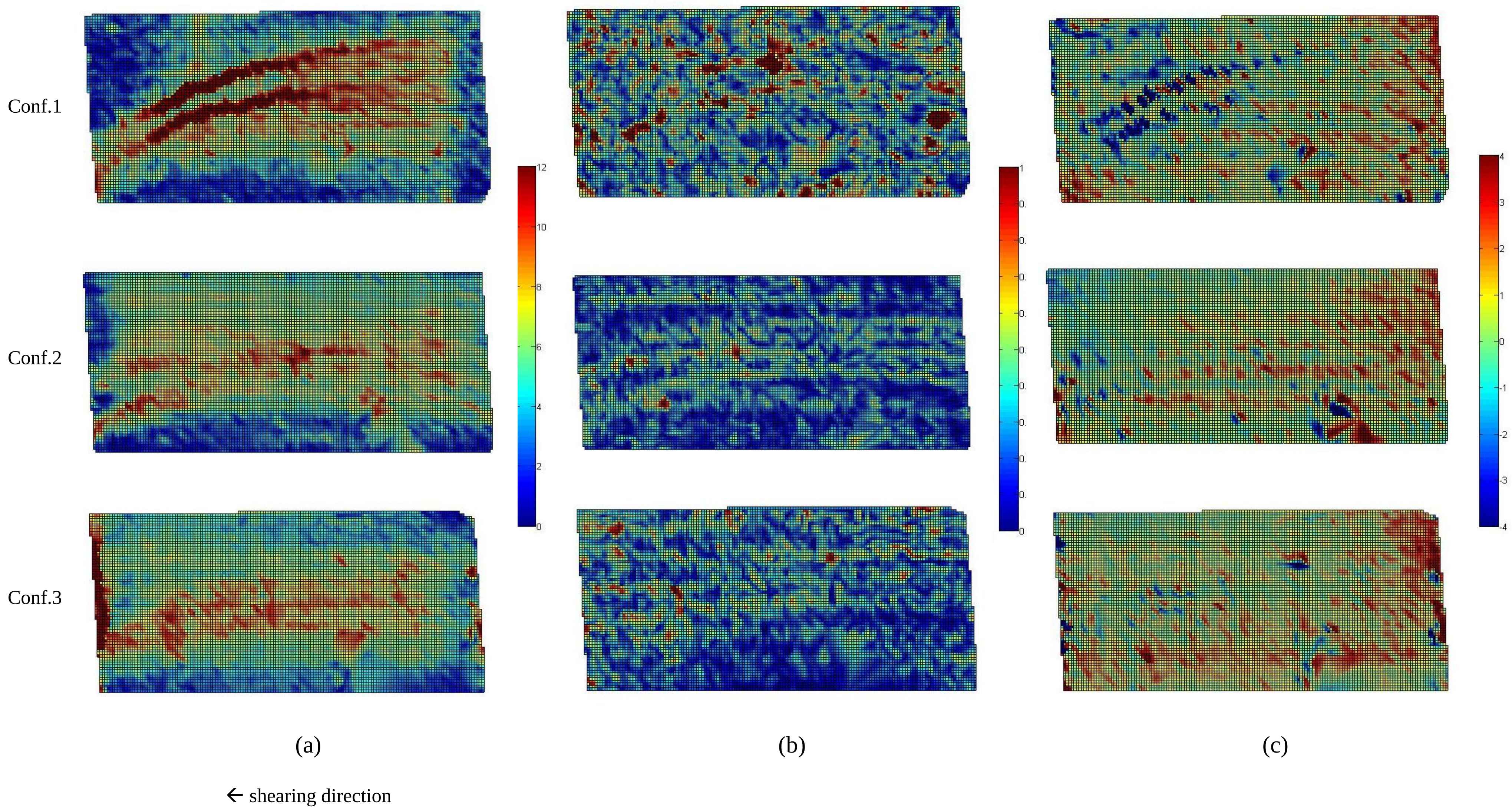

Figure 54 : Results from PIV analysis (γ=8%), (a) cumulative engineering shear strain, (b) maximum incremental shear strain and (c) volumetric strain

3.6 MODELLISATION OF THE PROTOTYPE CONDITIONS BY A FINITE ELEMENT METHOD

A finite element analysis of the direct simple shear prototype conditions has been performed with Plaxis 2D (version 10). The objective of this analysis is to obtain information concerning the stress/strain distribution inside of the sample. Two models are considered: one linear elastic perfectly plastic (Mohr Coulomb) and one visco-elasto-plastic (Soft Soil Creep), both in plane strain conditions. The use of rigid and smoother boundaries is discussed. A tentative of comparison with experimental results is also dealt.

3.6.1 GENERAL SETTINGS

The dimensions of the model are similar to the sample dimensions in conf.2 and conf.3 in the experimental work (65*124mm).

Each test is modelled by three different phases. The first phase is the initial stress generation, the second is the phase of consolidation and the third is the phase of shearing in a constant volume state. All the phases are performed in drained condition; the water table is fixed at the bottom of the sample. In this way, the development of pore pressure is ignored as it is the case in regular constant volume tests. The stresses and effective stresses are not differenced in the rest of the report. The saturated and unsaturated soil density is set equal to 18kN/m3.

The K_0 stress generation is performed automatically by the software. For advanced models, it determination depends on the Pre-Overburden Pressure (POP) or of the Over Consolidation Ratio (OCR) as detailed in 3.6.3

The consolidation phase is performed by applying a vertical load of 5kPa at the top of the sample. The soil is fixed at the sides in the horizontal direction but free in the vertical direction. The bottom of the sample is provided with total fixities.

The shearing phase is applied by prescribed displacement at the sides and at the top of the sample. The displacements are applied from the left to the right. At the top of the sample, the soil is displaced in the horizontal direction and fixed in the vertical direction. In this way, the height of the sample is kept constant; furthermore the contact between the soil and the top plate is always insured. Both rigid and smoother boundaries (with interface) are considered. Four types of prescribed displacement are used as illustrated in figure 55. The first configuration is modelled by applying a linear displacement equal to zero at the bottom and maximum at the top (equal to the displacement along the top). The second configuration is modelled by applying step displacements at the sides, the displacement between each strip being linear. This method was used already for the finite element modelling of a direct shear box (Potts, 1987). An idealized regular repartition of the points at the sides (42 points separated by 3.1mm) is used as well as a more realistic one with very small space between each strip (0.5mm spacing). The first solution (conf.2a) is easier to handle since it reduces the chance to have sharp elements at the sides and consequently reduces notably the calculation time. The influence of this homogenous repartition of points on the stress/strain state is discussed. The conf.3 is modelled with a method similar to the homogenous repartition of points and by adding four lines of 6mm deeper in the sample and by applying horizontal displacement to it. The influence of the vanes is supposed to be preponderant compared to the influence of the gap between each strip.

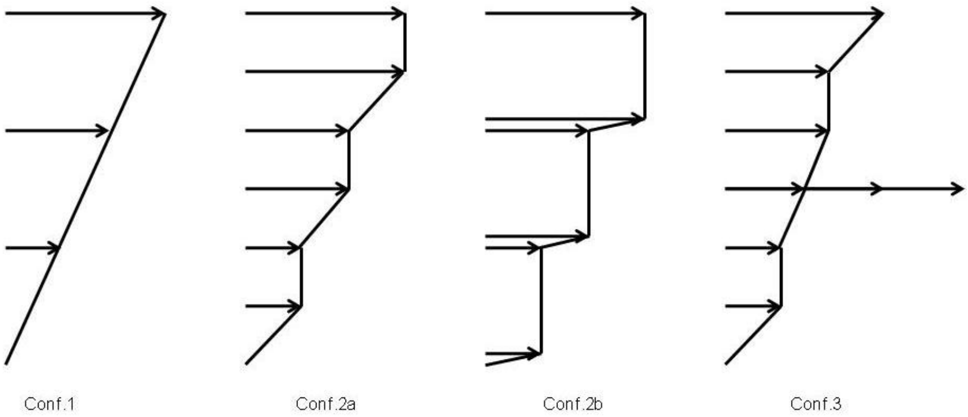

Figure 55: Prescribed displacement applied at the sides

For the case of rigid boundaries, the displacements applied at the sides leave the soil free to move in the vertical direction (except the displacement applied to the vanes). This method is equivalent to have a straight plate on the side with perfectly smooth. An assessment of this method has been made by reproducing a part of the study performed by Prevost and Hoeg (1976) and gave very satisfying results as detailed in appendix F. Fixing the soil in the vertical direction is creating ideal conditions which can be compared to pure shear conditions and induces an almost full homogeneity of stresses and strains in the sample.

For the Soft Soil Creep model, the time of the shearing phase is set similar to the one used in the experiments, equal to 5% of the height per hour.

3.6.2 MESH DEFINITION

A 15-noded elements mesh is used in this study. Since the boundaries are different for the three configurations, the meshes are also built slightly differently by the software. The detail of the mesh characteristics is given in table 6. A relatively large number of elements is used in order to get rid of the mesh influence in simulation results. For instance, the average stresses along the top cap are reaching a limit after a certain number of elements. The number of elements is chosen comfortably above it.

Table 6: Characteristics of the meshes used

	Conf.1	**Conf.2a**	**Conf.2b**	**Conf.3**
Elements	4554	5210	4640	3724
Nodes	36837	42117	37561	30237
Average element size (mm)	1,347	1,260	1,335	1;490

Sharp elements should be avoided in finite element modelling because it can lead to undesired outcome as divergence or unrealistic stress concentration. Poor mesh quality can also increase a lot the time of calculation especially with advanced models. The element quality is given by the ratio of the area of the inner circle and the area of the outer circle of an element. Therefore, an equal sided triangle element has a quality of one. The four mesh used in this study are presented in figure 56. The element size is lightly smaller at the sides than at the centre for conf.2a and conf.3. A more realistic mesh (conf.2b) is also considered with a space of 0.5mm between each strips and with a similar number of strips than for conf.2a. Two clusters are added at the sides to reduce the sharpness of the elements located between two strips. The mesh quality is still of poor quality (0.2 to 0.4) along the sides. It could be improved by tediously refining the mesh along each strip.

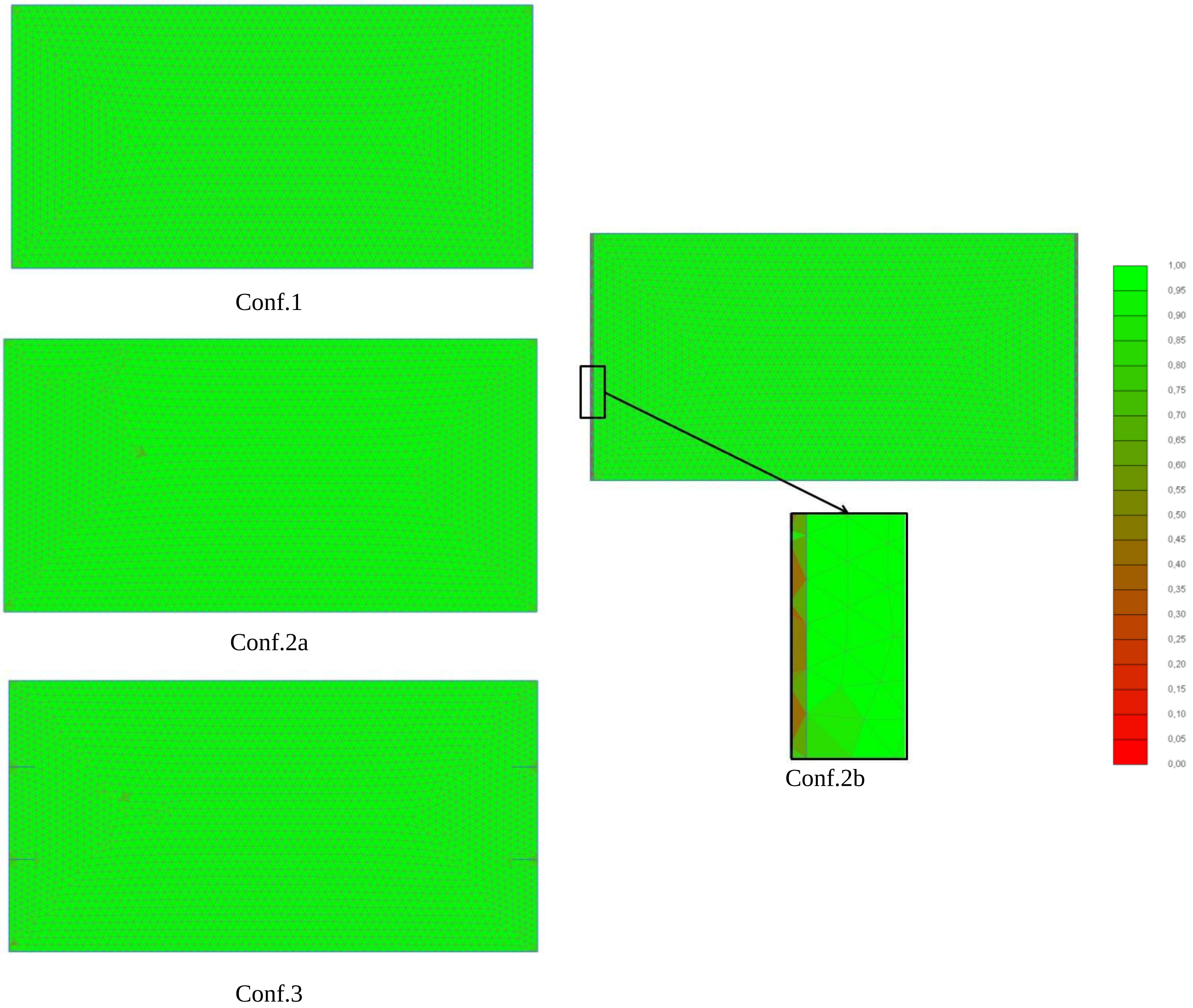

Figure 56: Quality of the meshes

3.6.3 MOHR COULOMB MODEL

The parameters used in the MC model are detailed in table 7. A small cohesion is given to the soil to avoid eventual problems of calculation with Plaxis (Brinkgreve et al. 2010). A tension cut off is used to set the tensile strength of the soil to zero.

The results from the consolidation phase are not shown. It should be noted anyway that even if a vertical stress of 5kPa is applied, the average vertical stress measured at the top of the sample is 5.65kPa. The vertical stress is 6.24kPa at the bottom of the sample.

The results from the shearing phase are presented at 5% external shear strain in figure 59. Three different features are shown: the cartesian shear strain (γ_{xy}), the principal stresses (direction and values) and the nature of the stress points. A distinction is done between tension points and Mohr Coulomb. With the Soft Soil Creep model, the visualisation of the cap points is also presented. This information give an insight into the state of failure of each point in the specimen.

Table 7: Mohr Coulomb parameters

E (Mpa)	4.23
ν	0.31
φ (°)	35
Ψ (°)	0
c (kPa)	0.2
K_0	0.58

Results from pure shear conditions at 5% external shear strain show an almost full homogeneity of the stresses and strains inside the soil sample as illustrated in figure 57. The scale of shear strain is similar to the scale used in figure 59.

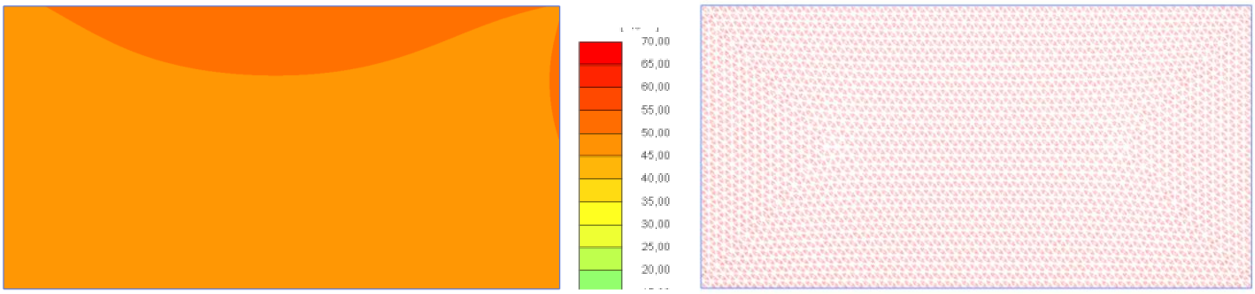

(a) Shear strain (b) Effective stresses

Figure 57 : Results of the simulation of pure shear conditions

Considering the figure.59, large similarities are observed between the conf.1 and conf.2a. The zone of homogenous shear strain (>4%) is concentred in the middle of the sample whereas the shear strain along the sides is close to zero. In conf.2a, a strain concentration is observed at the sides due to the large relative displacement imposed by the strips. A stress concentration takes place in the two obtuse (compression) angles whereas very small stresses develop in the acute (tension) angles for the conf.1 and conf.2a. The effect of the strips is limited to the sides. It does not influence the stress distribution in the core of the sample nor it improves the homogeneity of stresses in the tension corners. If the spacing between each strip is reduced, the shear strain homogeneity remains similar whereas the shear stress distribution is lightly influence especially in the obtuse corners where the number of tension points is reduced. Few points are not at failure yet along the front and back sides. The results obtained from the conf.3 show a much different pattern compared to the three previous ones. Due to the presence of the vanes, the zone of shear strain homogeneity is extended to a larger part of the sample. The stress repartition is notably improved as well. The zones of compression and tension are reproduced in all the obtuse corners and acute corners respectively. The area of tension zones at the top and bottom of the sample are notably reduced. Furthermore the stress intensity is reduced at the top and bottom compression corners.

The figure 58 presents the shear stress repartition along the top boundary of the sample at 5% shear strain, given for the Mohr Coulomb model. Two vertical scales are considered since high stresses develop in the left (obtuse) corner for conf.1. The presence of strips and even more vanes greatly reduces the high stresses in the first 15mm on the left. Between 15mm and 95mm, the shear stress is overestimated in conf.1, conf.2a and conf.2b. It is almost zero in the last 30mm for these configurations. The advantage brought by the conf.3 is obvious here, since the shear stress is greatly reduced in the corners and the fairly homogenous zone of shear stress is extended of about 40%

compared to the conf.1. The vertical stress shows the same evolution along the top boundary since almost all the points are on the Mohr Coulomb failure surface at 5% shear strain.

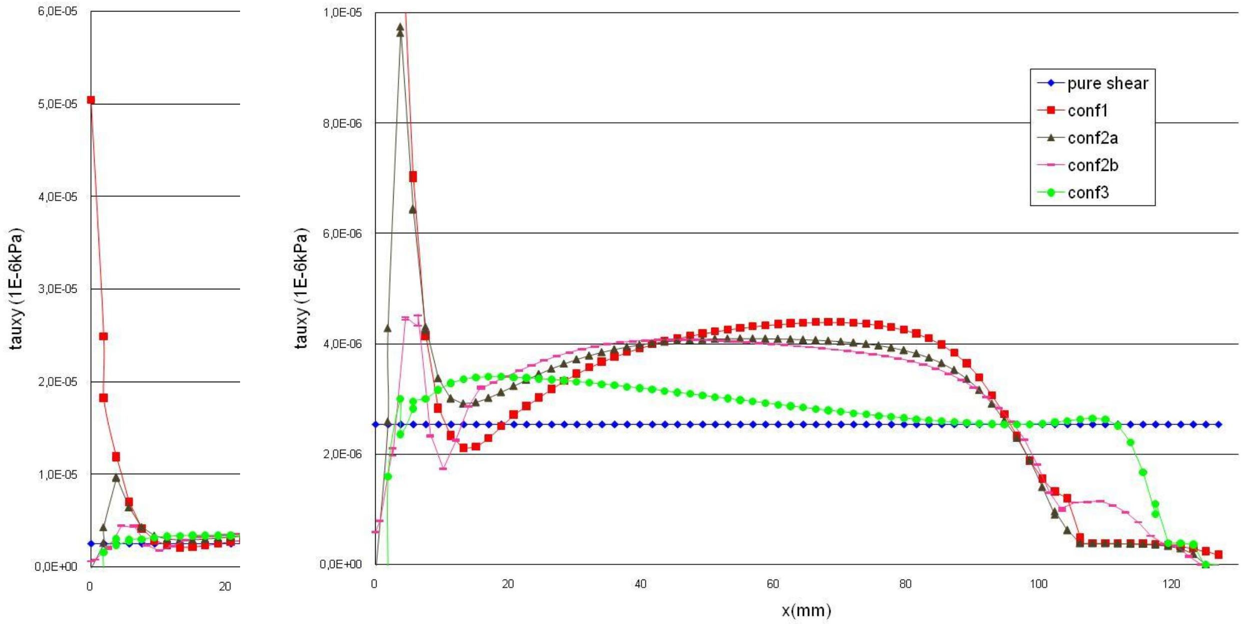

(a) (b)

Figure 58: Shear stress distribution on top of the sample with a Mohr Coulomb model, (a) real scale and (b) adapted scale

A comparison of the stress strain curves obtained with the three configurations and the pure shear condition would be desirable. However, the perfect boundary conditions considered here do not make possible such a comparison. Indeed, by taking the average shear stress or vertical stress along the top boundary (as it would be measured by a classical apparatus), the curves are increasing with the external shear strain applied without reaching a plateau as it would be expected. The rigid boundaries considered here must be responsible of this phenomenon. In particular, the high stresses in the obtuse angles are certainly overestimated. To be able to plot more realistic stress/strain curves, interfaces should be used at the sides and top and bottom of the sample. The use of interfaces is discussed in 3.6.6.

3.6.4 SOFT SOIL CREEP MODEL

An updated mesh is used with the Soft Soil Creep model since it reduces notably the time of calculation (surprisingly!). The parameters used in the simulation have been deduced from a K0-CRS test performed on the OVP clay. The results from this test are not presented here. The parameters used for the Soft Soil Creep model are presented in table 8.

For the Soft Soil Creep model, the K_0 value is influenced by the POP and OCR value according to the equation (17) (Brinkgreve et al. 2010).

$$K_0^{nx} = K_0^{nc}.OCR - \frac{\upsilon_{ur}}{1-\upsilon_{ur}}(OCR-1) + \frac{K_0^{nc}POP - \frac{\upsilon_{ur}}{1-\upsilon_{ur}}POP}{|\sigma_{yy}^0|} \quad (17)$$

The vertical stresses at the end of consolidation are similar to the one observed with the Mohr Coulomb model.

The results from the shearing phase are presented at 5% external shear strain in figure 60. Three different features are shown: the cartesian shear strain (γ_{xy}), the principal stresses (direction and values) and the nature of the stress points. A distinction is done between tension points, Mohr Coulomb and Cap points.

Table 8: Soft Soil Creep parameters

λ^*	0.111
κ^*	0.0138
μ^*	0.007
ν_{ur}	0.30
K_0^{nc}	0.5785
M	1.420
c (kPa)	0.2
φ(°)	35
Ψ (°)	0
POP (kPa)	34.5

The results differ notably from the results obtained with the Mohr Coulomb model. In the conf.1, the shear strain is localised only in the central area of the sample with more significant values in the four corners of this area. A zone all along the top, bottom and sides shows a very small shear strain. The stresses distribution is following an arching pattern. The major part of the sample is experiencing tension, especially at the sides and along the shortening diagonal of the sample. The conf.2a presents few differences considering the shear strain repartition; the strips bring only small influence at the corners. The stress homogeneity is reduced in the central part of the sample and logically increased along the strips. The major part of the specimen is still experiencing tension. Few cap points are observed at the top and bottom. The results are notably influenced by reducing the interval space between each strip (conf.2b). Shear strain is more significant locally in the four corners of the central shear strain zone. The stress homogeneity is greatly improved since tension points are only localised along the sides of the sample (and not anymore in the core). More cap points develop at the top and bottom. The results from conf.3 are showing a very different pattern for both stress and strain repartition. The shear strain is very inhomogenous in thin bands, it can reach very high values (more than 40% in these bands). The stress repartition is much more homogenous than for the two previous configurations but tension points, Mohr Coulomb points and cap points are cohexisting in all the sample. A large amounts of artefacts do not make possible to present reliable data along the top of the sample for instance.

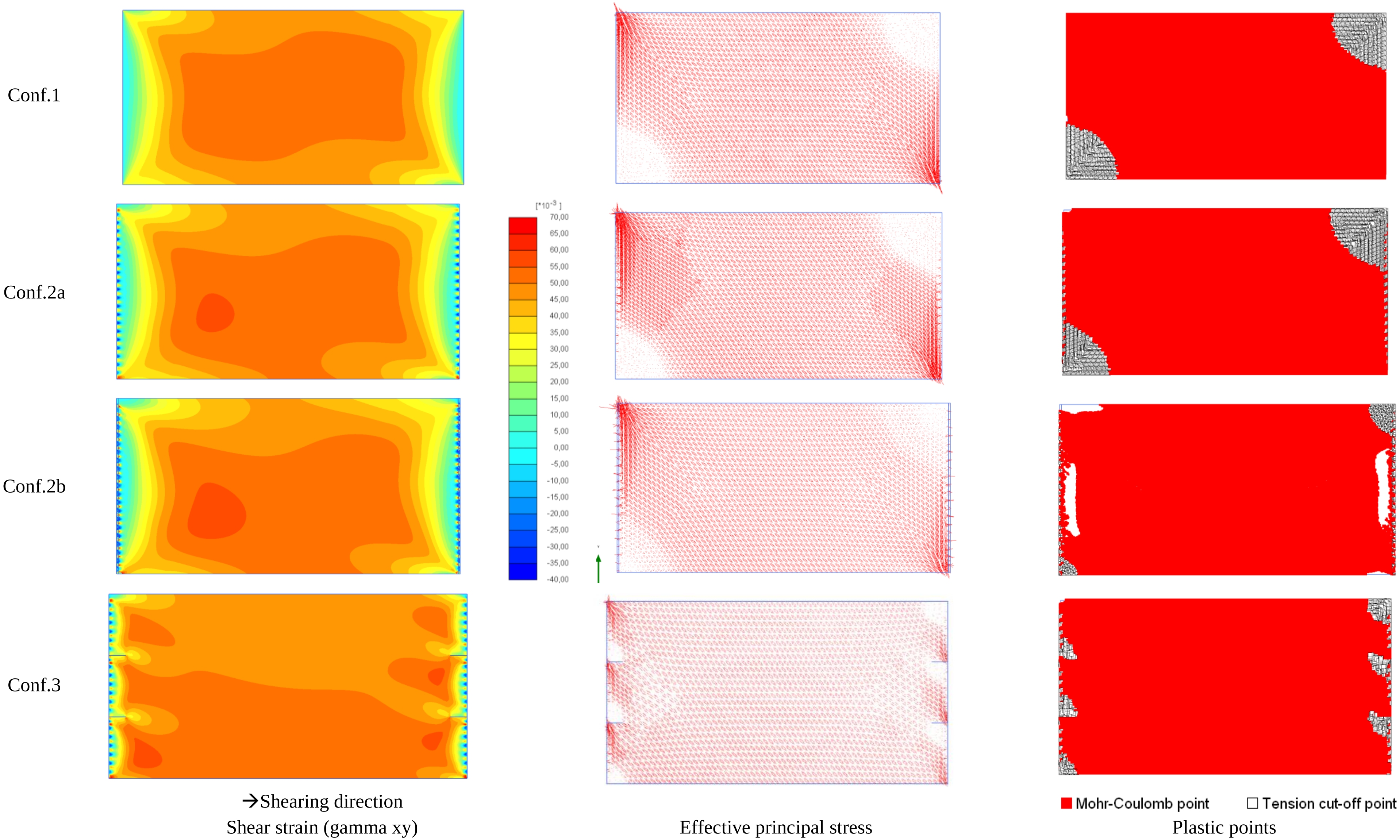

Figure 59: Results obtained with a Mohr Coulomb model (γ=5%) with perfectly rough boundaries at the top and bottom and perfectly smooth at the sides

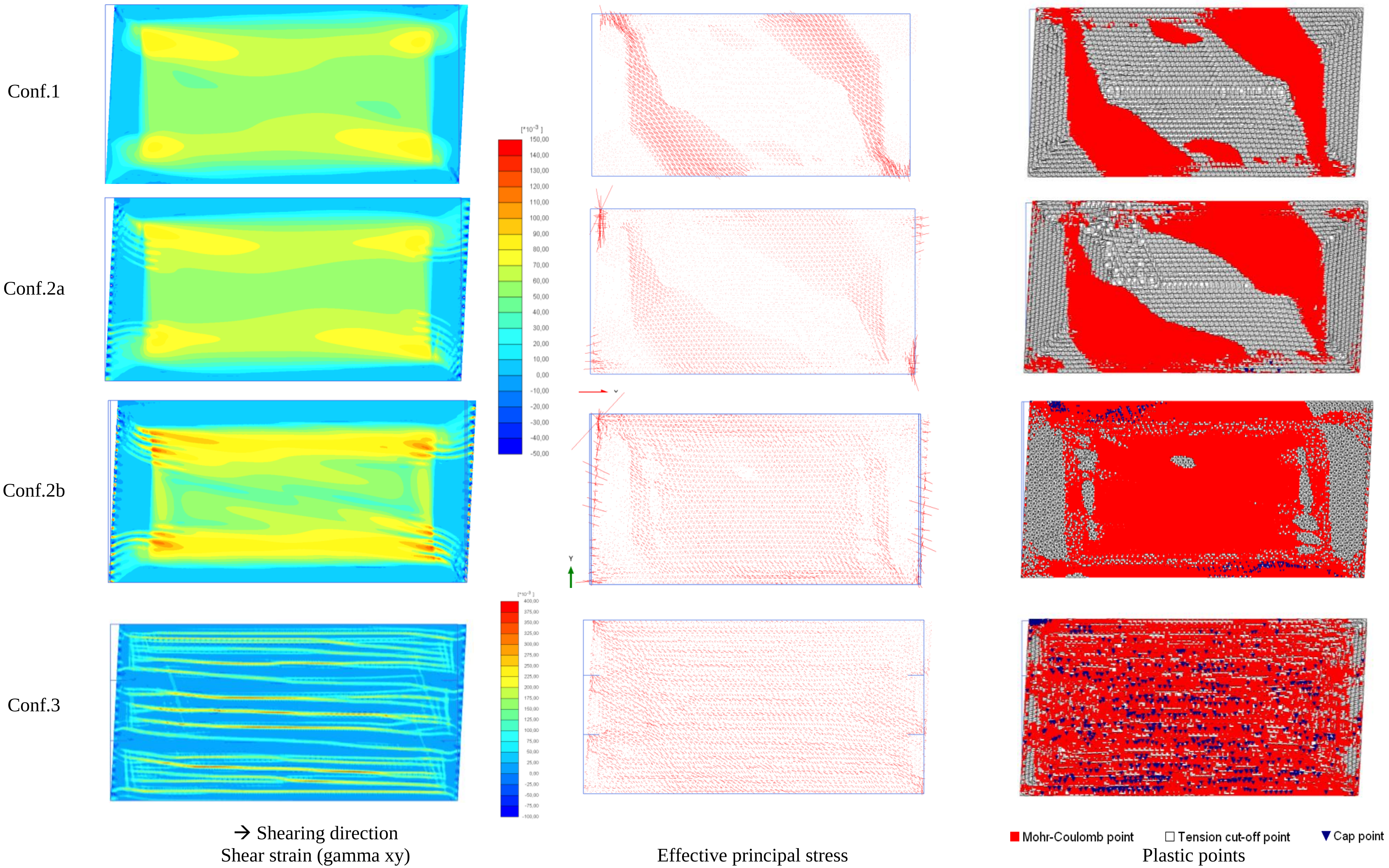

Figure 60: Results obtained with a Soft Soil Creep model (γ=5%) with perfectly rough boundaries at the top and bottom and perfectly smooth at the sides

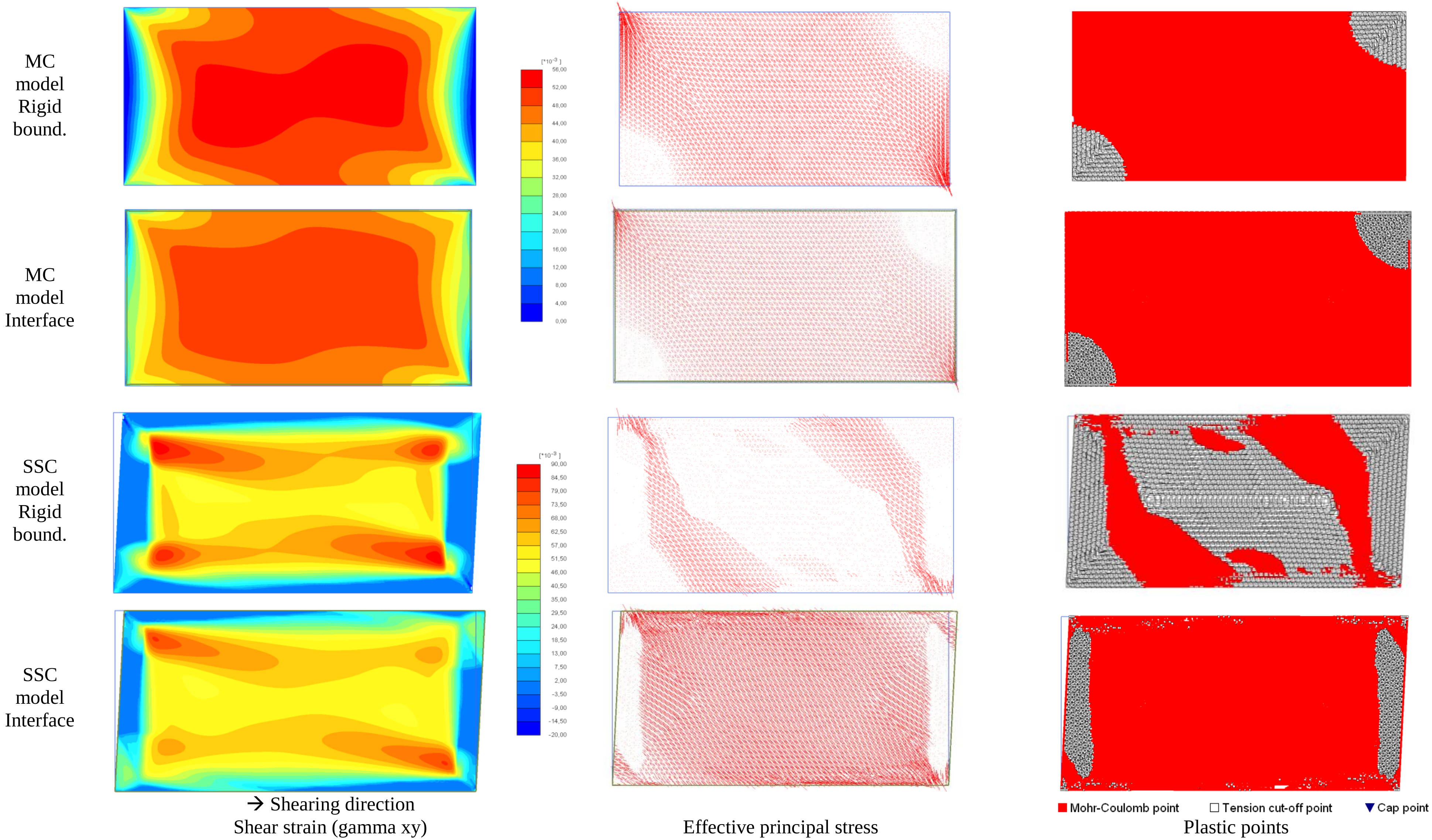

Figure 61: Comparison between rigid boundaries and interfaces with the Mohr Coulomb model and theSoft Soil Creep model

3.6.5 INTERFACES

An interface can be defined at along the boundaries of the sample. Its purpose is to give a certain amount of elastic deformation at the boundaries and in this way reduce their rigidity. Two factors are governing the behaviour of the interface: its strength factor (R_{inter}) and its virtual thickness factor. The strength factor defines its rigidity, it is 1 for rigid boundaries and 0 for completely smooth boundaries. The virtual thickness is obtained by multiplying the virtual thickness factor by the average element size. The interface characteristics considered are presented in table 9. A larger virtual thickness is considered at the top compared to the sides to simulate the effect of the sand paper. The factor of rigidity is smaller at the sides than at the top since small friction is expected.

Table 9: Interfaces characteristics

	R_{inter}	Virtual thickness factor	Equivalent thickness (mm)
Top and bottom	0.8	0.2	0.27
Sides	0.3	0.1	0.13

The influence of interface has been studied for the conf.1, for both the Mohr Coulomb model and the Soft Soil Creep model. The prescribed displacements applied at the sides do not allow the soil to move in the vertical direction anymore. The influence of the virtual thickness of the sides showed negligible variations in the results.

Concerning the results from the Mohr Coulomb model, the boundaries bring small influence on the general pattern of both shear strain and shear stresses. The shear strain is logically more homogenized by the presence of interfaces, in particular it is not zero anymore along the sides. The highest value in all the core of the sample is also lightly reduced. The stress concentration is less significant in the obtuse angles and the nature of stress points is similar.

The results from the Soft Soil Creep model are presented at the bottom of the figure 61. As for the Mohr Coulomb model the extreme values in the shear strain distribution disappear at the sides (low values) and in the core (high values). The stress distribution is greatly influenced since all the tension points have been replaced by Mohr Coulomb points in the core of the sample. Tension points are only observed along the sides, but not localised in the obtuse angles. Nonetheless, this pattern is certainly more realistic. As illustrated in figure 62, the shear stress obtained at the top boundary with an interface is much reduced in the left corner and also in the central part.

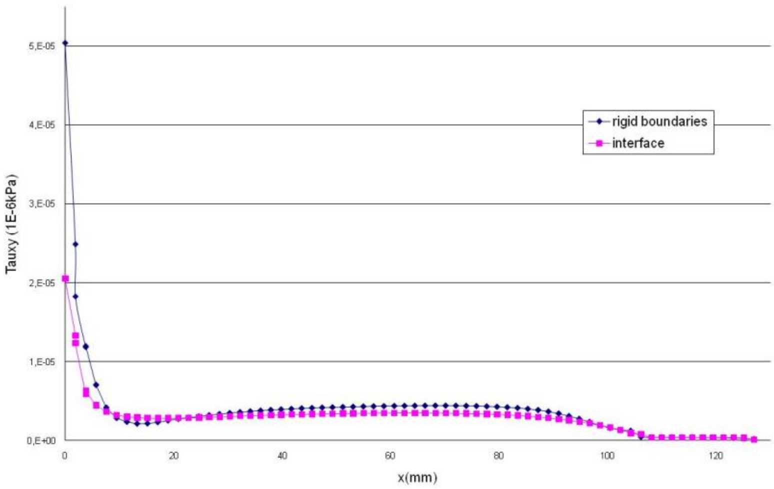

Figure 62: Shear stress distribution at the top of the sample with and without interface

Note the stress disturbance along the top and bottom boundaries. It can be reduced by reducing the virtual thickness of the interface.

3.6.6 CONCLUING REMARKS

Two models have been considered, one linear elastic perfectly plastic (Mohr Coulomb) and one visco-elasto-plastic (Soft Soil Creep).

Care has to be given to the mesh definition to avoid as possible sharp elements, especially if an advanced model is used. In particular, the time of calculation is notably improved.

The results obtained from the Mohr Coulomb model shows a positive influence of the strips the stress homogeneity if the spacing between each strip is realistic. The adding of vanes notably increases the stress and strain homogeneity, in particular along the top boundary. Much more than the typical central third of stress homogeneity is obtained.

The results of Soft Soil Creep model show large zones of tensions throughout the soil sample for straight perfectly smooth boundaries. The stress homogeneity is largely influenced by the presence of strips with thin spacing at the sides. The results obtained with the vanes (conf.3) appear unrealistic and might be due to the rigid interface considered. Furthermore, many artefacts are observed with this model.

In general the conf.2a is too close to conf.1 to show clear differences. The stress-strain homogeneity might be even more reduced with a thinner spacing between each strip in conf.3. It could not be considered with the actual model and very fine mesh.

The rigid boundaries on top and bottom and perfectly smooth boundaries on the sides are certainly overestimating the stress concentration in the obtuse (compression) corners. This effect is increasing with the external shear strain applied. These boundaries do not make possible to plot realistic stress/strain curves as it would be measured in classical apparatus. A closer modellisation of the experimental conditions can certainly be obtained by using interface of appropriate thickness at the sides and top and bottom. This method might reduce the differences observed between the three configurations considered. Further modellisation should be performed in this direction since the purpose of such a study would be to evaluate the effect of the boundaries on stress-strain curves. The improvement should provide curves closer to the ideal pure shear curves.

The comparison of the modellisation results of strain distribution with experimental results is a difficult task. Indeed, the boundaries considered in the modellisation are perfectly rigid at the top and perfectly smooth along the front and back side which is obviously not the case in the experimental device. Some similarities can be observed anyway. The shear strain homogeneity is localised in the central part of the sample and remains low along the sides at least in conf.1. This result is also given by the finite element software. Furthermore, the reduction of tension zones in the obtuse angle with the Mohr model is also visible in the experiment by separation of the soil from the platen.

CONCLUSION

For now sixty years, the direct simple shear device has been in use in the geotechnical laboratories since it can mimic closely certain in situ conditions. One major advantage of this test is the rotation of the principal stress direction which is not observed in triaxial device for instance. Due to the lack of additional shear stresses provided at the front and back side of the specimen, stress inhomogeneities develop along all the boundaries. Therefore, the sides of the specimens are made as smooth as possible to reduce this effect and very thin geometries of samples (height over diameter ratio of 0.2-0.3) are used to limit the development of the inhomogeneities at the sides and keep the major part of the sample in a homogenous state of stress and strain. Due to the occurrence of peat dyke failure or peat slope failure in the Netherland and all over the world (Pigott et al. 1992, Van Baars 2005, Boylan and Jennings 2006) the direct simple shear tests knows a renewed interest for peat testing at low vertical stress. The behaviour of peat is largely governed by its anisotropy and fibrosity. Therefore, it is desirable to use larger sample with larger height over diameter ratio to take into account the influence of the peat structure (fibres, wood remnants). Some promising work has been done in this direction already (Boylan and Long, 2009).

A series of tests has been performed at various vertical stresses, on a wood and sedge peat from the North of the Netherlands with a classical Geonor device. The results obtained from two different boundaries, the classical reinforced membrane and an unreinforced membrane surrounded by a stack of rings, were compared. The results from each boundary show small differences in term of cohesion, friction angle and initial shear modulus. A more adapted compliance test for the horizontal resistance would be necessary in case of the stack of rings. Furthermore, some limitations of the Geonor device have been observed in case of peat testing at low normal stress.

- The simple shear state cannot be ensured since the shearing is applied at the top of the specimen and not at the sides. Most of the time, the sides do not remain in a straight shape during the shearing.
- Normal loads smaller than 10kPa cannot be reached in the actual configuration. It can certainly be fixed by updating the vertical load system (amplifier).
- A significant portion of the shear resistance measured is due to the friction of the apparatus and to the stiffness of the boundaries. It should be reduced to ensure accurate measurements at low vertical stresses. Being able to get rid of the membrane between the stack of rings would reduce notably the shear stress due the apparatus itself.
- No visual assessment of the sample deformation is possible to check if slippage is occurring or not at the top and bottom of the sample. It is desirable at low vertical stress.

A prototype of direct simple shear test has been developed for larger samples at low vertical stress. The effect of two innovative rough boundaries on the strain homogeneity of the sample has been investigated. A visual assessment of the deformation as well as a Particle Image Velocimetry analysis has been performed. The results from remoulded soft clay samples are encouraging since the shear strain homogeneity is increased inside of the sample. Furthermore, the separation of the soil from the top platen is reduced in the acute corners and so should be tensile forces. These results are limited since slippage has been observed at the top of the sample and no load measurements could be performed. The vertical load applied might have been different in the three cases considered and then influence the strain homogeneity during shearing. Further developments of the prototype are needed in order to provide reliable results. Fixing the slippage and adapt load cells to the prototype should be the first steps. The comparison of the stress-strain curves measured with each boundary is desirable in order to quantify the improvement. Various peat samples should be tested as well.

A finite element analysis of the prototype boundaries has been performed with two models, the Mohr Coulomb model and the Soft Soil Creep model. The influence of the new boundaries has been investigated with perfect rigidity at the top and perfect smoothness at the sides. The stress and strain homogeneity is increasing in the sample with the presence of strips and vanes compared to classical straight boundaries. The spacing between each strip is found to have a clear influence on the state in the core of the specimen. The initial mesh has to be defined with care to avoid sharp elements since small spacing between points are used. Results from the Soft Soil Creep model show a large amount of tension developing in the entire specimen, probably due to the rigid boundaries considered. Realistic stress/strain curves could not be obtained with a method similar to the measurements in classical tests, by averaging the shear and normal stress from the top of the sample. The use of interfaces with different characteristic at the top and bottom might solve these limitations and give more realistic results. Though, the differences between the different configurations might be less obvious. A three dimensional analysis would be desirable, in particular if cylindrical samples are considered in the future to investigate the assumption of plane strain deformation.

BIBLIOGRAPHY

Aas G. (1980), Vurdering av korttidsstabilitet i leire pa basis av undrenert skjaerfasthet, *NGI publication 132*, Beretning over NGIs virksomhet fra 1 Jan 1978-31 Dec 1979, 21-30

Airey D.W. and Wood D. (1984), Discussion on: Specimen size effect in simple shear test, *Journal of Geotechnical Engineering Division*, ASCE Vol.110 No.3, 439-442

Airey D. W., Budhu M. and Wood D. M. (1985), Some aspects of the behaviour of soils in simple shear, *Developments in soil mechanics and foundation engineering*, Banerjee P.K. and Butterfield R. (Editors), Vol.2, London: Elsevier

Airey D. W. and Wood D.M. (1986), Pore pressure in simple shear, *Soils and foundations*, Vol.26 No.2, 91-96

Airey D. W. and Wood D.M. (1987), An evaluation of direct simple shear tests on clay, *Géotechnique*, Vol.37 No.1, 25-35

Bjerrum L. and Landva A. (1966), Direct simple shear tests on a Norwegian quick clay, *Géotechnique*, Vol.16 No.1, 1-20

Boylan N., Jennings P. and Long M. (2008), Peat slope failure in Ireland, *Quarterly Journal of Engineering Geology and Hydrogeology*, 41, 93-108

Boylan N. and Long M. (2009), Development of a direct simple shear apparatus for peat soils, *Geotechnical testing journal*, Vol.32 No.2, 1-13

Brinkgreve R.B.J., Swolfs W.M. and Engin E. (2010), *Plaxis 2D 2010*, Plaxis bv, Delft

Budhu M. (1984a), Discussion on: Specimen size effect in simple shear test, *Journal of Geotechnical Engineering Division*, ASCE Vol.110 No.3, 442-445

Budhu M. (1984b), Nonuniformities imposed by simple shear apparatus, *Canadian Geotechnical Journal*, Vol.21 No.1, p125-137

Budhu M. and Britto A. (1987), Numerical analysis of soils in simple shear devices, *Soils and foundations*, Vol.27 No.2, 31-41

Christian J.T. (1981), Discussion on: State of the Art: Laboratory strength testing of soils, *Laboratory shear strength of soils*, ASTM STP 740, Young R.N. and Townsend F.C. (Editors), 638-640

DeGroot D.J., Germaine J.T. and Gedney R. (1991), An automated electropneumatic control system for direct simple shear testing, *Geotechnical testing journal*, Vol.14 No.4, 339-348

Doherty J.P. and Fahey M. (2011), A three dimensional finite element study of the direct simple shear test, *Frontiers in offshore geotechnics II*, Gourvenec and White (editors), 341-346

Duncan J.M. and Dunlop P. (1969), Behavior of soils in simple shear tests, *Proc 7th ICSMFE*, 1, 101-109

Dyvik R., Berre T., Lacasse S. and Raadim B. (1987), Comparison of truly undrained and constant volume direct simple shear tests, *Géotechnique*, Vol.37 No.1, 3-10

Farrell, E.R. and Hebib S. (1998), The determination of the geotechnical parameters of organic soils, *Proceedings of international symposium on problematic soils*, IS-TOHOKU 98, Sendai, Japan, 33-36

Farrell E.R., Jonker S.K., Knibbeler A.G.M. and Brinkgreve R.B.J. (1999), The use of direct simple shear test for the design of a motorway on peat, *Geotechnical engineering for transportation infrastructure*, Barends et al. (editors), Balkema, Rotterdam, 1027-1033

Finn W.D.L., Pickering D.J and Bransby P.L. (1971), Sand liquefaction in triaxial and simple shear tests, *Journal of the soil mechanics and foundations division*, SM4, 639-659

Franke E., Kiekbusch M. and Schuppener B. (1979), A new Direct Simple Shear device, *Geotechnical testing journal*, Vol.2 No.4, 190-199

den Haan E.J. (1987), Het simple shear apparatus, technical report, Grondmechanica Delft

den Haan E.J. and Kruse G.A.M. (2007), Characterisation and engineering properties of Dutch peats, *Characterisation and Engineering Properties of Natural Soils,* Tan, Phoon, Hight & Leroueil (Editors).Taylor & Francis, London, 2101-2133.

Den Haan E.J. (2009), Deformatie en sterkte van ophogingen en dijken op slappe Nederlandse grond, *Geotechniek* vol 55, 52-55

Hayashi S., Ochiai H., Yoshimoto A., Sato K. and Kitamura T. (1988), Functions and effects of reinforcing materials in earth reinforcement, *Proceedings of International Geotechnical Symposium on Theory and Practice of Earth Reinforcement*, Fukuoka, 5-7 October, pp 99-104.

Hobbs N.B. (1986), Mire morphology and the properties and behaviour of some British and foreign peats, *Quarterly Journal of Engineering Geology*, London, Vol.19, 7-80

de Jong A.K. (2007), *Modelling peat dike stability: back analysis of direct simple shear test results,* MSc thesis report, Delft University of Technology

de Josselin de Jong G. (1971), Discussion on stress-strain behavior of soils, *Proc. Roscoe Memorial Symposium*, Parry R.H.G. (Editor), 258-261, Cambridge: Foulis

Kjellman W. (1951), Testing the shear strength of clay in Sweden, *Géotechnique*, Vol.2, No. 3, 225-235

Kondner R.L. (1963), Hyperbolic stress-strain response: cohesive soils, *Journal of the soil mechanics and foundation division*, SM1, 115-143

Kovacs, W.D. (1973), Effect of sample Configuration in simple shear testing, *Proc symposium on behaviour of Earth and Earth structures subjected to Earthquakes and other dynamic loads*, Roorkee, India, 1973, 82-86

Lacasse S. and Vucetic M., (1981), Discussion on: State of the Art: Laboratory strength testing of soils, *Laboratory shear strength of soils,* ASTM STP 740, Young R.N. and Townsend F.C. (Editors), 633-637

Ladd C.C. (1981), Discussion on: State of the Art: Laboratory strength testing of soils, *Laboratory shear strength of soils*, ASTM STP 740, Young R.N. and Townsend F.C. (Editors), 643-652

Landva A.O. and Pheeney P.E. (1980), Peat fabric and structure, *Canadian geotechnical journal* 17, 416-435

Landva A.O., Korpijaakko E.O. and Pheeney P.E. (1983), Geotechnical classification of peats and organic soils, *Testing of peats and organic soils*, ASTM STP 820, Jarrett P.M. (Editor), American Society for Testing Material, 37-51

Landva A.O. and La Rochelle P. (1983), Compressibility and shear characteristics of Radforth peats, *Testing of peats and organic soils*, ASTM STP 820, Jarrett P.M. (Editor), American Society for Testing Material, 157-191

La Rochelle P. (1981), Discussion on: State of the Art: Laboratory strength testing of soils, *Laboratory shear strength of soils,* ASTM STP 740, Toung R.N. and Townsend F.C. (Editors), 653-658

Long M. and Jennings P. (2006), Analysisof the peat slide at Pollatomish, County Mayo, Ireland, *Landslides* 3 51-61

Lucks A.S., Christian J.T., Brandow G.E. and Hoeg K. (1972), Stress condition in NGI simple shear test, *Journal of the soil mechanics and foundation division*, ASCE, Vol.98 SM1, 155-160

MacFarlane I.C. and Radforth M.W. (1964), A study of the physical behaviour of peat derivatives under compression, *Proceedings of the 10th Muskeg Conference*, Technical Memorandum 85, Ottawa

Magnan J.P. (1994), Construction on peat: state of the art in France, *Advances in understanding and modelling the mechanical behaviour of peat*, den Haan, Termaat and Edil (Editors), Balkema, Rotterdam, 369-379

Morgenstern N.R. and Tchalenko J.S. (1967), Microscopic structures in Kaolin subjected to direct shear, *Géotechnique* Vol.17, 309-328

NEN-5104 (1989), Classificatie van onverharde grondmonsters, Nederlands Normalisatie instituut, Delft

Oda M. and Konishi J. (1974): Rotation of principal stresses in granular material during simple shear, *Soils and foundations*, Vol.14, No.4, 39-53

Pigott P.T., Hanrahan E.T. and Somers N. (1992), Major canal reconstruction in peat areas, *Proc. Instn Civ. Engrs Wat. Marit. And Energy*, Vol.96 (sept), 141-152

Potts D.M., Dounias G.T. and Vaughan P.R. (1987), Finite element analysis of the direct shear box test, *Géotechnique* 37, No.1, 11-23

Prevost J. H. and Hoeg K. (1976), Reanalysis of simple shear soil testing, *Canadian geotechnical journal*, Vol.13 No.4, 418-429

Radforth N.W. (1952), Suggested classification of Muskeg for the engineer, *The engineering journal*, Nov 1952

Roscoe K.H. (1953), An apparatus for the application of simple shear to soil samples, *Proceedings third ICSMFE* 1, 186-191

Roscoe K.H., Bassett R.H. and Cole E.R.L. (1967), Principal axes observed during Simple Shear of sand, *Proc. Conference on shear strength properties of natural soils and rocks*, Oslo, Vol 1, 231-237

Saada A.S. and Townsend F.C., (1981), State of the Art: Laboratory strength testing of soils, *Laboratory shear strength of soils*, ASTM STP 740, Young R.N. and Townsend F.C. (Editors), 7-77

Saada A.S., Fries G. and Ker C.C. (1983), An evaluation of laboratory testing techniques in soil mechanics, *Soils and foundations*, Vol.23 No.2, 98-112

Shen C.K. Sadigh K. and Herrmann L.R. (1978), An analysis of NGI simple shear apparatus for cyclic soil testing, *ASTM Dynamic geotechnical testing*, STP 654, 148-162

Sintubin M, Debacker T.N. and Van Baelen H. (2009), Early Palaeozoic orogenic events north of the Rheic suture (Brabant, Ardenne): a review, *C.R. Geoscience 341*, 156-173

Skempton A.W.and Petley D.J. (1970), Ignition loss and other properties of peats and clays from Avonmouth, King's Lynn and Cranberry Moss, *Géotechnique* 20, No.4, 343-356

TAW (1996), *Technisch rapport Geotechnische classificatie van veen*, Technische adviescommissie voor de Wateringen, Delft

Terzaghi, K., Peck, R. B. and Mesri (1996), G., *Soil Mechanics in Engineering Practice, 3rd Ed.* Wiley-Interscience

Uesugi M. and Kishida H. (1986), Frictional resistance at yield between dry sand and mild steel, *Soils and foundations* Vol.26, No.4, 139-149

Van Baars S. (2005), The horizontal failure mechanism of the Wilnis peat dyke, *Géotechnique* 55 No.4, 319-323

Van Baelen H. And Sintubin M. (2008), Kinematic consequences of an angular unconformity in simple shear: an example from the southern border of the Lower Palaeozoic Rocroi inlier (Naux, France), *Bull. Soc. Geol.. Fr.*, t.179, No1, 73-87

Von Post L. (1922), Sveriges Geologiska Undersoknings torvinventering och nogra av dess hittils vunna resultat (SGU peat inventory and some preliminary results), *Svenska Mosskulturforeningens Tidskrift*, Jonkoping, Sweden, 36, 1-37

Vucetic M. and Lacasse S. (1982), Specimen size effect in simple shear test, *Journal of Geotechnical Engineering Division*, ASCE Vol.108 GT12, 1567-1585

Wood D.M., Drescher A. and Budhu M. (1979), On the determination of stress state in the simple shear apparatus, *Geotechnical testing journal*, Vol.2 No.4, p211-221

White D.J., Take W.A. and Bolton M.D. (2003), Soil deformation measurement using particle image velocimetry (PIV) and photogrammetry, *Géotechnique* 53, No.7, 619-631

Wright D.K., Gilbert P.A. and Saada A.S. (1978) Shear devices for determining dynamic soil properties, *Proc specialty conference on Earthquake Engineering and soil dynamics*, ASCE, Vol 2, 1056-1075

Wroth C.P. (1984), The interpretation of in situ soil tests (24th Rankine lecture), *Géotechnique* 34, No.4, 449-489

Wroth C.P. (1987), The behaviour of normally consolidated clay as observed in undrained direct shear tests, *Géotechnique* 37, No.1, 37-43

LIST OF FIGURES

LIST OF TABLES

APPENDIX A: ON POST CLASSIFICATION SYSTEM

Degree of humification	Decomposition	Plant structure	Content of amorphous material	Material extruded on squeezing (passing between fingers)	Nature of residue
H_1	None	Easily identified	None	Clear, colourless water	
H_2	Insignificant	Easily identified	None	Yellowish water	
H_3	Very slight	Still identifiable	Slight	Brown, muddy water; no peat	Not pasty
H_4	Slight	Not easily identified	Some	Dark brown, muddy water; no peat	Somewhat pasty
H_5	Moderate	Recognizable, but vague	Considerable	Muddy water and some peat	Strongly pasty
H_6	Moderately strong	Indistinct (more distinct after squeezing)	Considerable	About one third of peat squeezed out; water dark brown	
H_7	Strong	Faintly recognizable	High	About one half of peat squeezed out; any water very dark brown	
H_8	Very strong	Very indistinct	High	About two thirds of peat squeezed out; also some pasty water	Plant tissue capable of resisting decomposition (roots, fibres)
H_9	Nearly complete	Almost not recognizable		Nearly all the peat squeezed out as a fairly uniform paste	
H_{10}	Complete	Not discernible		All the peat passes between the fingers; no free water visible	

Figure 63: Degree of humification according to the Von Post system (1922)

APPENDIX B: PEAT CHARACTERISTICS AND DETAILED TEST RESULTS

Table 10 Detail of the peat sample characteristics
Samples with blue color have been tested with a reinforced membrane, samples with red lines have been tested with the stack of rings

Sample	Wood content (%)	bulk density wet (Mg/m3)	Unit weigth (kN/m3)	W(%) initial	W(%) after test	Loss on ignition (%)	Org content (%) Skempton	CaCO3 (%)	Spec gravity (Skempton) Mg/m3	e	Sr (%)	Initial vert. stress (kPa)	h initial (mm)	settlement (mm)	H/D	tau (10%)	sigv (10%)	tau (40%)	sigv (40%)	G (Buisman)
a1	30	0,976	9,58	581	535	79	78	1,603	1,55	10,09	0,89		20	1,98						
a2	10	0,954	9,36	580	490	79	78	1,523	1,56	10,36	0,87		20	2,08						
a3	5	0,805	7,89	573	562	81	81	1,588	1,54	12,14	0,72	31,1	20	2,6	0,28	11,31	24,95	14,22	21,33	0,4006
a4	10	0,887	8,70	508	461	68	67	1,74	1,65	10,60	0,79		20	3,84						
a5	10	0,984	9,66	572	577	80	79	1,541	1,55	9,82	0,90	30,6	20	4,42	0,25	11,44	22,95	15,03	16,37	0,27
a6	50	1,050	10,30	557	537	77	76	1,563	1,58	9,08	0,97	29,8	20	3,16	0,27	10,89	23,27	14,08	17,77	0,4221
a7	10	0,952	9,34	569	527	82	81	1,491	1,53	10,02	0,87	30	20	2,32	0,28	11,96	23,48	15,36	19,61	0,4092
a8	10	0,928	9,11	579	575	76	75	1,593	1,58	10,84	0,84	10,6	20	0,95	0,30	6,57	9,61			0,3729
a9	40	1,039	10,19	552	523	70	68	1,599	1,64	9,51	0,95	10,5	20	1,06	0,30	6,91	8,89	9,09	9,48	0,2657
a10	10	0,919	9,01	539	550	69	68	1,519	1,64	10,68	0,83	11	20	1,23	0,30	9,1	9,25	10,13	9,97	0,54
a11	50	0,992	9,73	588	541	74	73	1,399	1,60	10,31	0,91	11,2	20	0,92	0,30	7,81	9	11,32	9,75	0,2557
a12	30	0,935	9,17	620	539	74	73	1,437	1,60	11,60	0,85		20	0,68	0,31	7,41	7,69	9,27	8,84	
a13	20	0,911	8,93	630	455	75	74	1,362	1,59	12,07	0,83	53,2	20	7,34	0,20	17,66	47,34	22,69	41,21	0,571
a14	20	0,955	9,37	635	525	85	85	1,424	1,51	10,84	0,88		20	7,05						
a15	40	0,903	8,85	528	461	74	73	1,326	1,60	10,40	0,81	49,5	20	5,96	0,22	19,06	41,08	21,98	34,09	0,418
a16	15	0,928	9,11	535	428	70	69	1,672	1,63	10,44	0,84	49	20	7,18	0,20	16,16	40,99	20,62	30,6	0,321
a17	20	0,935	9,17	512	375	64	62	1,416	1,70	10,35	0,84	49,6	20	6,88	0,21	17,52	41,96	23,77	32,82	0,364
a21	30	0,936	9,18	542	321	70	69	1,249	1,63	10,44	0,85	112,7	30	16,12	0,22	40,65	93,07	50,53	76,71	0,98
a22	30	0,977	9,26	588	329	75	74	1,216	1,59	10,87	0,86	115,6	30	16,63	0,21	41,86	96,87	48,41	72,02	1
a23	20	0,920	9,24	586	331	71	70	1,352	1,60	10,89	0,86	110,7	30	16,53	0,21	42,91	94,67	50,01	78,36	2,45
a24	5	1,030	9,23	516	269	62	60	1,326	1,60	9,68	0,85	108,7	30	15,663	0,2	37,26	94,83	45,91	75,06	0,971
min	**5**	**0,887**	**8,70**	**508**	**269**	**62**	**60**	**1,216**	**1,51**	**9,08**	**0,79**									
max	**50**	**1,050**	**10,30**	**635**	**577**	**85**	**85**	**1,74**	**1,70**	**12,07**	**0,97**									
average	**22**	**0,948**	**9,26**	**566**	**472**	**74**	**73**	**1,47**	**1,59**	**10,44**	**0,86**									

APPENDIX C : CONSOLIDATION CURVES FROM GEONOR TESTING

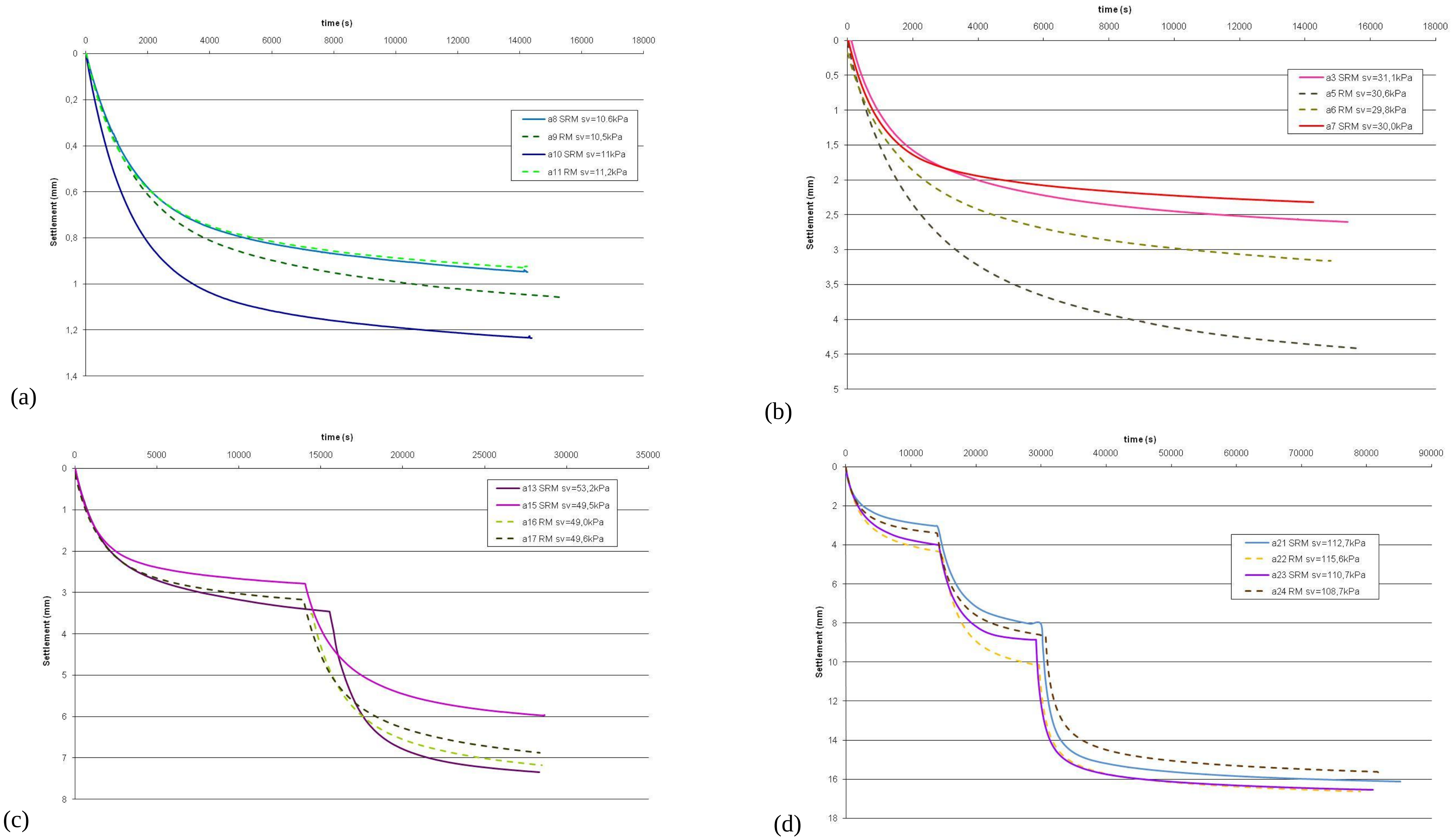

Figure 64 : Consolidation curves obtained at vertical stress of 10kPa (a) 30kPa (b) 60kPa (c) and 120kPa (d)

APPENDIX D: DETAILS OF THE KONDNER METHOD

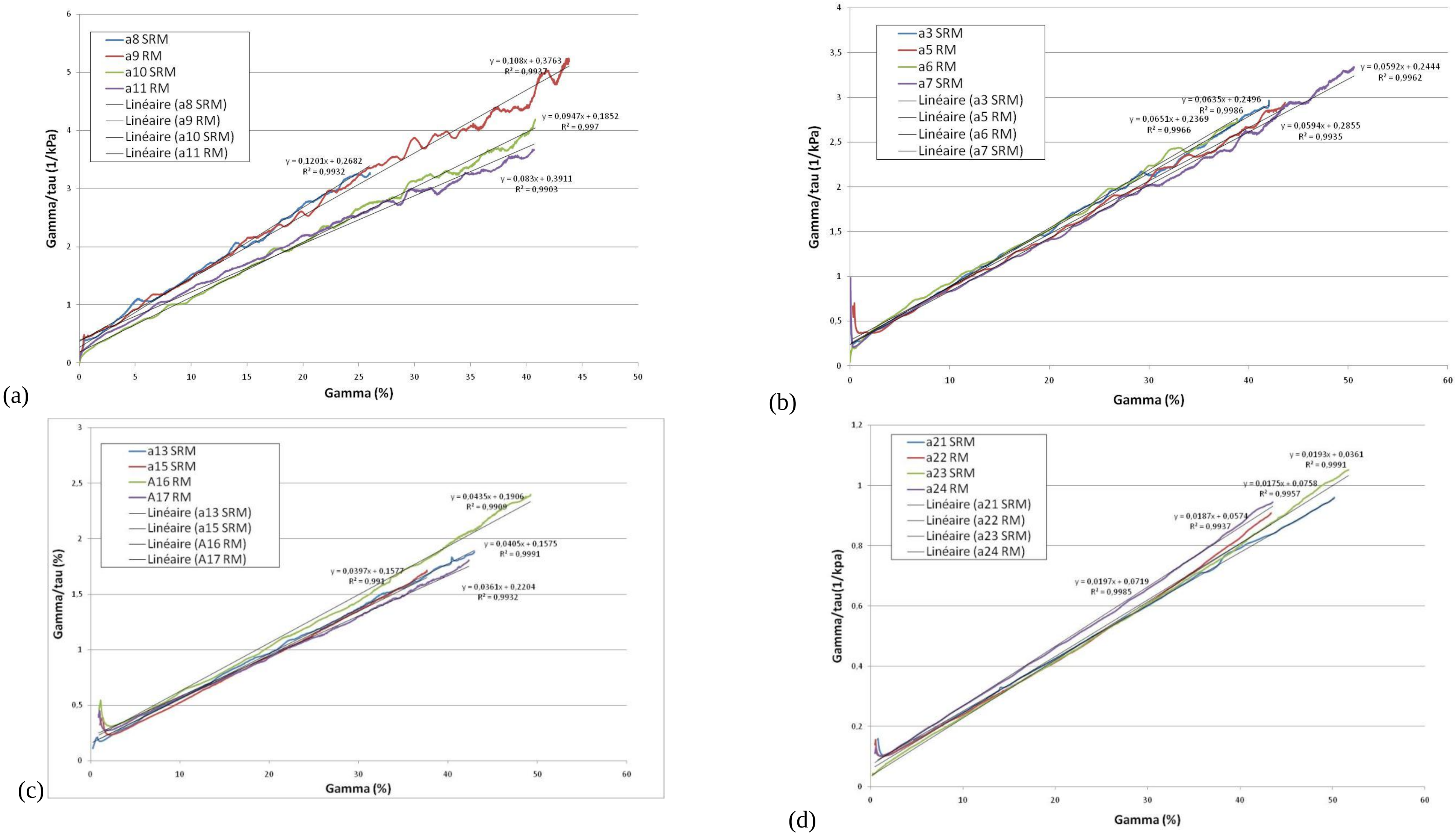

Figure 65: Transformed hyperbolic representation (Kondner 1963) for tests performed at vertical stress of 10kPa (a), 30kPa(b), 60kPa (c) and 120kPa(d)

APPENDIX E: FINITE ELEMENT MODELLISATION OF THE GEONOR DEVICE FOR MEMBRANE CALIBRATION PURPOSE

The purpose of this finite element study is to obtain the horizontal stress evolution during shearing in the Geonor device. This variation of horizontal stress is then used with the correction method (3) to apply a non linear correction on the tests results. One single test at 120kPa vertical stress is considered. The stresses are measured as the average stresses along the top or side boundaries (as it would be measured in the Geonor device). The Soft Soil Creep model is used with the parameters similar to the one used by den Haan (2009).

The mesh is presented in figure 65, the sample dimension are h=16mm and l=63mm. The shearing is applied by prescribed displacement with rough boundary at the top and bottom and with smooth boundary at the sides.

The results from the modellisation are presented in figure 66 and figure 67. A rough correspondence with test results can be observed and is suitable enough for the correction considered. The parameters of the model can be adapted to obtain a better fit with test results according to de Jong (2007) study.

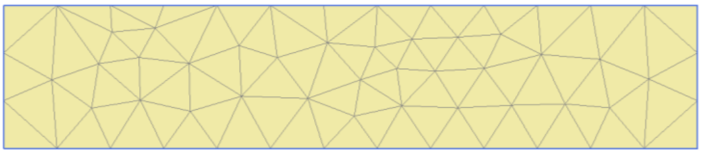

Figure 66: Mesh Geonor sample

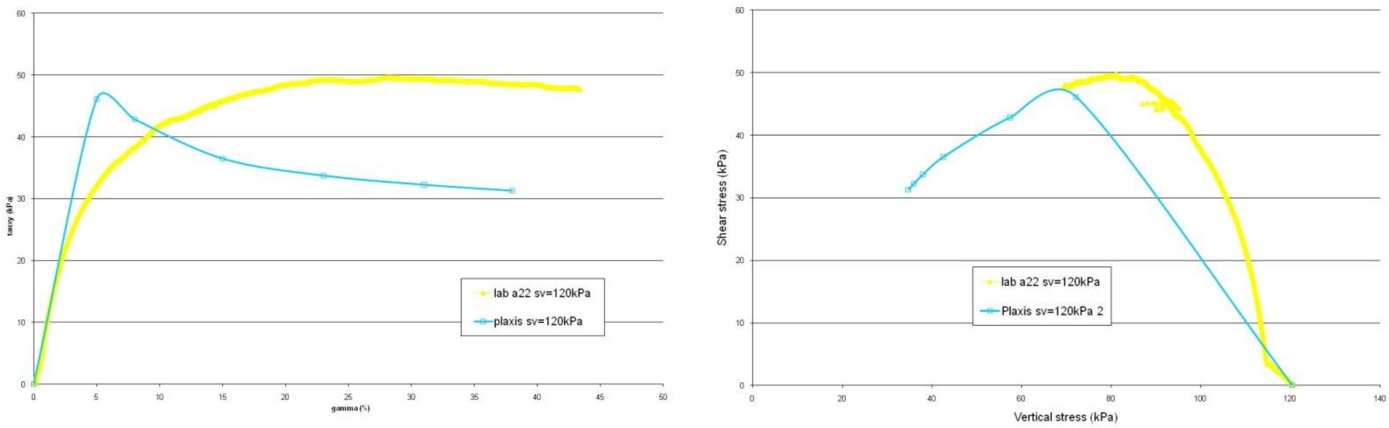

Figure 67 : Results from finite element modellisation of the peat sample in the Geonor device

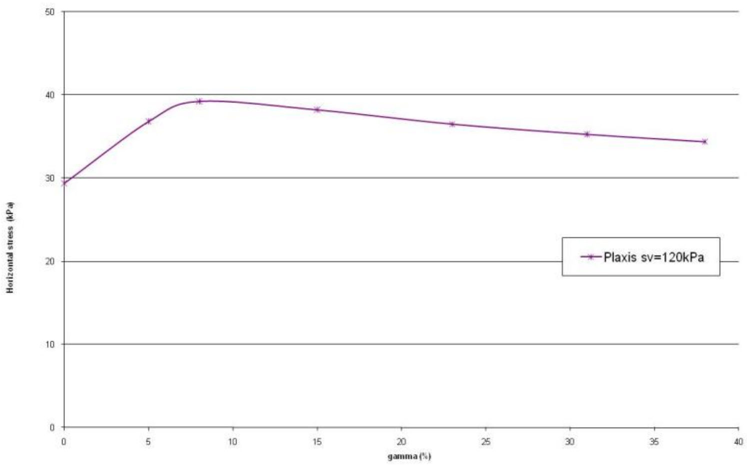

Figure 68: Horizontal stress along the sides

APPENDIX F: FINITE ELEMENT MODELLING OF THE DIRECT SIMPLE SHEAR DEVICE AND DIRECT SHEAR DEVICE (REPRODUCTION OF SOME RESULTS FROM THE LITERATURE)

Key studies have been selected from the literature and reproduced with Plaxis 2D. The purpose of these reproductions is to gain confidence with the software and become familiar with the methods already used to model shear tests.

F-1 THE EFFECT OF SLIPPAGE ON DIRECT SIMPLE SHEAR TEST (LINEAR ELASTIC ANALYSIS): PREVOST AND HOEG (1976)

Prevost and Hoeg (1976) expanded the mathematical analysis proposed by Roscoe (1953) in order to investigate the effect of slippage on stress and strain distribution in the direct simple shear sample. This study assumes a linear elastic material. Its characteristics are detailed in table 11. The sample dimensions are l=80mm h=20mm. A vertical load of 200kPa is applied on top of the sample. Lambda is the factor of slippage varying between 0 ans 0.5 in the study. A sinusoidal displacement was considered by Prevost and Hoeg (figure 68) but was not possible to apply with Plaxis. A linear approximtion was used instead as detailed in figure 69. The mesh considered (630 15 noded-elements) is illustrated in figure 70. The boundaries considered are perfectly smooth at the sides: a prescribed is applied in the horizontal direction and the soil displacement in the vertical direction is free.

Table 11: Elastic parameters (Prevost and Hoeg 1976)

ν	0,333
E (MPa)	2 667

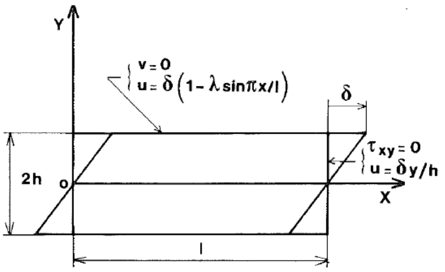

Figure 69: Boundary conditions from Prevost and Hoeg(1976)

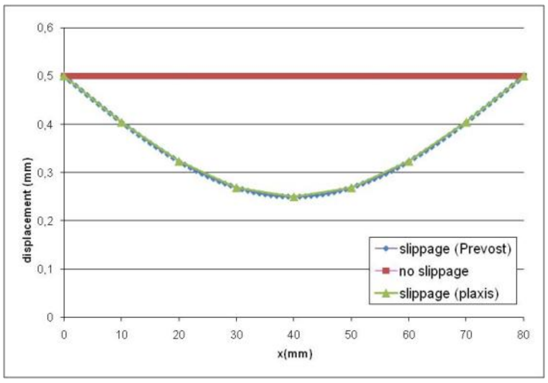

Figure 70: Displacement applied with Plaxis (lambda=0.5)

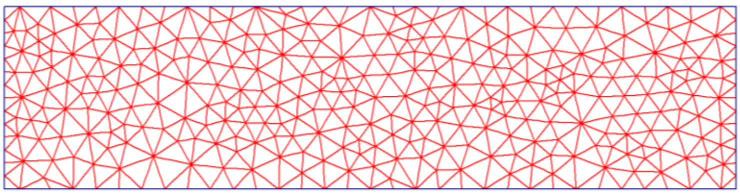

Figure 71: Mesh of the dss sample

The comparison between the mathematical analysis results and the finite element analysis results is presented in figure 71. A good correspondence is observed for all the curves. The disturbance in the shear stress and vertical stress curves is a consequence of the linear approximation of the sinusoidal displacement in Plaxis. The only significant difference observed is the shear stress in the two corners which is zero with the mathematical analysis and not with finite element analysis. Furthermore, the results from the mathematical analysis show infinite values of the vertical and horizontal stress in the corners of the sample. Roscoe (1953) noted that there is a slight incompatibility in the boundary conditions imposed by the mathematical analysis. It is not physically possible to impose an angle of shear at the corner and at the same time require that the shear stress is zero. Further details are given about the shear stress, vertical stress and vertical displacement in the sample in figures 72, 73 and 74 respectively.

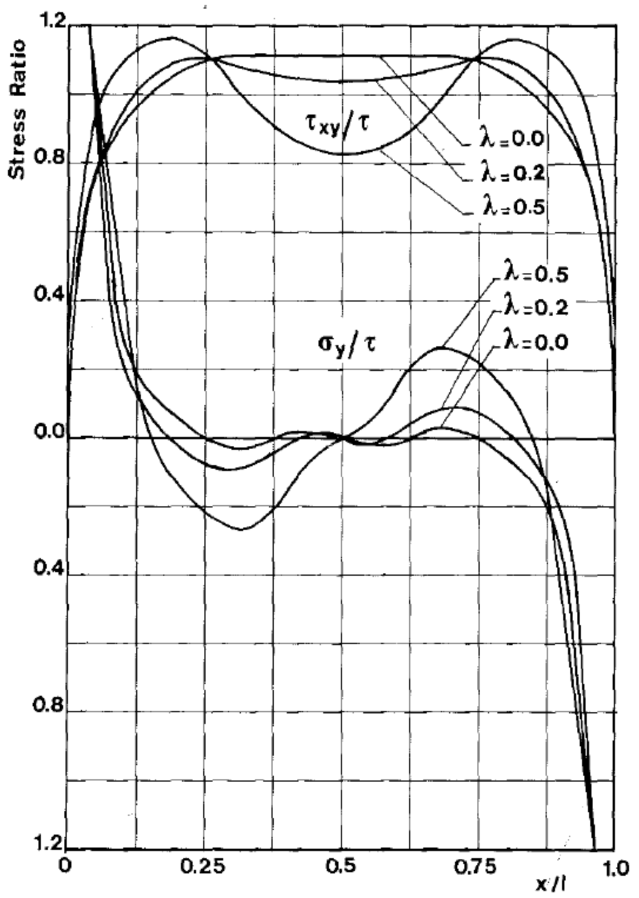

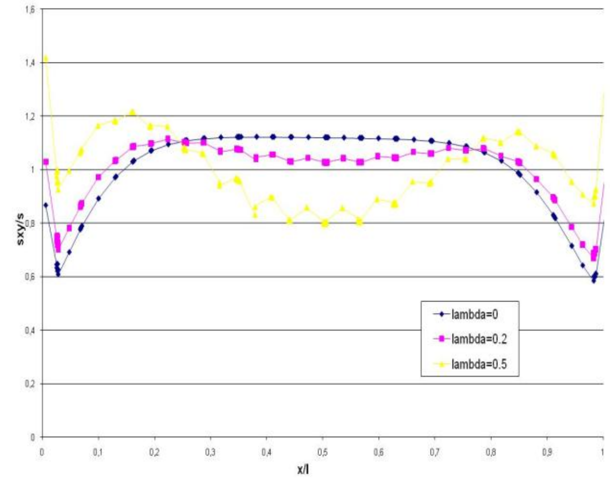

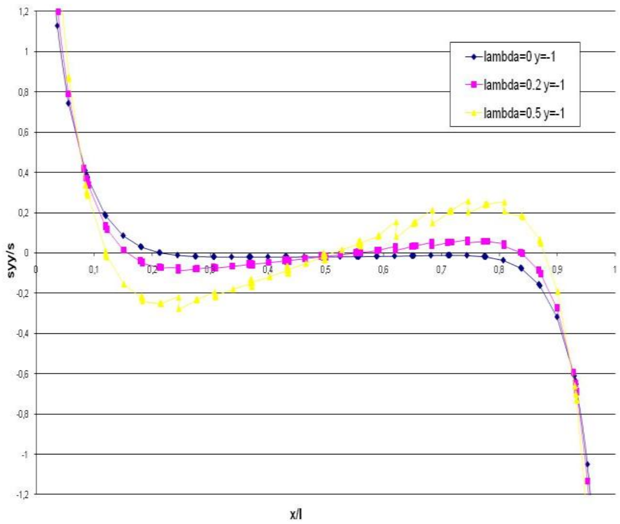

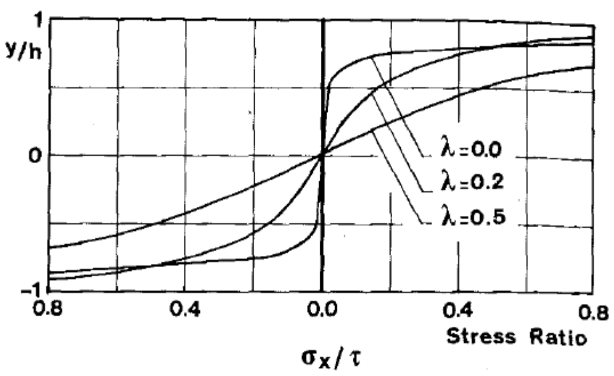

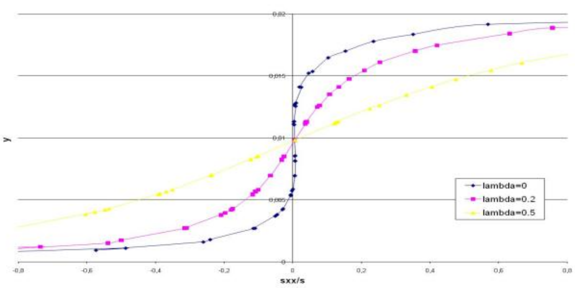

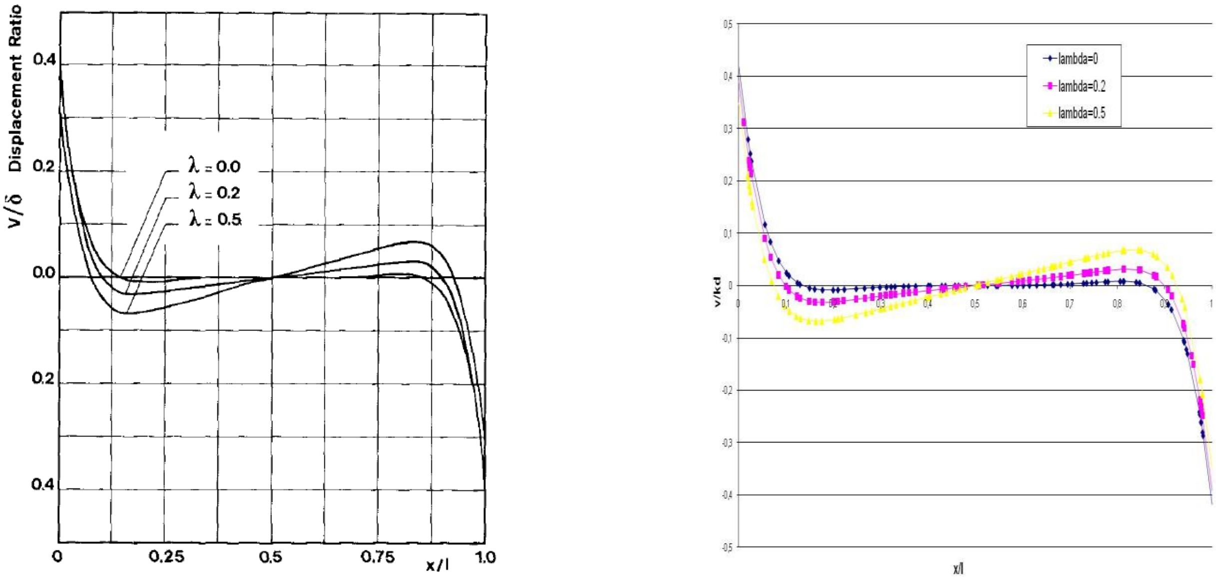

(a) (b)

Figure 72 : Comparison between Prevost and Hoeg results (a) and Plaxis results (b)

λ=0

λ =0.5

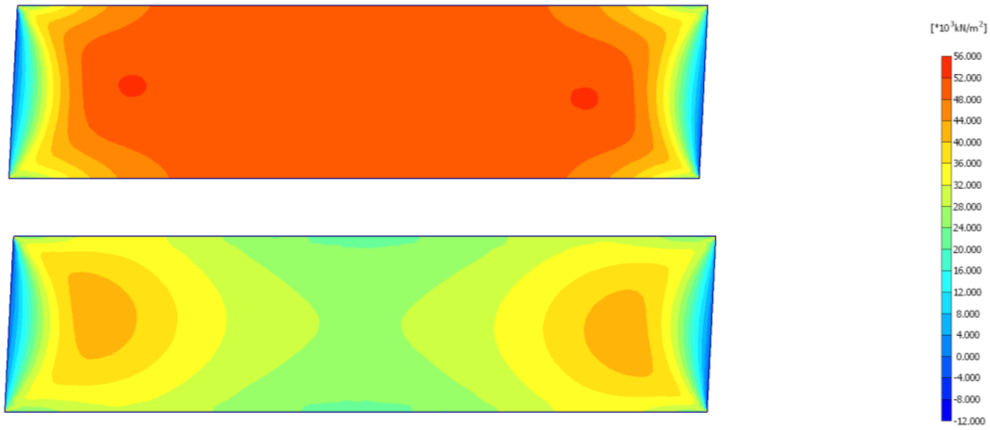

Figure 73 : Shear stress distribution

λ =0

λ =0.5

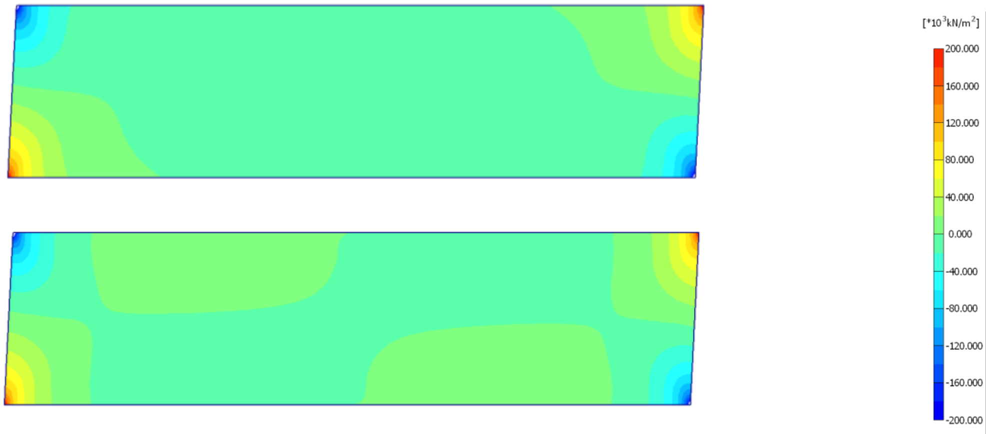

Figure 74: Vertical stress distribution

λ =0

λ =0.5

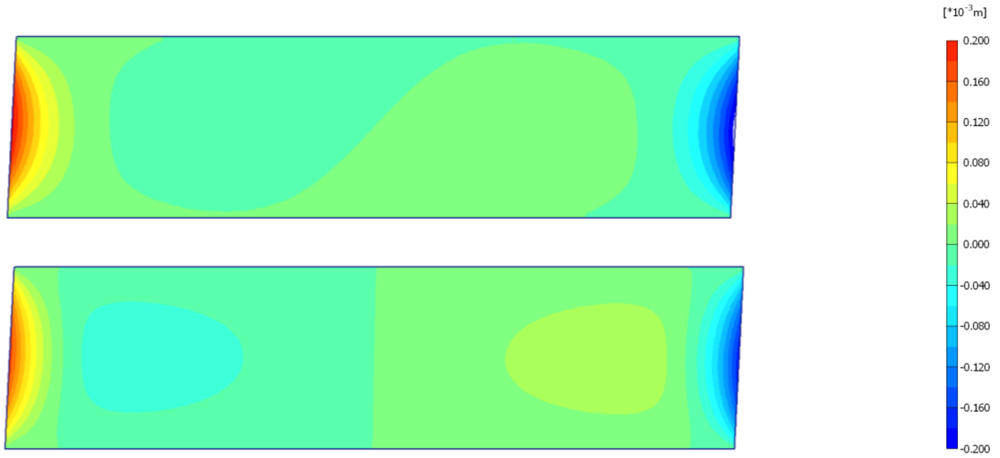

Figure 75 : Vertical displacement distribution

F-2 MODELLISATION OF THE DIRECT SHEAR BOX WITH THE MOHR COULOMB MODEL: POTTS ET AL. (1987)

Potts et al (1987) modelled a direct shear box with a finite element study considering various models. The analysis (A) which uses an elastic perfectly plastic model (Mohr Coulomb) is reproduced here with Plaxis. The meshes considered is presented in figure 75. The dimensions of the sample are h=20mm and l=60mm. A vertical stress of 200kPa is applied at the top of the sample. The boundaries are rough around the sample. Horizontal prescribed displacements are applied on the top and sides of the top half of the sample. The bottom half remains fixed. A horizontal linear displacement is applied in between the two halves on the sides.

Table 12 : Parameters considered in analysis (a)

φ	35
c	0,2
Ψ	0
K_0	0,43
E (MPa)	26
ν	0,3

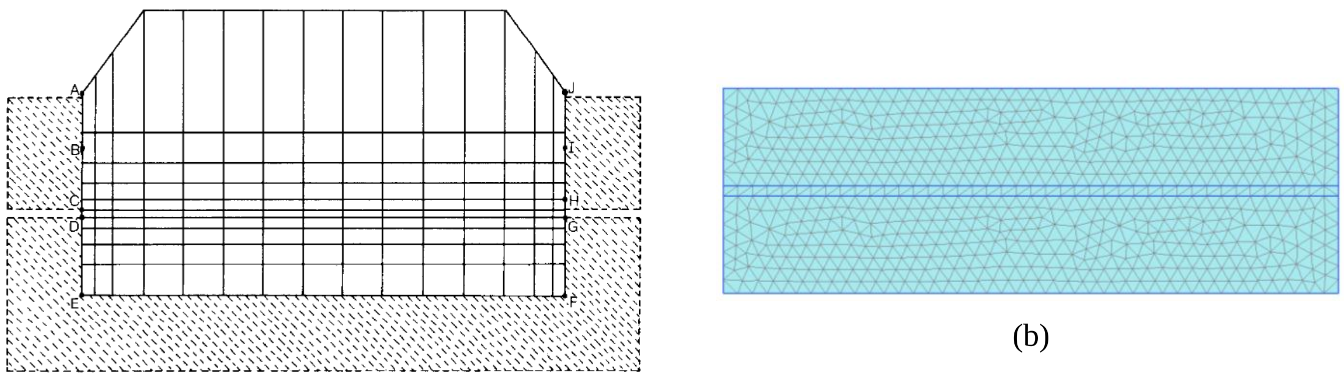

(b)

(a)

Figure 76 : Mesh considered (a) Potts et al and (b) plaxis

The results from the two finite element studies are compared. The states (a) (b) and (c) are illustrated in figure 76 on the stress-strain curve. The evolution of the relative shear stress and shear strain are given in figure 77 and figure 78 respectively. The present study is bringing more details since the mesh considered with Plaxis is much finer and each element contain more nodes (1600 15-noded elements with Plaxis instead of 150 8-noded with the original study).

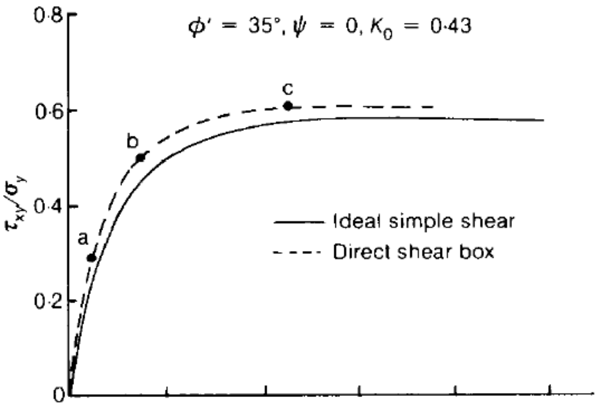

Figure 77: Stress-strain curve from analysis (a) (Potts et al. 1987)

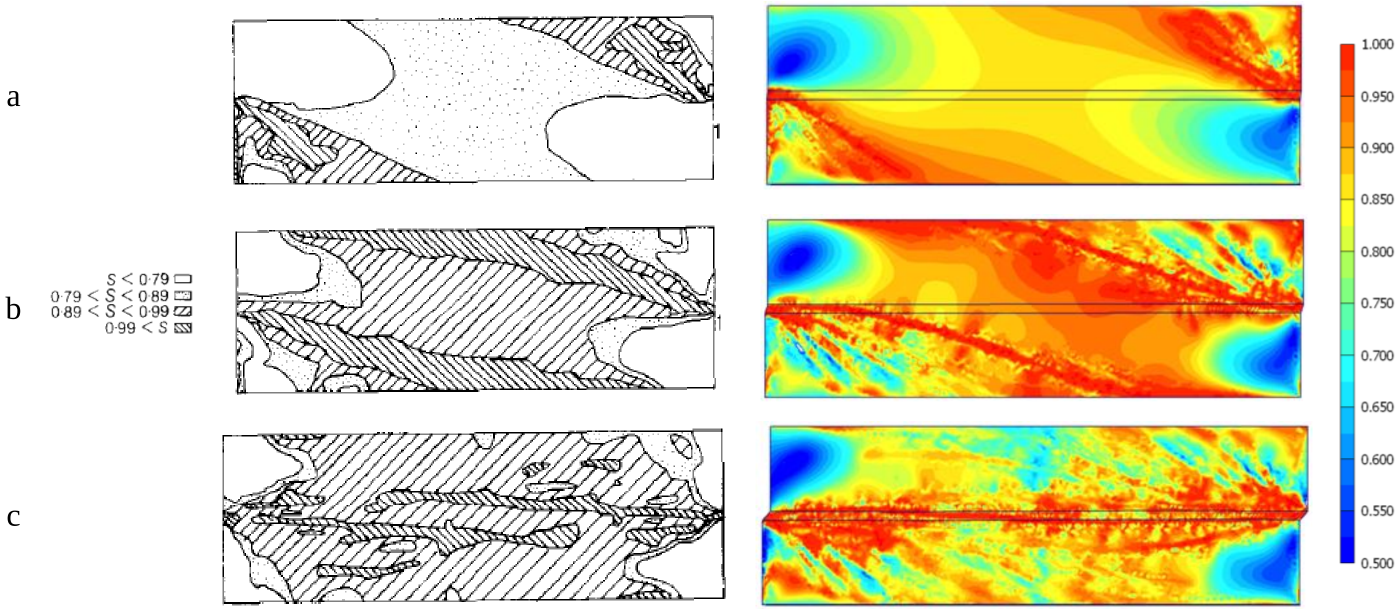

Figure 78: Evolution of the relative shear stress within the direct shear box, Potts et al. on the left and Plaxis on the rigth

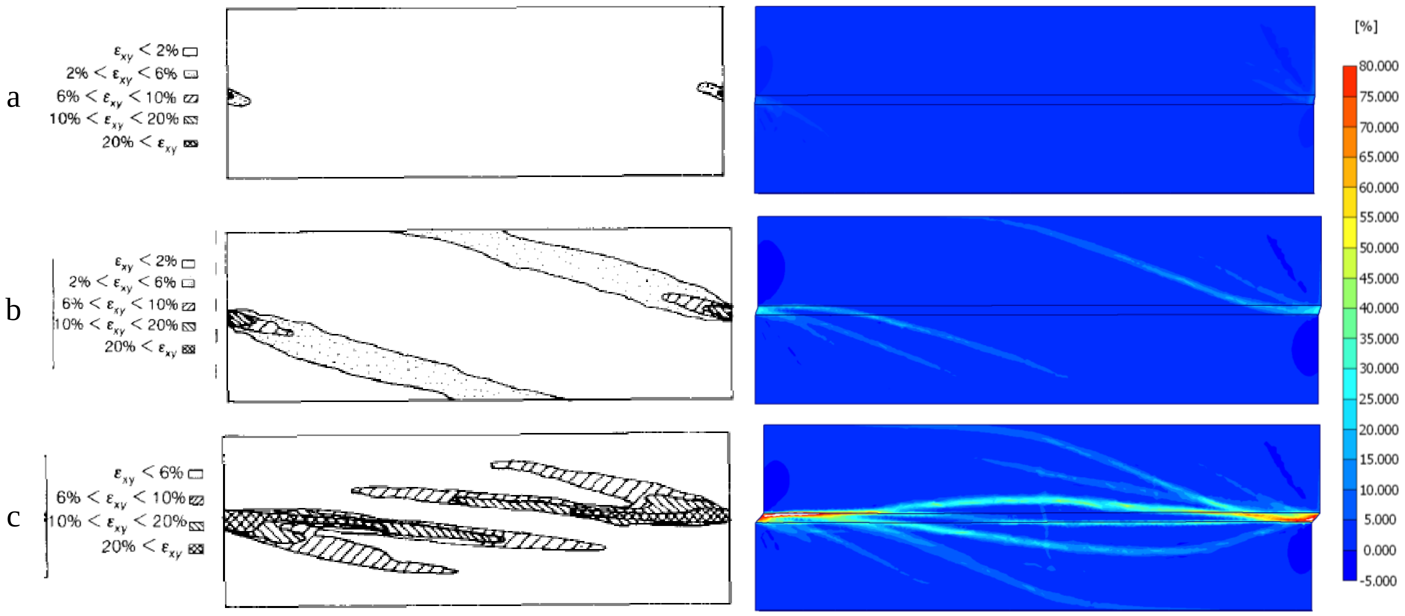

Figure 79: Evolution of the shear srain within the direct shear box, Potts et al. on the left and Plaxis on the rigth